Challenges in IR and MDI design

Manuela Boscolo (INFN-LNF)

ICFA mini workshop on Beam-Beam Effects in Circular Colliders
EPFL, Lausanne, Switzerland
2-5 September 2024

INFN LNF
Istituto Nazionale di Fisica Nucleare

CERN

Introduction

Key challenges for the machine detector integration of future colliders:

- e^+e^- circular: SuperKEKB (in operation), FCC-ee, CEPC
- e^+e^- linear: CLIC, ILC
- pp: FCC-hh, SppC
- e^- ion: EIC (approved), LHeC, FCC-eh
- $\mu^+\mu^-$

Different projects are at **different level of maturity**, have different time scales, either under commissioning, approved or to be approved for the far future.

Rich field with mutual influence and interplay in accelerators design as well as in R&D on the various technologies and systems.

Future Colliders IR Overview

e^+e^- Linear

high instantaneous luminosity within bunch train (low O(10Hz) rep rate)

higher occupancy at the same ave Luminosity

no hope to mitigate with a fast readout, cannot resolve within a bunch train

very low-β demands for the ultimate final focus quads design

smallest beam size ever demands for tightest alignment specs, and fast feeback for beam steering

IP bkgs, radiative beam-beam (beamstrahlung), pairs

e^+e^- Circular

uniform luminosity distribution in time (CW), top-up injection

lower rates than hh, but higher accuracy required

new concept for luminosity, very far from LEP2 rates and step forward also from flavour factories: nano-beams go toward LC,

compact IR (L*↓)

tight mechanical space constraints, including FF quads and correctors

high crossing angle

High beam energy → SR

High intensity → heating, vacuum

Beamstrahlung relevant like for LC (FCC-ee), pairs

hh Circular

continuous beam, luminosities comparable to that of e+e-, higher cross-sections

beam size (and emittance) much larger → higher rates

luminosity and MDI driven by detector performance reach capability

large IR (L* ↑)

head-on

shielding and activation issues

beam halo

e^- ion Circular

e- beam like that of e+e- circular future colliders:
high current issues
SR

4π solid angle detectors,
very low angle is required for the physics (for e+e- 50-100 mrad typical physics cone)

enormous beam apertures required,
FF quads and IR magnets very difficult

Future Colliders IR Overview

e^+e^- Linear	e^+e^- Circular	hh Circular	e^- ion Circular
SLC (1989)	(AdA,1962)	ISR (1971)	HERA (1992)
	long history	SPS	
ILC	LEP	Tevatron	**EIC**
CLIC	*Factories*	RHIC	**LHeC**
	(high current)	LHC → **HL-LHC**	**FCC-eh**
	PEP-II		
	KEKB	**FCC-hh**	
	DAFNE	**SppC**	
	..	*(high field magnets)*	
	Super factories		
	(nanobeam concept)		
	SuperKEKB		
	FCC-ee		
	CEPC		

Please note:
Not exhaustive list

Future Colliders Performance

e+e-

[FCC-ee CDR]

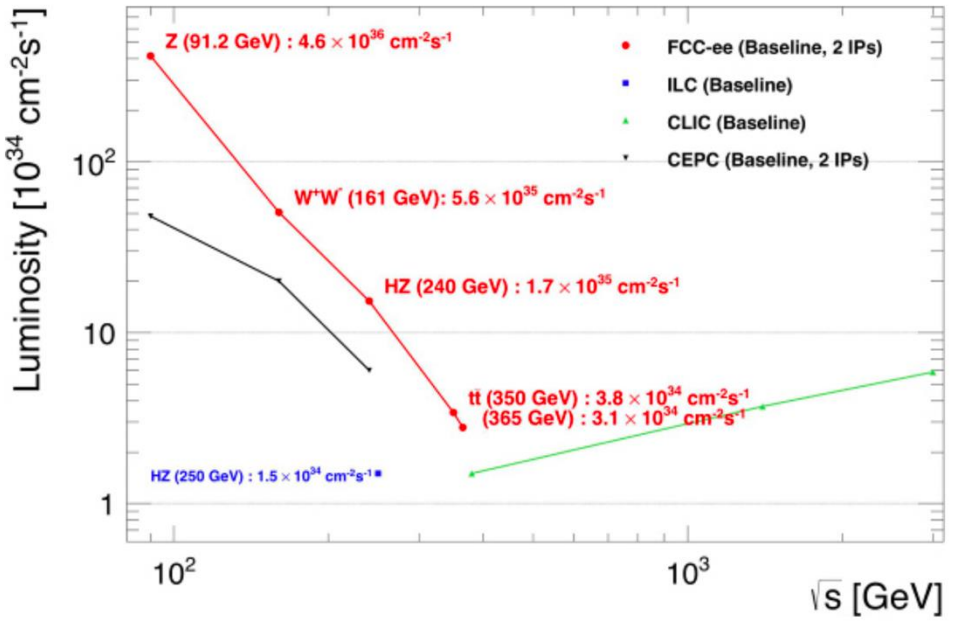

hh

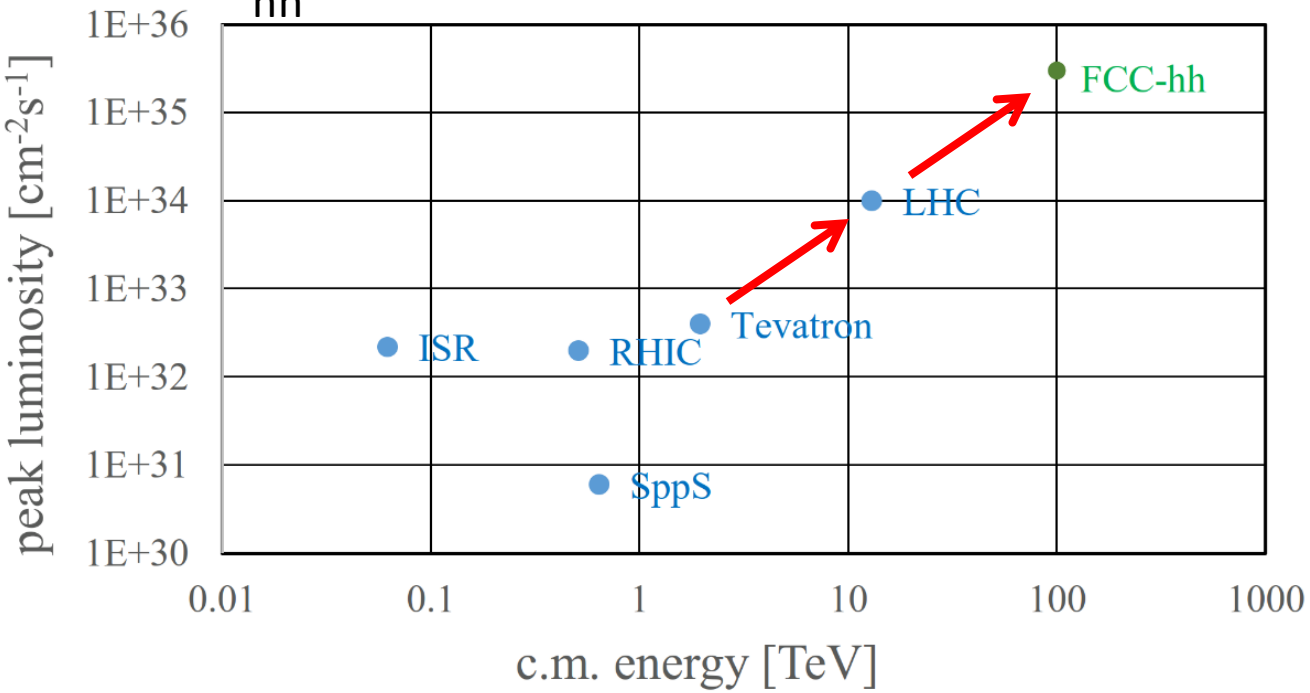

e+e- circular: vertical squeeze at IP

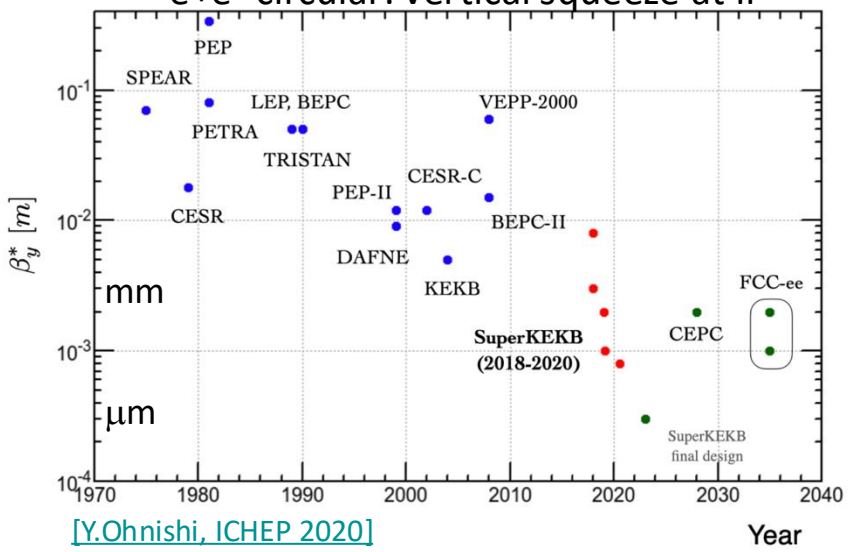

[Y.Ohnishi, ICHEP 2020]

- **order of magnitude performance increase** in both **energy & luminosity**
- **100 TeV cm collision energy** (vs 14 TeV for LHC)
- **20 ab^{-1} per experiment collected over 25 years** of operation (vs 3 ab^{-1} for LHC)
- similar performance increase as from Tevatron to LHC
- **key technology: high-field magnets**

IR future colliders Parameter Table

particle		e^+e^-				pp			e^- - ion	
type		circular		linear		circular			circular/ ERL	
collider name		SuperkekB	FCC-ee	ILC	CLIC	LHC	HL-LHC	FCC-hh	EIC	LHeC
Beam Energy	GeV	LER (e+) 4 HER (e-) 7	45.6, 120,182.5	125, 250	190 / 1500	7000	7000	50000	(e-) 10 (h) 275	(e-) 49.19 (p) 7000
$\mathcal{L}$ (peak)	$10^{34}cm^{-2}s^{-1}$	80	230, 8.5, 1.6	1.4, 1.8	1.5, 6	2.1	5	5-30	1	23
crossing angle	mrad	83	30	14	16.5, 20	0.26	0.5		25	0
Bunch spacing	ns	4	20	554, 5Hz train	0.5, 50Hz 312 train	25	25	25	10	50
L* (free region)	m	L 0.77 H 1.22	2.2	4.1	6	23	23	40	4.5	10
β_x*	cm	L 3.2 H 2.5	15,30, 100	1.3, 2.2	80 / 70	25	15	110-30	45 80	(e-) 6.45 (p) 10
β_y*	mm	L 0.27 H 0.3	0.8, 1, 1.6	0.41, 0.8	0.1 / 0.12	250	150	1100-300	56 72	(e-) 64.5 (p) 100
Normalised emittance x	μm	L 25 H 63	24, 148, 479	5, 10	0.95/ 0.66	3.5	2.5	2	(e-) 391 (h) 3.3	(e-) 50 (p) 2.5
Normalised emittance y	nm	L 68 H 177	89, 235, 1000	35, 35	30/20	3500	2500	2000	(e-) 25400 (h) 290	(e-) 50000 (p) 2500
B_{det}	T	1.5	2	5 (SiD)	3.5-5	Atlas 2T, CMS 4T			1.4	3.5
central pipe radius	cm	1	1 (1.5 CDR)	1	3	2.35 Atlas, 2.1 CMS	2.35 Atlas, 2.1 CMS	2.5	elliptical	elliptical

Boundary Conditions to IR design

- **Ideal case:**
  - High luminosity
  - Full (4π) detector acceptance
  - Low background conditions

- **Real life:**
  - Achievable Luminosity high enough as required by physics program
  - Good detector acceptance in forward/rear direction
  - Tolerable background rates

Luminosity and acceptance requirements depend very much on the physics program

Extra-constraints: injection, crossing angle, synchrotron radiation

Detector Constraints for the accelerator design

- Highest physics acceptance from the nominal beam axis
- Smallest possible beam pipe radius
- Thinnest possible beam pipe wall
- Detector solenoid – compensation needed
- Separation scheme (only for circular)
- Compromise on L* (free distance between the IP and the first final focus quad)

IR and MDI for e^+e^- Linear Colliders

- **Squeezed beams at the IP: requires extreme final focus quads gradient**
- **Extreme mechanical precision mandatory to reach goal luminosity**, two necessary ingredients:
  - **active and passive alignment system,** R&D
  - **fast feedback** (beam steering at nm precision level)
- **Beam-induced backgrounds ->** constraints on beam pipe radius and geometry, vertex detector radius
  ($\gamma\gamma$ -> hadrons)
- **Challenge on MDI mechanics, electronics, services, minimal tolerances**
- **Low mass tracker supports with integrated cooling** –R&D performed through past years
- **The very different bunch structure between LC (bunch trains) (even if ILC/CLIC are different wrt each other) and circular (uniform fill) leads to very different detector solutions:**
  - **In-time pile-up of hadronic backgrounds, sufficient granularity for topological rejection**
  - **At CLIC: ns-level timing in many detectors systems (0.5 ns micro-bunch spacing, 312 bunches)**
  - **Power pulsing of front-end electronics, reduced power consumption**

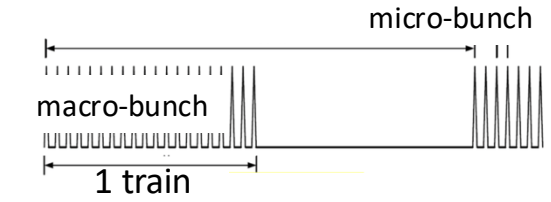

LC bunch structure

CLIC MDI

ArXiv:1903.08655 (2018)

simpler design

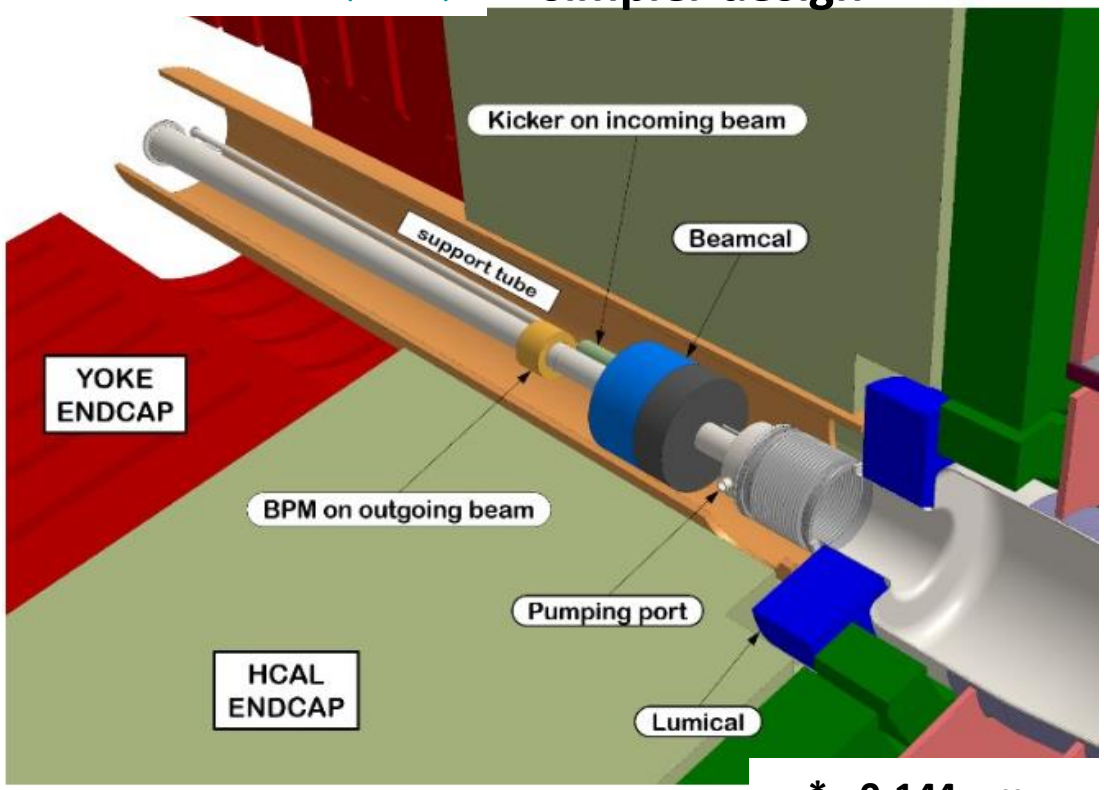

$\sigma_x^* = 0.144\ \mu m$
$\sigma_y^* = 2.97\ nm$ @380 GeV

L* = 6 m both 380 GeV and 3 TeV

QD0 outside the detector at 380 GeV and 3 TeV

QD0 mounted on the tunnel floor (much smaller vibrations)

no pre-absorber, no cantilever support for QD0

divided in three segments, much smaller gradient (25 T/m), larger aperture radius (25 mm)

no anti-solenoid needed

ArXiv:1202.6511 (2011)

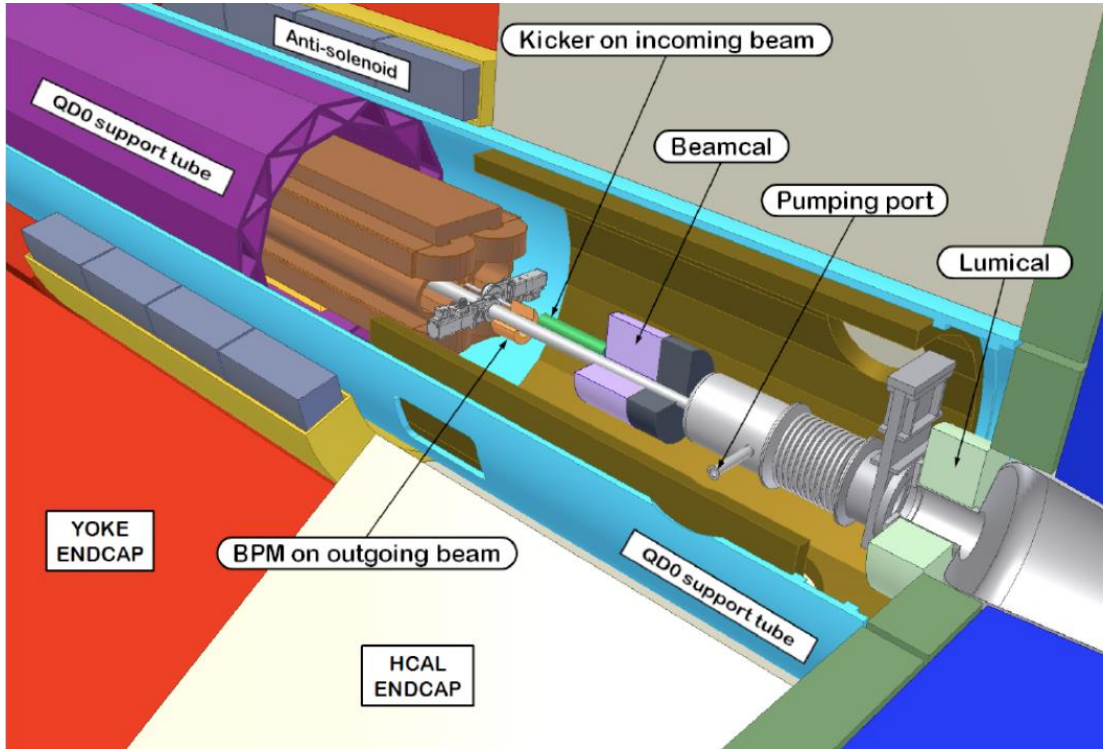

L* = 4.3 m at 500GeV

L* = 3.5 m at 3TeV

CLIC MDI

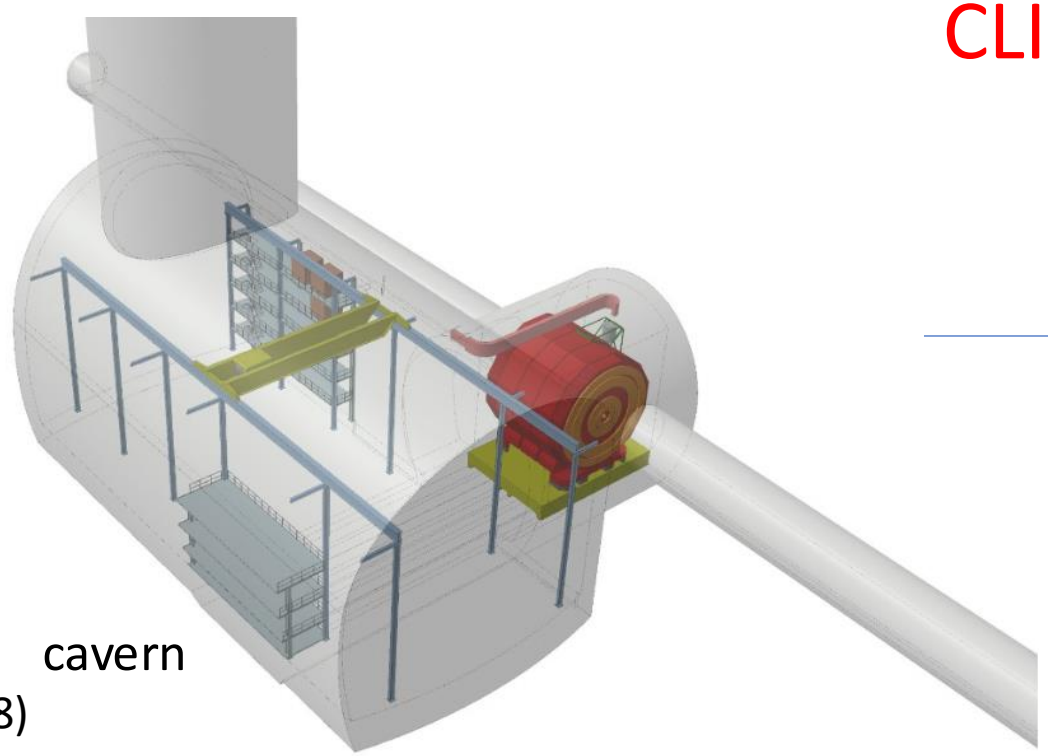

new cavern (2018)

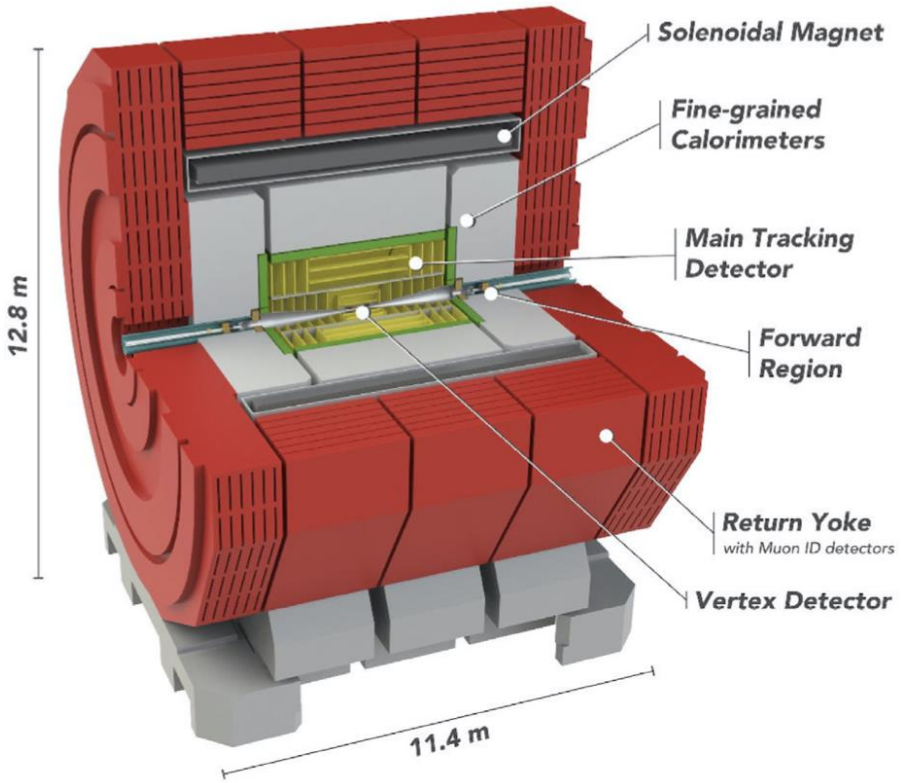

(Most of the detector elements unchanged)

Key issues:

- Minimization of radiation:

  Collimators and masking to suppress bkg from beam-beam and beam dumps

  - Background suppression and radiation shielding

    NIM A 983 (2020) 164522 link

Lower backgrounds from incoherent pairs at 380 GeV allow for a **smaller central vacuum chamber**, and thus a **smaller radius of the innermost vertex detector layer**

Radiation effects and beam-beam at 3 TeV determine the design constraints

CLIC QD0 Prototype

https://arxiv.org/pdf/1202.5952.pdf

- **QD0** requirements (**2009**) **L*=3.5, 4.3 m, inside detector**
- The magnetic requirements for the QD0 are quite severe: the extremely high gradient needed, the small aperture of the magnet bore, the length of the magnet, the required tunability.

- Distance between post collision line beam pipe and beam axis ~35 mm
- **Active stabilisazion of the quadrupole**: sufficient rigidity and with a well known dynamic behaviour (vibration eigenmodes, no source of vibration (ex. coil coolant flux)

Parameter	Value
Nominal field gradient	575 T/m
Nominal integrated field gradient	1570 T
Magnetic length	2.73 m
Magnet bore diameter	8.25 mm
Good field region(GFR) radius	1 mm
Integrated field gradient error inside GFR	< 0.1%
Adjustment	+0 to -20%

Table 1: Magnetic and geometric requirements for the QD0 quadrupole

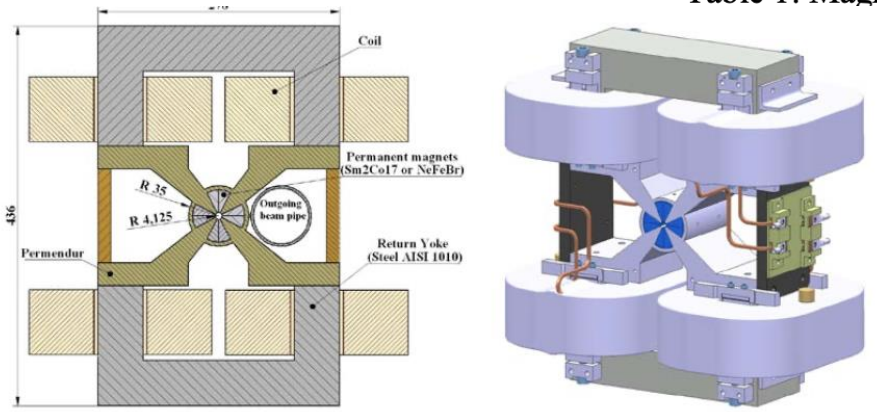

Figure 2-3: Conceptual design of the QD0 cross section and full assembly

CLIC QD0 Main Parameters		100mm prototype	Real magnet 2.7m
Yoke			
Yoke length	[m]	0.1	2.7
Coil			
Conductor size	[mm]	4×4	4×4
Number of turns per coil		18×18=324	18×18=324
Average turn length	[m]	0.586	5.786
Total conductor length/magnet	[m]	0.586×324×4=760	5.786×324×4=7500
Total conductor mass/magnet	[kg]	26.8×4=107.2	265.2×4=1060.8
Electrical parameters			
Ampere turns per pole	[A]	5000	5000
Current	[A]	15.432	15.432
Current density	[A/mm^2]	1	1
Total resistance	[mOhm]	896	8836
Voltage	[V]	13.8	136.4
Power	[kW]	0.213	2.1

Table 2: Magnetic and geometric parameters for the QD0 "Short Prototype" and "Full Size" magnet.

ILC IR and MDI

	FCC-ee	ILC	CLIC
Transv. rms emittance (pm)	H: 270, 630, 1340 V: 1, 1, 3	H: 20, 10 V: 0.14, 0.07	H: 2.4, 0.22 V: 0.8, 0.01

Very small beams at IP - determine a challenging MDI design

$\sigma_x^* = 0.52\ \mu m$
$\sigma_y^* = 7.7\ nm$

squeezed beams can be obtained with strong FF quads

[Arxiv_2019] **L* = 4.1 m**

[TDR (2013)] L* 4.5 m (ILD) 3.51m (SiD)

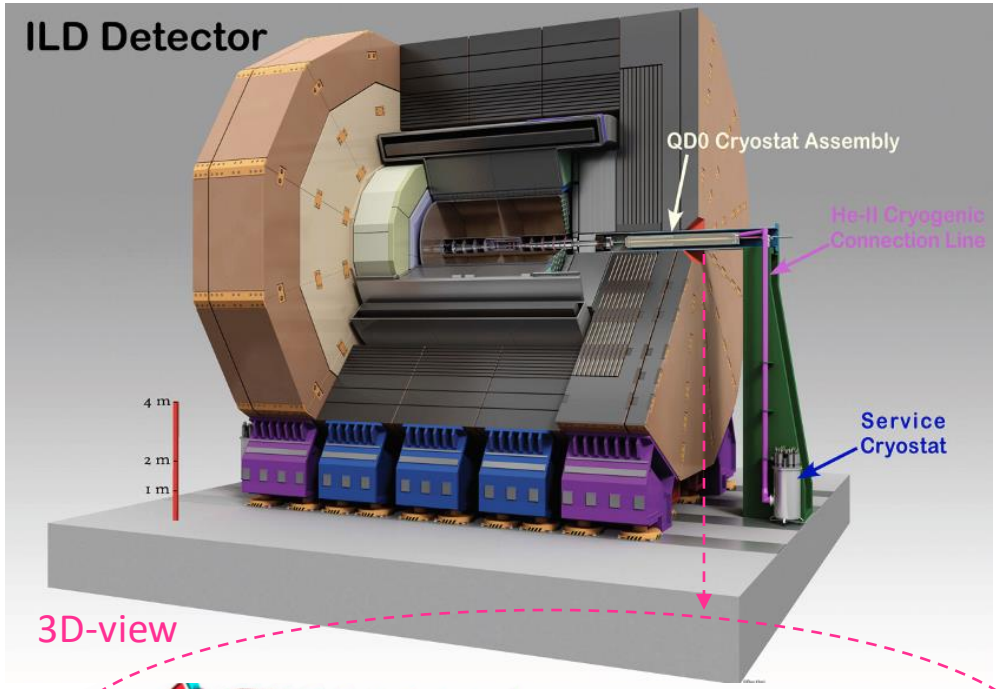

3D-view

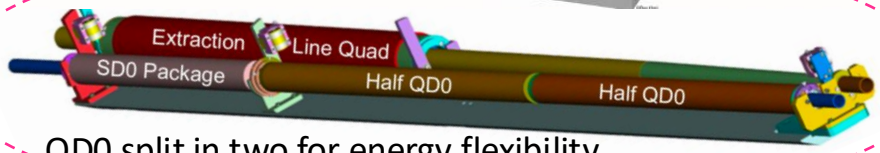

QD0 split in two for energy flexibility

- Strong SC **QD0**, as compact as possible, inside the detector, shielded coils, correctors needed (BNL direct-wind technology) **R&D**
  [see B. Parker, LCWS2021]
- **alignment** system : vertical position of the centre of the incoming-beam-line quadrupole field O(50 nm) challenging

- **Overall integration with push-pull system** in less than 24hrs
- Stable luminosity with **train-by train** and **intra-train feedbacks**
  -> BPMs at μm/ sub-μm level
- **Luminosity feedback**
- **Luminosity measurement:** precision of $\approx 10^{-3}$,
- Lumical: Bhabha rate in the 30-90mrad polar angle region in front the FF quads @500Ecm 10 bhabhas/bunch train; 1.5k pairs/BX for fast lumi diagnostics at 5-30mrad

Two independent cryostats, with **QD0 cryostat almost entirely into the detector.** Only the QD0 cryostat is moved together with detector during push-pull operation.

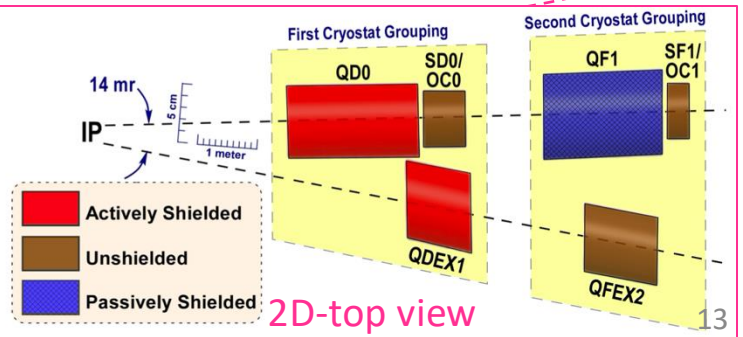

2D-top view

Collision scheme adopted by all future e^+e^- circular colliders

Crab-waist scheme, based on two ingredients:

- concept of **nano-beam scheme:**
  - vertical squeeze of the beam at IP and large horizontal crossing angle
  - large ratio σ_z/σ_x reducing the instantanous overlap area, allowing for a lower β_y^*
- concept of **crab-waist sextupoles:**
  - placed at a proper phase advance they suppress the hourglass effect by inducing a constant β_y along the larger coordinate of the beams overlap.

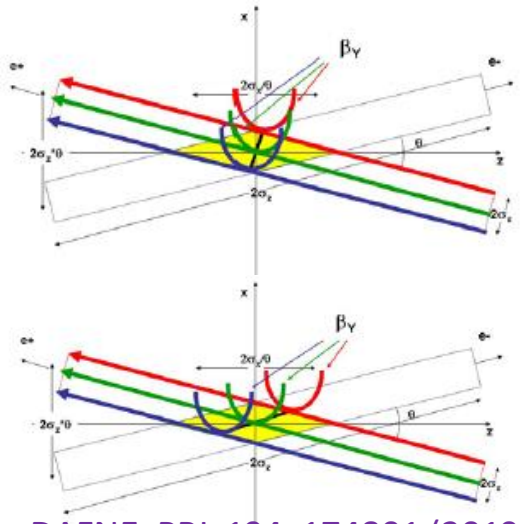

crab sextupoles off

crab sextupoles on

DAFNE, PRL 104, 174801 (2010)

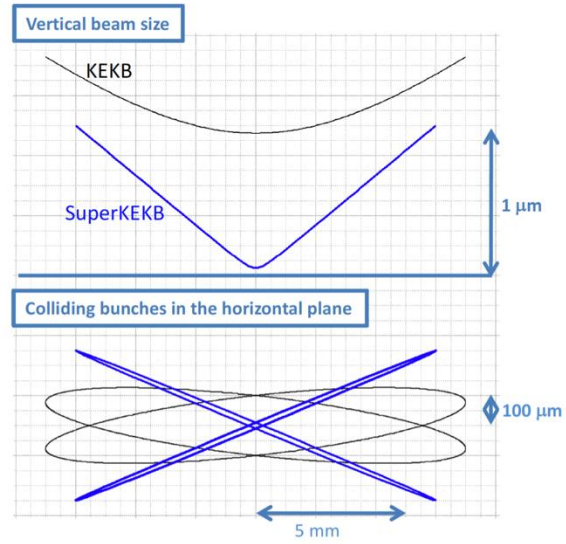

Figure 2: Schematic view of the nanobeam collision scheme.

SuperKEKB https://arxiv.org/pdf/1809.01958.pdf

IP beam distributions (SuperB case)

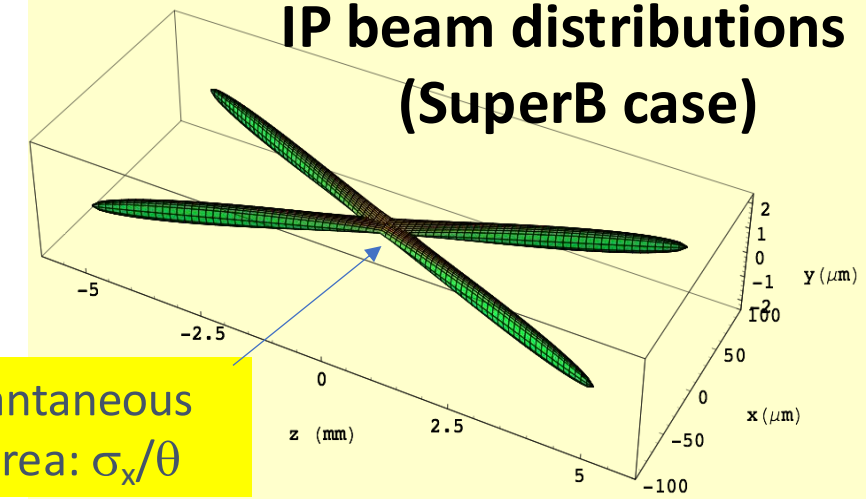

Small instantaneous collision area: σ_x/θ

Collision scheme adopted by all future e^+e^- circular colliders

Crab-waist scheme, based on two ingredients:

- concept of **nano-beam scheme:**
  - vertical squeeze of the beam at IP and large horizontal crossing angle
  - large ratio σ_z/σ_x reducing the instantanous overlap area, allowing for a lower β_y^*
- concept of **crab-waist sextupoles:**
  - placed at a proper phase advance they suppress the hourglass effect by inducing a constant β_y along the larger coordinate of the beams overlap.

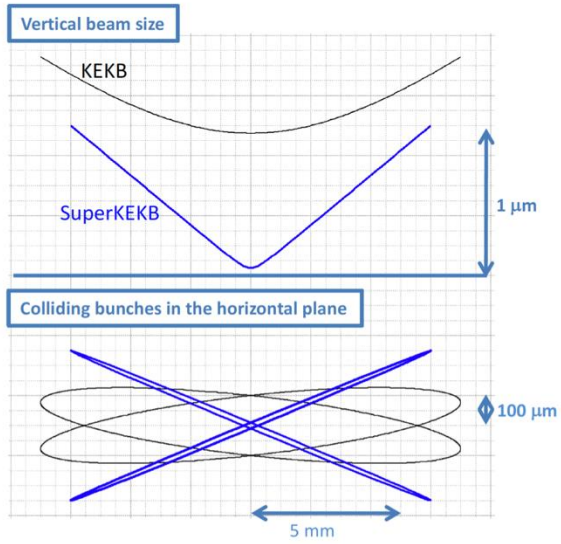

Figure 2: Schematic view of the nanobeam collision scheme.

SuperKEKB https://arxiv.org/pdf/1809.01958.pdf

IMPACT on MDI design:

- Tight and packed interaction region → small L*, QD0 inside detector, mechanical constraints
- Beam pipe design, as splitting in two pipes is very close to the IP
- Robustness against machine induced and IP backgrounds
- Radiation damage, and occupancy and spurious hits
- Higher trigger rate to cope

KEKB and SuperKEKB IR relevant parameters

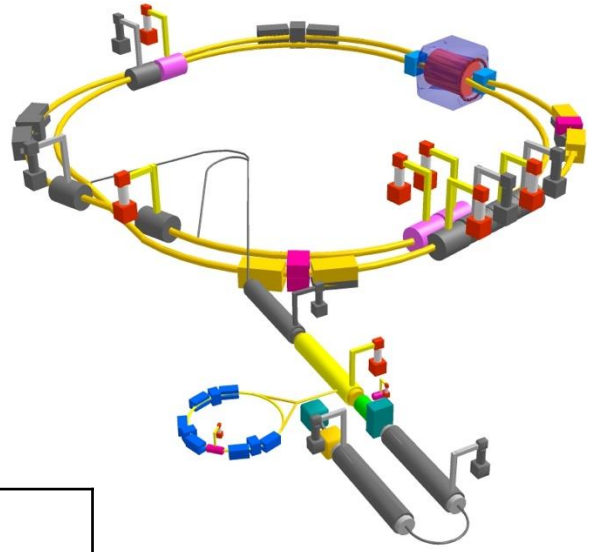

Parameters	unit	KEKB		SuperKEKB	
		LER(e+)	HER(e-)	LER(e+)	HER(e-)
Luminosity	10^{34} $cm^{-2}s^{-1}$	2.11		**60 (4.7 achieved)**	
Circumference	m	3014		3014	
Energy	GeV	3.5	8.0	4	7.007
I (beam)	A	1.64	1.2	**2.8**	**2**
I (bunch)	mA	1.0	0.75	1.77	1.13
ε_x/ ε_y transv. rms	**nm /pm**	18 / 150	24 / 150	**3.3**	**4.6**
σ_x/σ_y(IP)	**μm /nm**	150 / 940	170 / 940	**10 / 48**	**11 / 62**

target values 2031

SuperKEKB FF magnets and detector

σ_x^*= 10.7 μm σ_y^*= 62 nm

σ_x^*= 10.1 μm σ_y^*= 48 nm

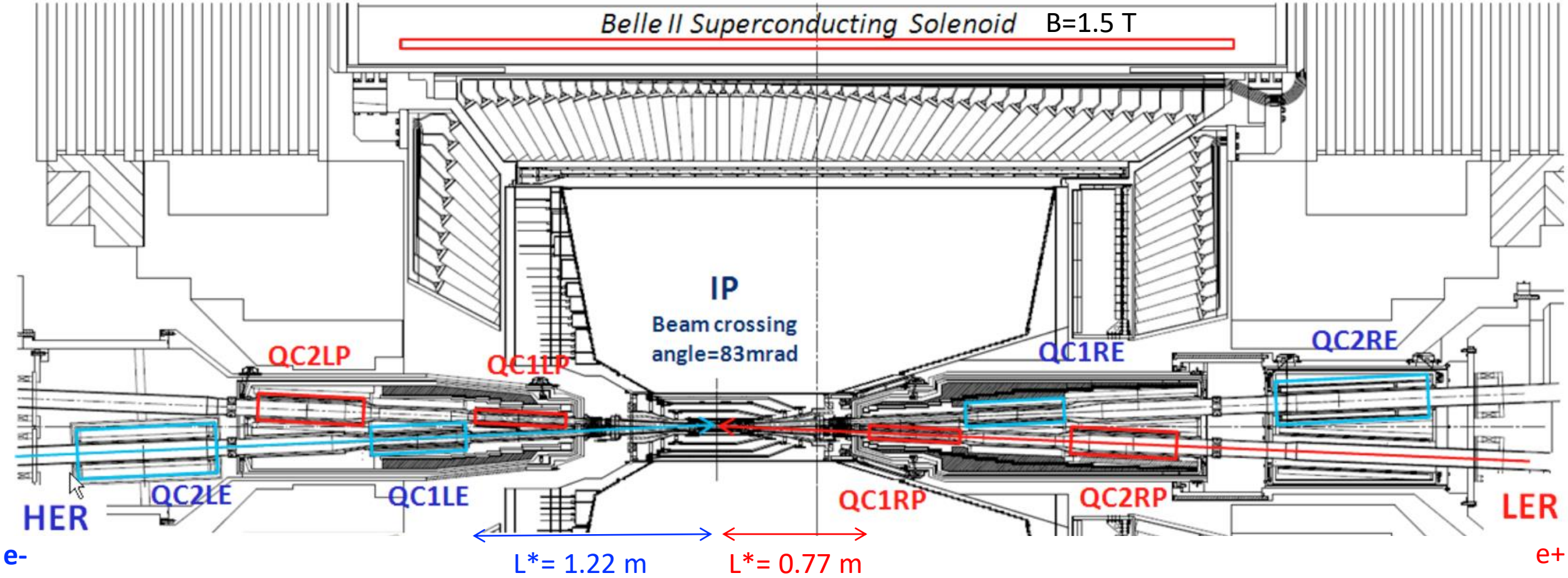

SuperKEKB beam pipe & synchrotron radiation

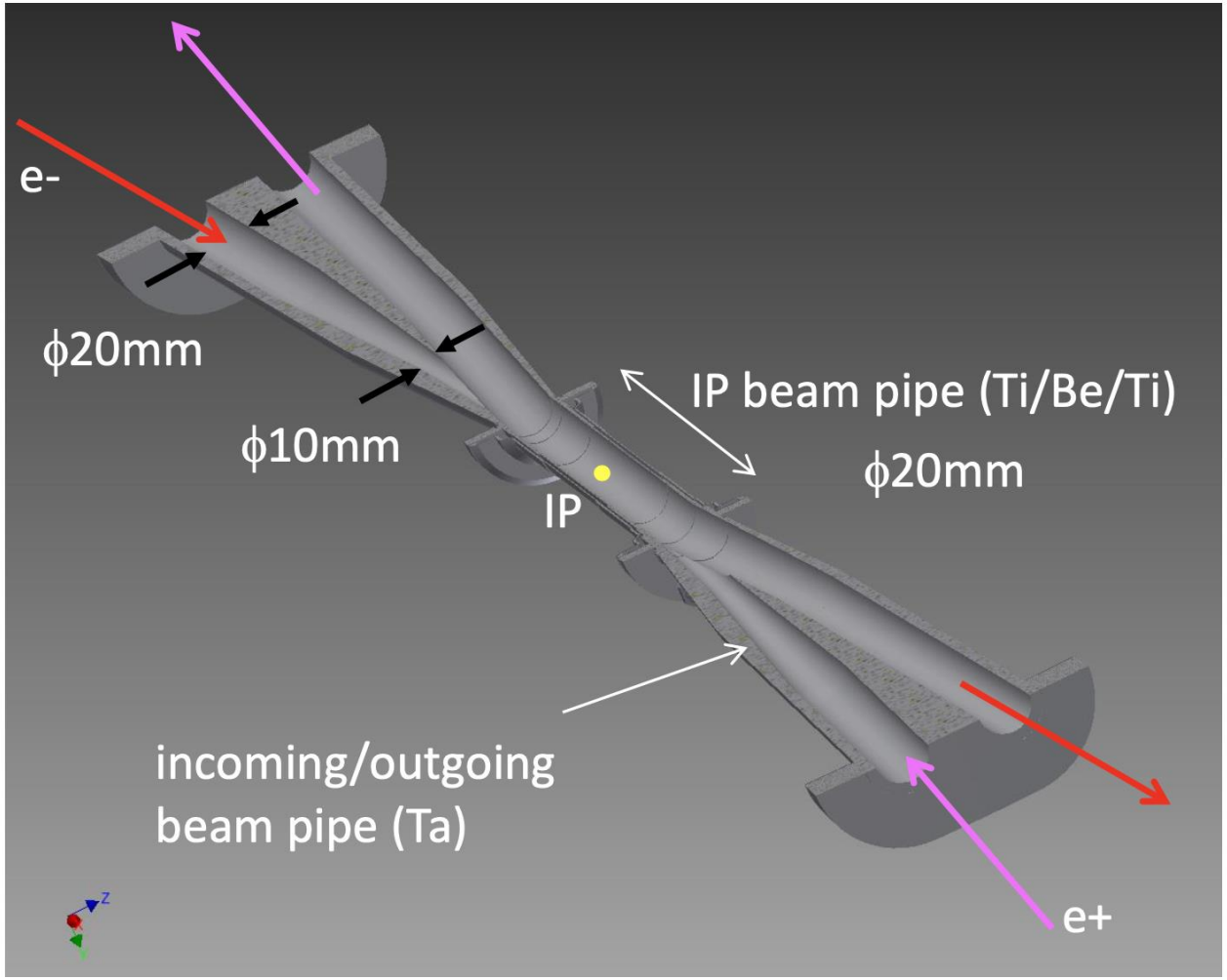

- ϕ20mm→ϕ10mm collimation on incoming beam pipes (no collimation on outgoing pipes, HOM can escape from outgoing beam pipe)

- Most of SR photons are stopped by the collimation on incoming pipe.
- Direct hits on IP beam pipe is negligible

- To hide IP beam pipe from reflected SR, "ridge" structure on inner surface of collimation part.

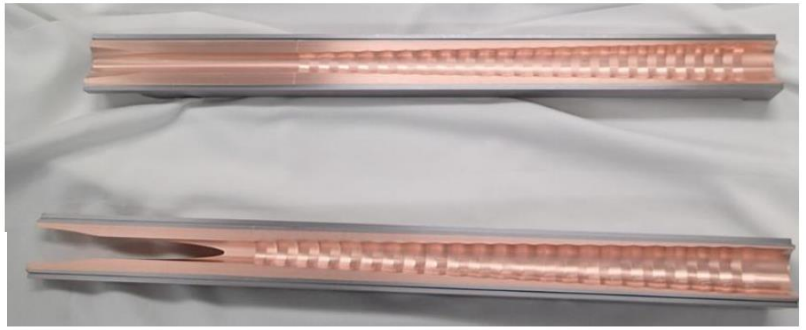

Inner surface of Be pipe are coated with **Au layer (10 μm)** to protect detectors from SR

SuperKEKB Be beam pipe at IP

- The beam pipe at the IP is a double pipe, each consists of middle (Be) and side (Ti) parts, brazed to each other.
- The inside of inner pipe is Au coated (10 μm thickness via 0.3 μmTi) by magnetonsputtering
- Paraffin runs between them

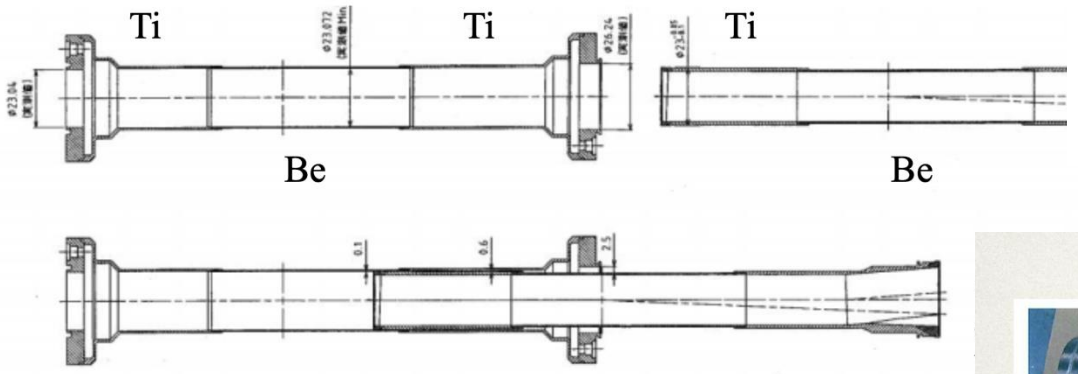

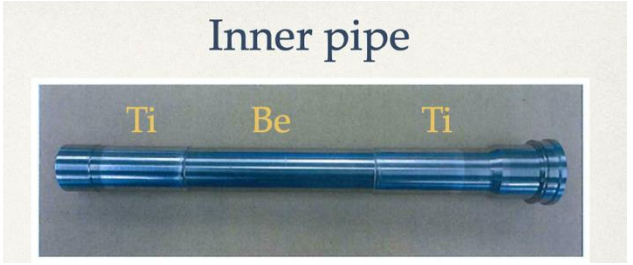

•Outer Be: 0.4 mm thick
•Inner Be: 0.6 mm thick
•Gap: 1 mm

Courtesy K. Kanazawa

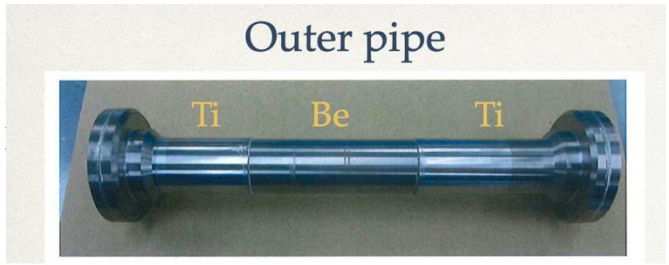

Light material (Be) inside detector acceptance
Paraffin ($C_{10}H_{22}$) flow to remove heat from image charge (~80 W)
Gold plating on inner wall protects detectors

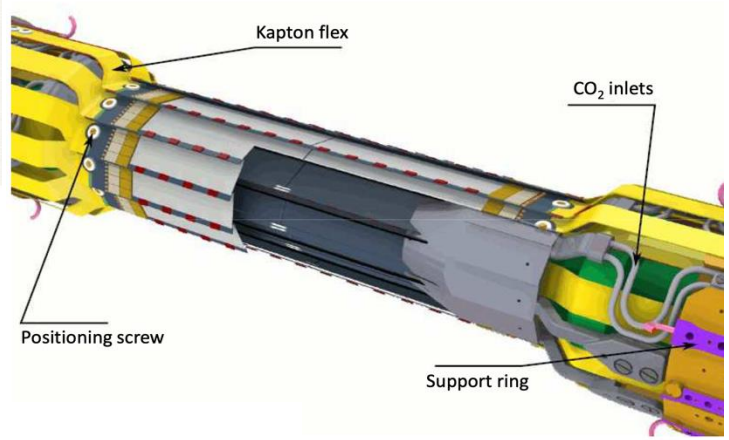

➢ Low material budget cooling
- Massive structures outside the acceptance to cool down the readout chips
- The center of the ladder rely on cold air

Challenge of SuperKEKB IR magnet integration

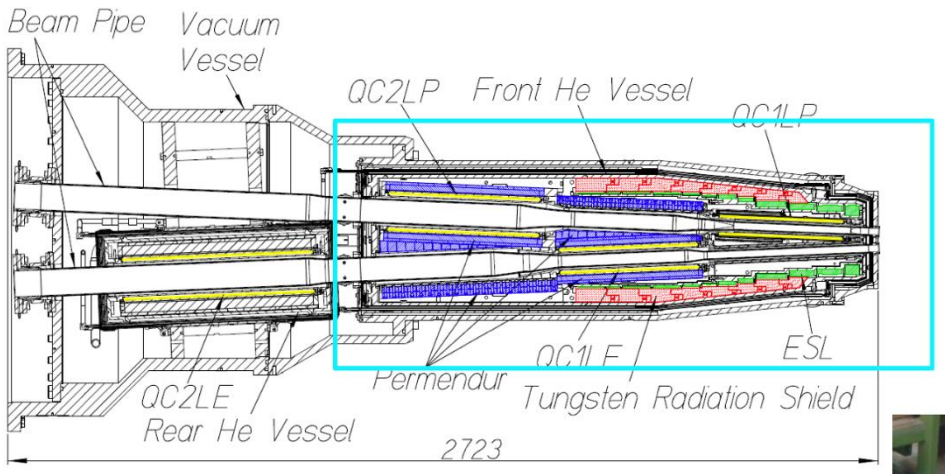

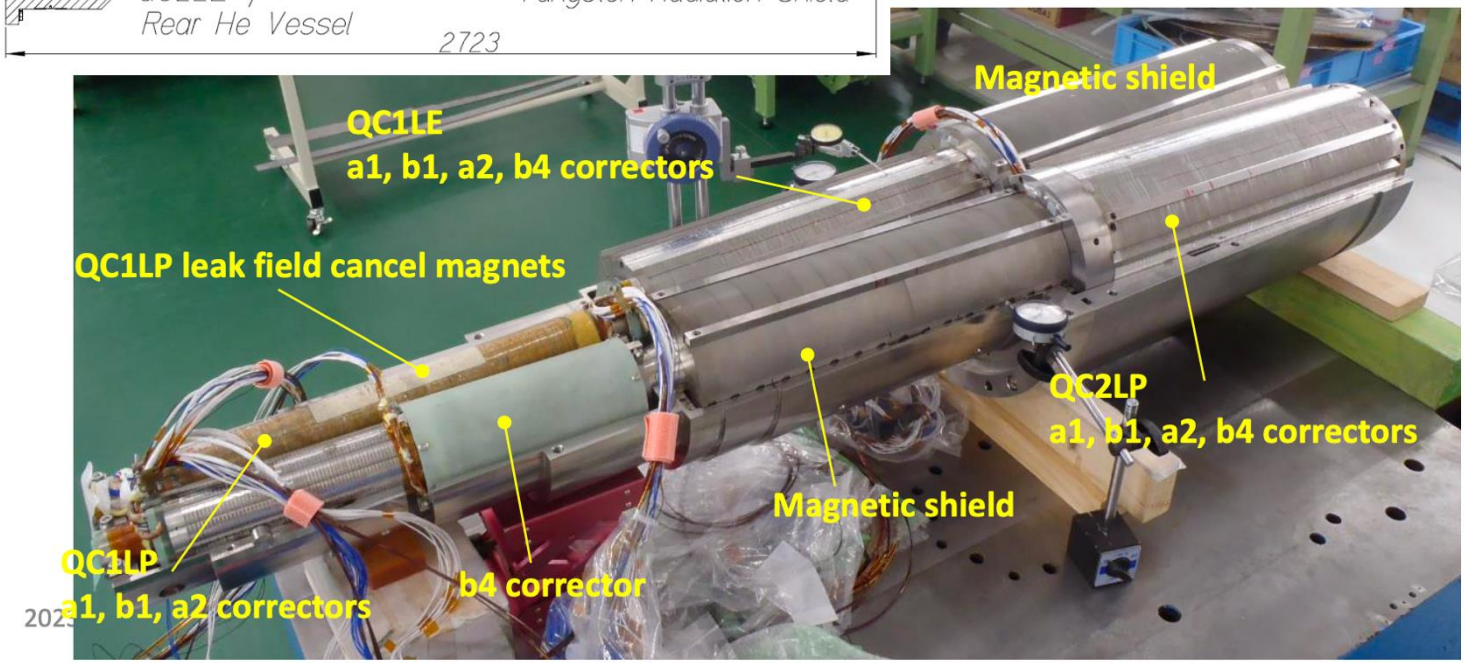

Courtesy N. Ohuchi

Challenge of SuperKEKB IR magnet integration

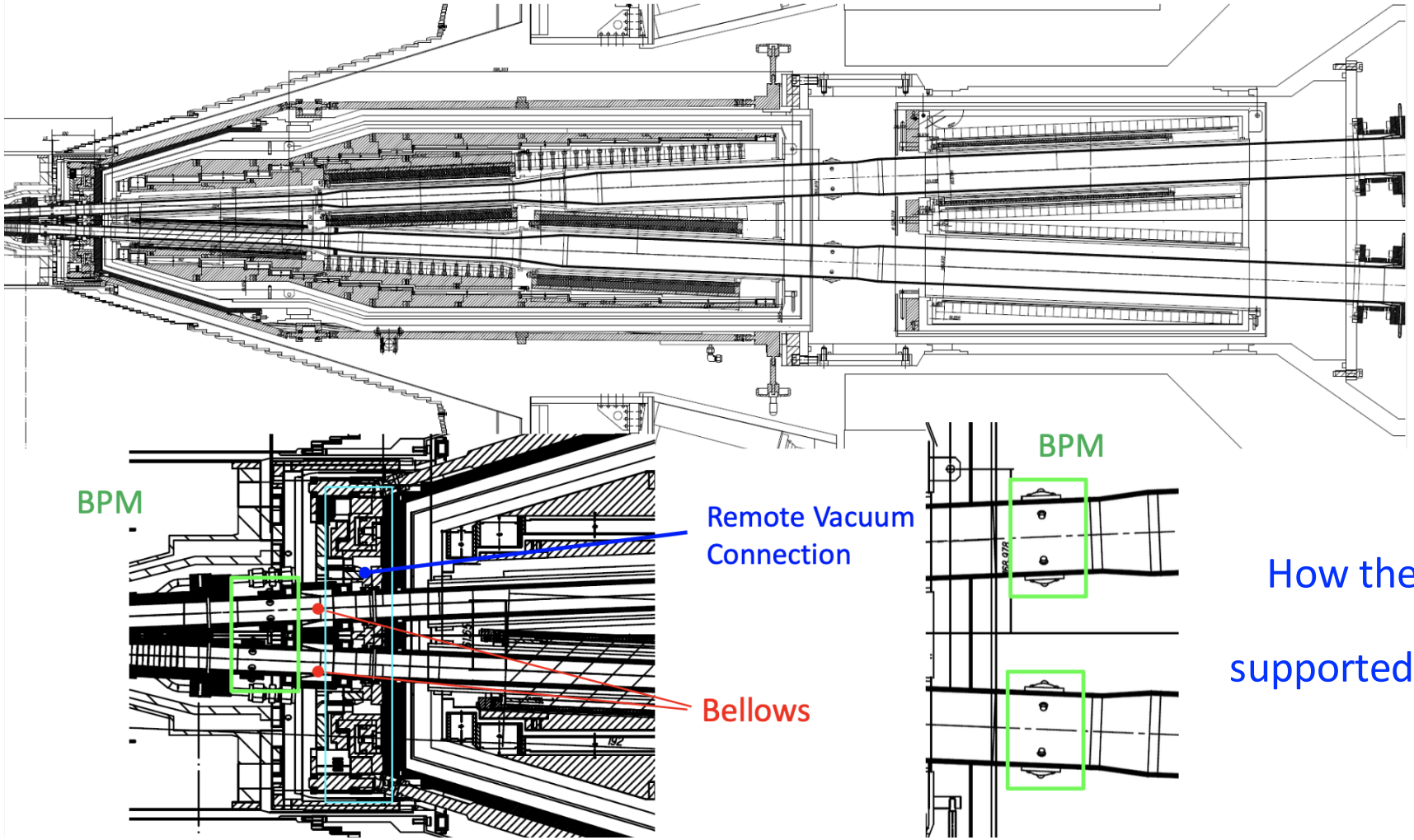

How the in-board BPM, bellows and magic flange are positioned and supported, overall alignment, vibration control

Courtesy N. Ohuchi

Challenge of SuperKEKB/Belle II backgrounds

- **Data/MC signals now within a factor of 2-3 with many down to the 20% level or better**

  This includes detector background signals for large radius detector subsystems

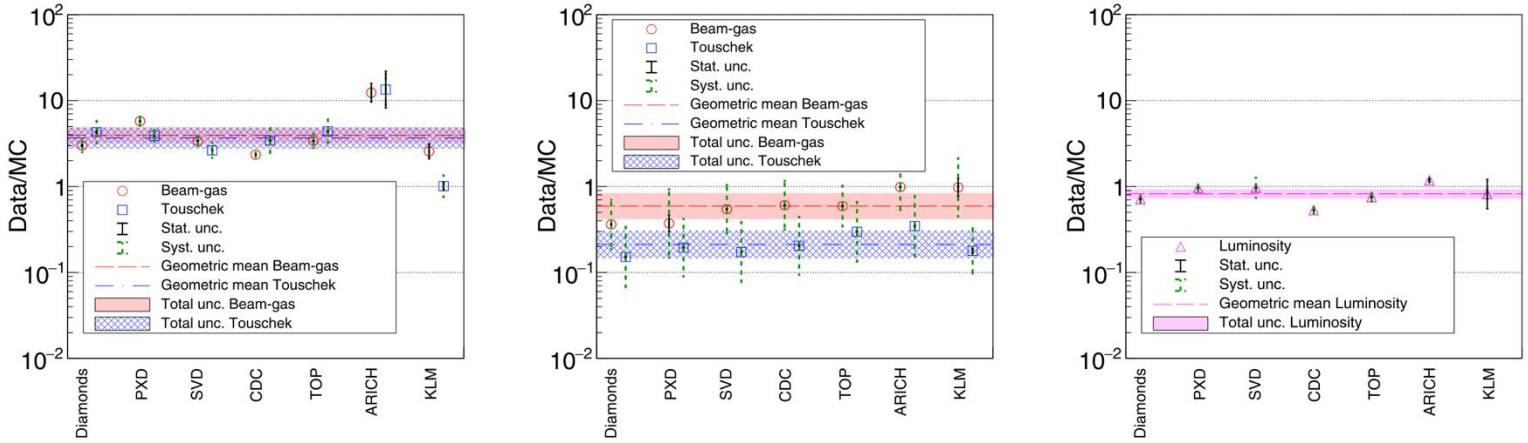

(a) LER single-beam background. (b) HER single-beam background. (c) Luminosity background.

Fig. 15. Belle II detector-level Data/MC ratios in Belle II over 2020 and 2021 dedicated background studies.

Table 7
Combined Belle II Data/MC ratios over 2020–2021 collected data.

Background	LER	HER
Beam-Gas	$3.94^{+0.92}_{-0.74}$	$0.59^{+0.25}_{-0.18}$
Touschek	$3.67^{+1.22}_{-0.92}$	$0.21^{+0.10}_{-0.07}$
Luminosity	$0.82^{+0.11}_{-0.10}$	

[NIM A 1055 (2023) 168550]

Backgrounds in Belle-II

Measured 16 June 2021

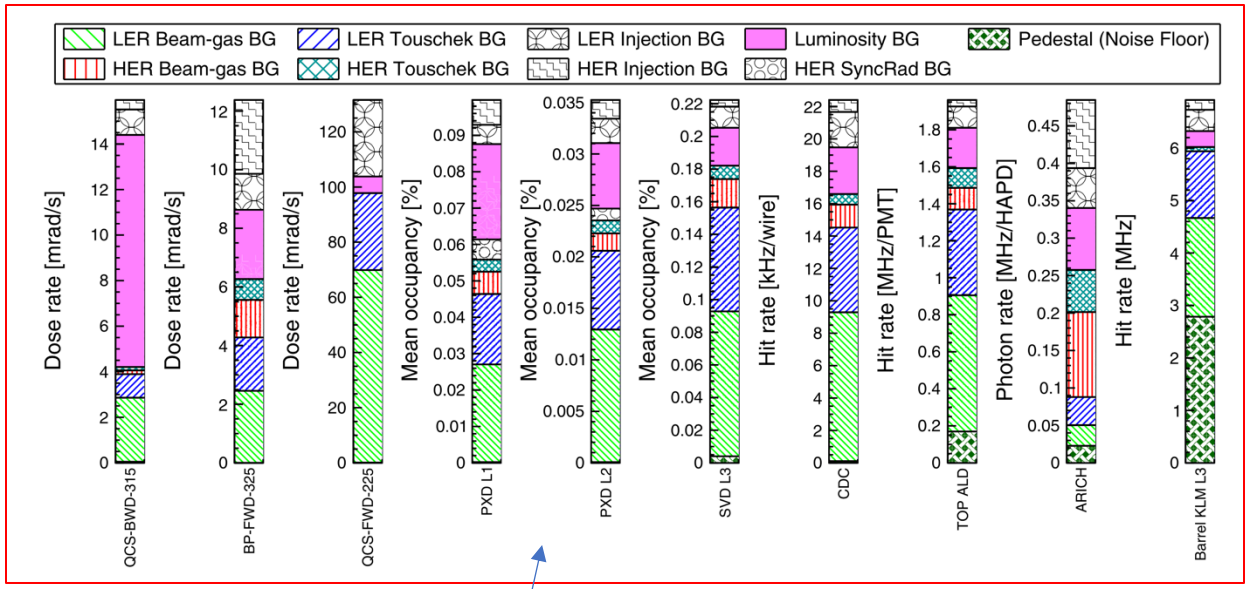

Extrapolation to L = 2.8 x 10^{35} $cm^{-2}s^{-1}$

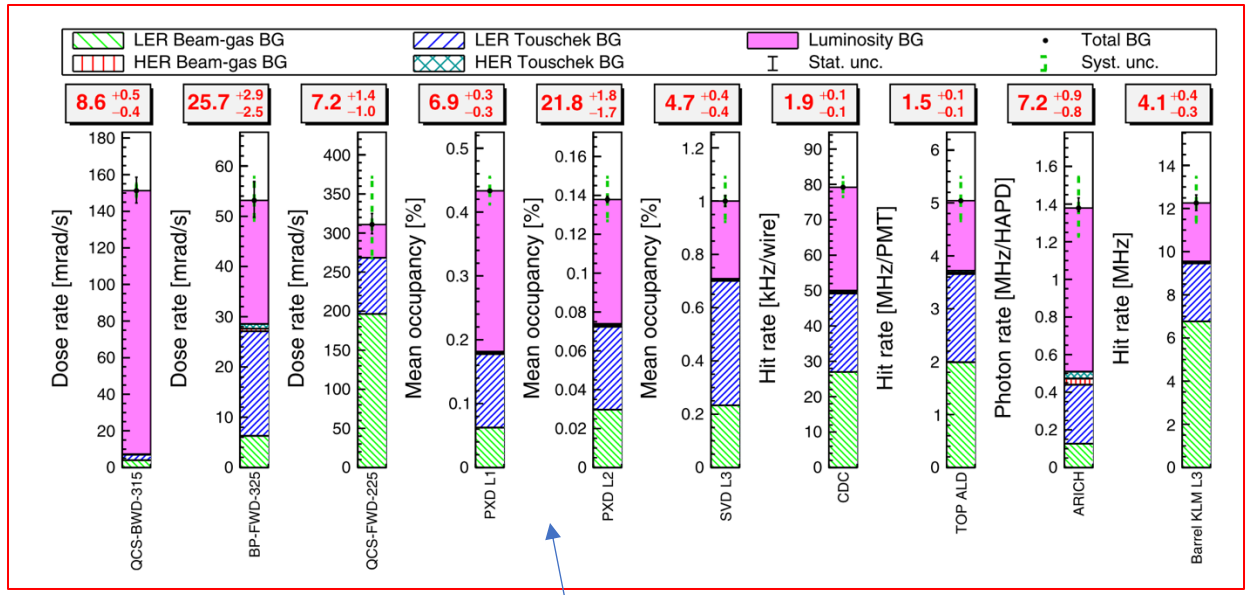

[NIM A 1055 (2023) 168550]

Initial conditions in the vertex detector:
beam gas & **Touschek**

- SVD and fully-equipped PXD mounted around modified beam pipe (Au coating, cooling)

Pixel detector @ full Lumi:
Luminosity & **Touschek**

SuperKEKB backgrounds experience

Major upgrades of LS1 (June 2022- Jan 2024) for backgrounds mitigation and reach full $\mathcal{L}$

- Replacement of damaged collimator heads on both rings
- IR radiation shield modifications
- QCS-R cryostat vacuum leak
- Non-linear collimator in LER
- Aperture enlargment of injection channel
- Installation of monitors for sudden beam loss events (e.g. beam loss monitors, bunch oscillation monitors)

Sudden beam loss

- Beam loss that occus suddenly within 1 (10 μs) or 2 turns without clear (large) precursory phenomena.
- The cause is still unclear.
- A significant percentage of the beam is lost before the beam abort. Harmful for vacuum components and detector, especially innermost detector (PXD, SVD).
- Damage to collimator heads and other accelerator components
- Quench of the final focus quadrupole magnet systems (QCS)
- Large backgrounds to the Belle-II detector
- Challenges to store higher beam current due to frequent beam abort

SuperKEKB continuous injection background

- Beam currents reached 1400 mA (half the design)
- permanent injection up to 25 Hz per ring:
  - single or double bunch top-up
  - injected bunch creates background spikes
  - every 10 μs for a few ms
  - detectors stay active during injection
  - **first 0.5 ms masked out in trigger (deadtime)**
  - pixel detector always integrates over 2 turns

Pixel detector hits during top-up injection

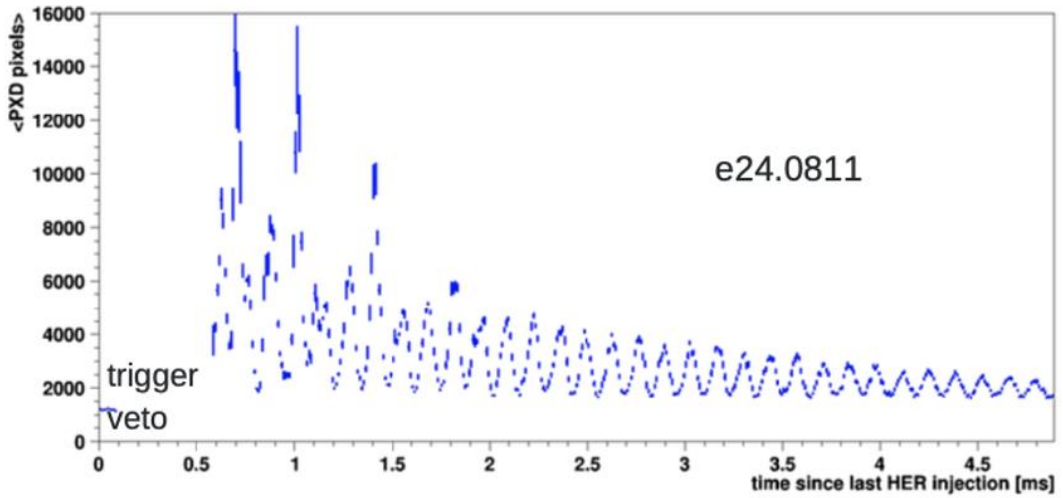

At FCC-ee: preference to longitudinal injection to prevent the SR fans produced by the off-axis injected beam
The effect of injection backgrounds on vertex detector should be smaller, to be studied (also due to a smaller frequency 0.1 Hz)

FCC-ee layout

Double ring e+e- collider with 91 km circ.

Common footprint with FCC-hh, except around IPs

Perfect 4-fold super-periodicity allowing 2 or 4 IPs; large horizontal crossing angle 30 mrad, crab-waist collision optics

Synchrotron radiation power 50 MW/beam at all beam energies

Top-up injection scheme for high luminosity

Requires booster synchrotron in collider tunnel and 20 GeV e+/e- source and linac

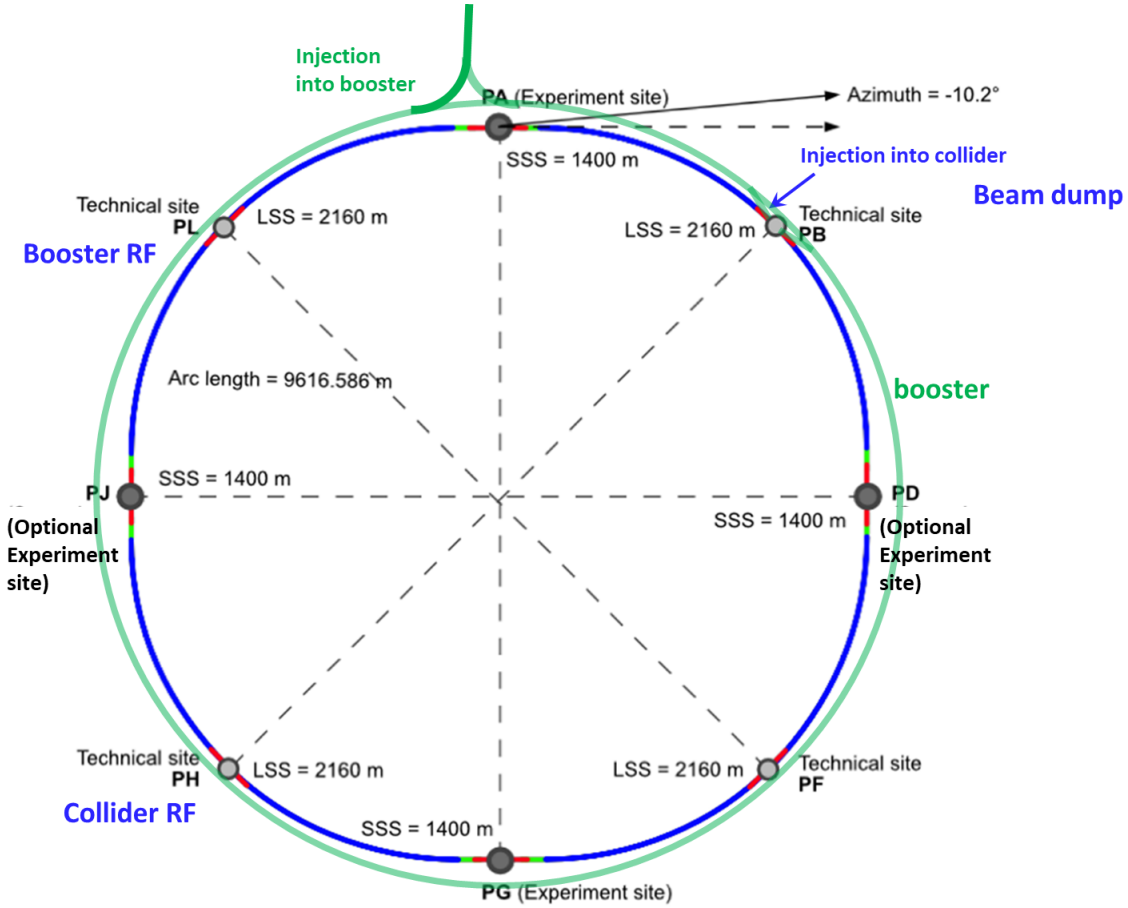

FCC-ee main machine parameters

horizontal crossing angle 30 mrad = 1.7 deg

Parameter	Z	WW	H (ZH)	ttbar
beam energy [GeV]	45.6	80	120	182.5
beam current [mA]	1270	137	26.7	4.9
number bunches/beam	11200	1780	440	60
bunch intensity [10^{11}]	2.14	1.45	1.15	1.55
SR energy loss / turn [GeV]	0.0394	0.374	1.89	10.4
total RF voltage 400/800 MHz [GV]	0.120/0	1.0/0	2.1/0	2.1/9.4
long. damping time [turns]	1158	215	64	18
horizontal beta* **[m]**	0.11	0.2	0.24	1.0
vertical beta* [mm]	0.7	1.0	1.0	1.6
horizontal geometric emittance [nm]	0.71	2.17	0.71	1.59
vertical geom. emittance [pm]	1.9	2.2	1.4	1.6
horizontal rms IP spot size [μm]	9	21	13	40
vertical rms IP spot size [nm]	36	47	40	51
beam-beam parameter ξ_x / ξ_y	0.002/0.0973	0.013/0.128	0.010/0.088	0.073/0.134
rms bunch length with SR / BS [mm]	5.6 / 15.5	3.5 / 5.4	3.4 / 4.7	1.8 / 2.2
luminosity per IP [10^{34} $cm^{-2}s^{-1}$]	140	20	≥5.0	1.25
total integrated luminosity / IP / year [ab^{-1}/yr]	17	2.4	0.6	0.15
beam lifetime rad Bhabha + BS [min]	15	12	12	11
	4 years 5 x 10^{12} Z LEP x 10^5	2 years > 10^8 WW LEP x 10^4	3 years 2 x 10^6 H	5 years 2 x 10^6 tt pairs
Bunch spacing	20 ns			

Design and parameters dominated by the choice to allow for 50 MW synchrotron radiation per beam.

C = 90.7 km

50 ps rms

FCC-ee Interaction Region

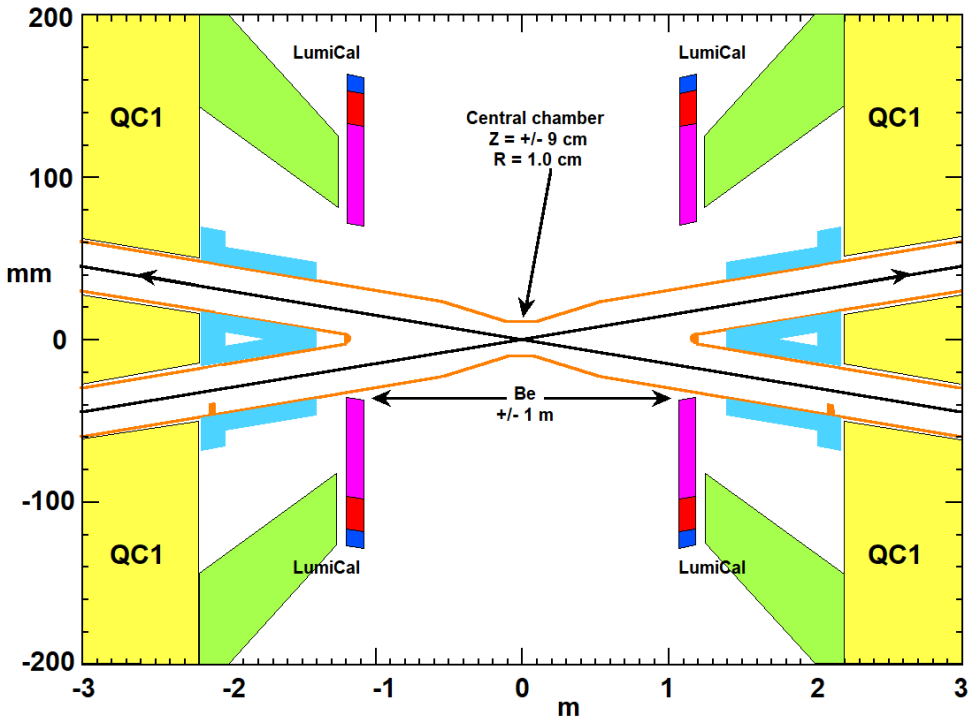

FCC-ee IR layout.

L*, is 2.2 m. The 10 mm central radius is foreseen for ± 9 cm from the IP, and the two symmetric beam pipes with radius of 15 mm are merged at 1.2 m from the IP.

B(detector) = 2 T

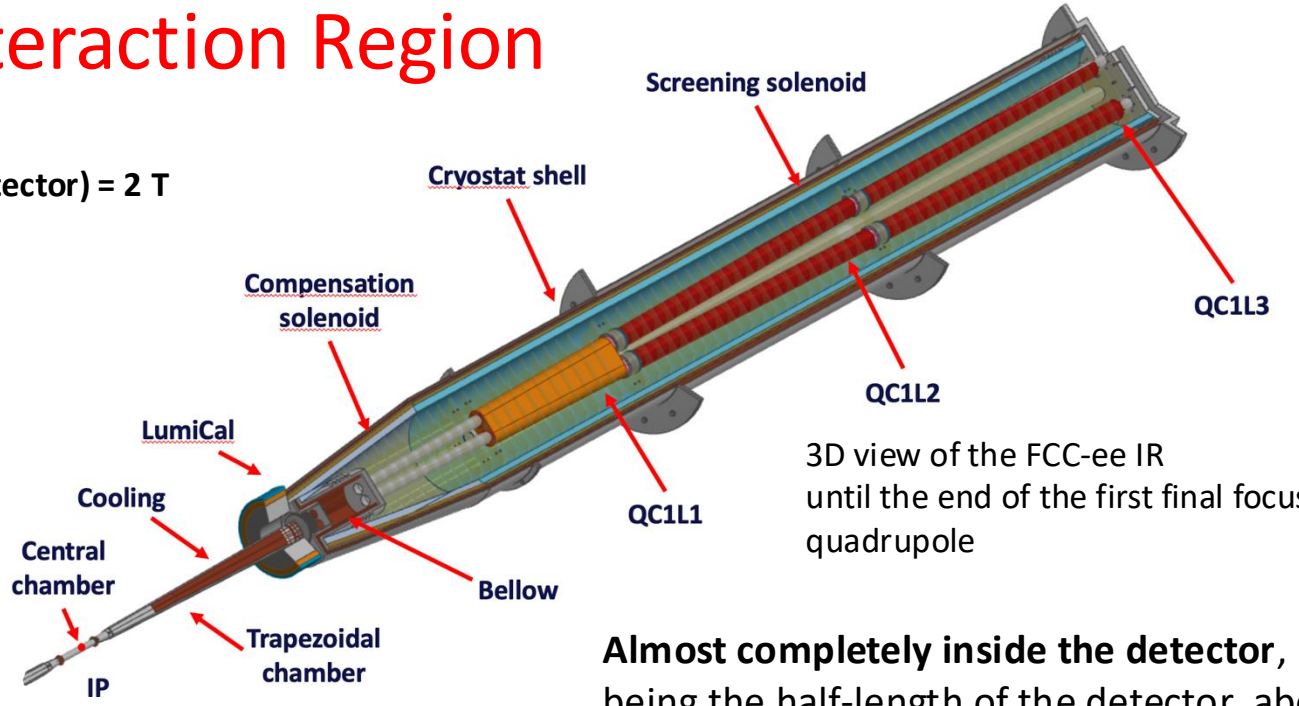

3D view of the FCC-ee IR until the end of the first final focus quadrupole

Almost completely inside the detector, being the half-length of the detector about 5.2 m and the end of QC1L3 at about 5.6 m.

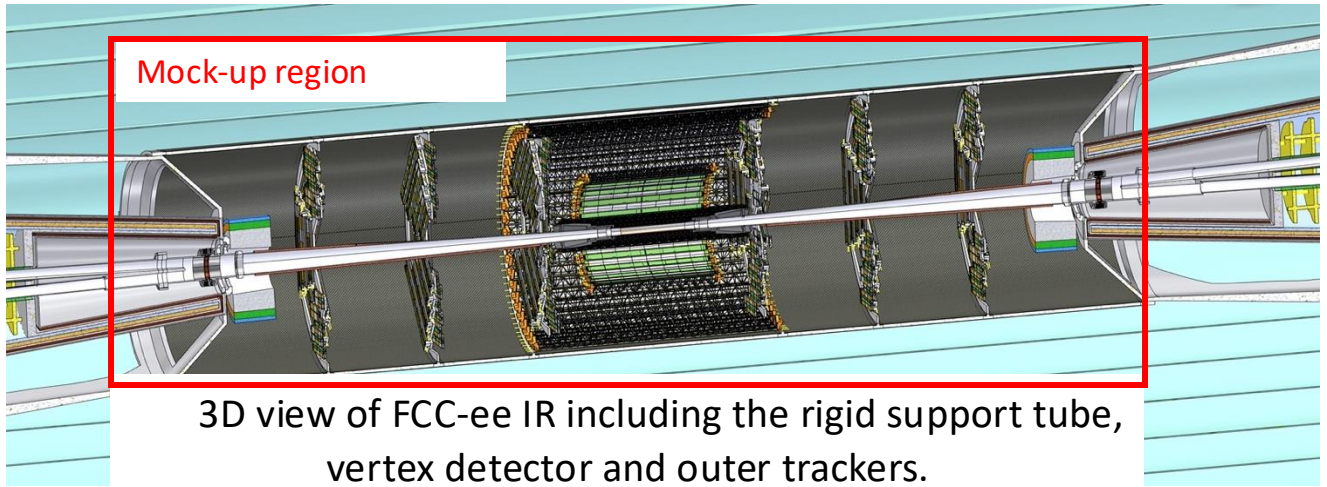

3D view of FCC-ee IR including the rigid support tube, vertex detector and outer trackers.

Low-impedance IR vacuum chamber

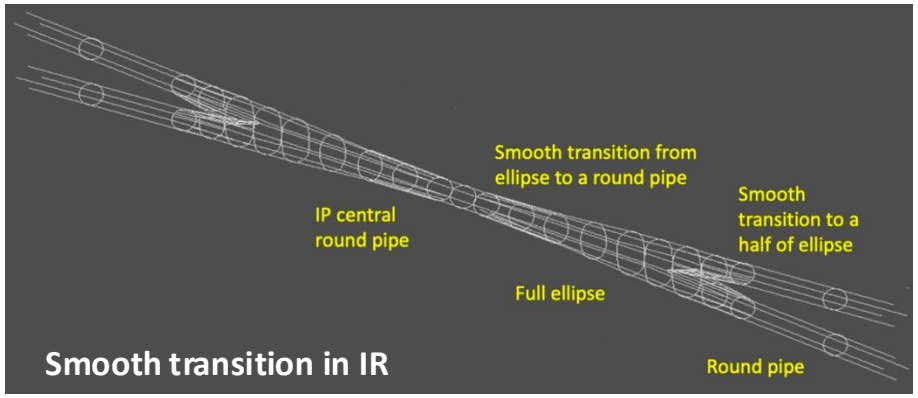

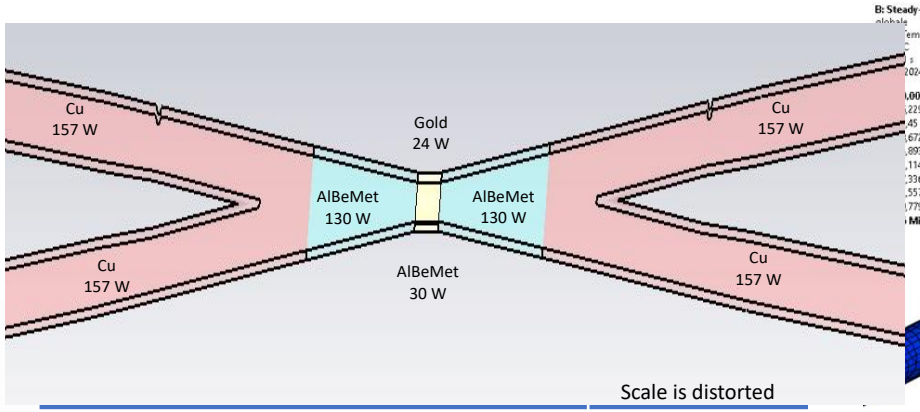

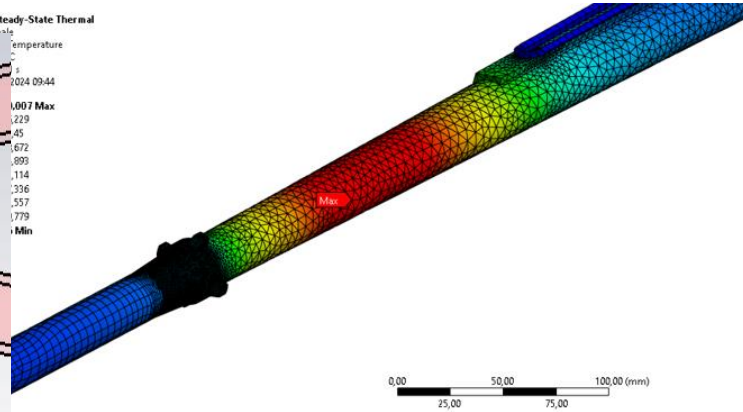

Scale is distorted

beam energy [GeV]	45
beam current [mA]	1280
number bunches/beam	1000
rms bunch length with SR / BS [mm]	4.38 / 14.5
bunch spacing [ns]	32

	conical chamber	central chamber
coolant	water	paraffin
T_{max} (chamber)	50°C	29°C
T_{max}(coolant)	18 °C	20 °C

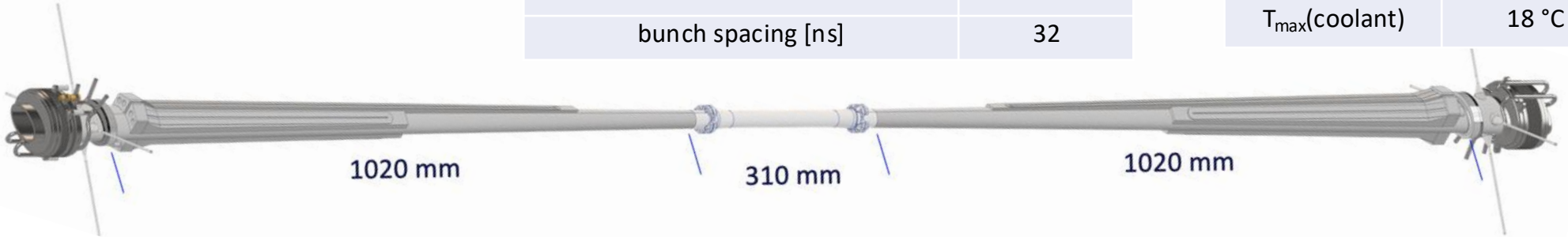

Study and optimization of the material budget for the beam pipe has been performed and is in progress. LumiCal requirements and material budget minimization considered, also comparing Be with AlbeMet.

Vertex detector design and integration

Integration with the machine elements being developed
Services integration and cooling being finalised:
$\Delta T < 10^{o}C \; - 1.5 \mu m \; RMS \; displacement$

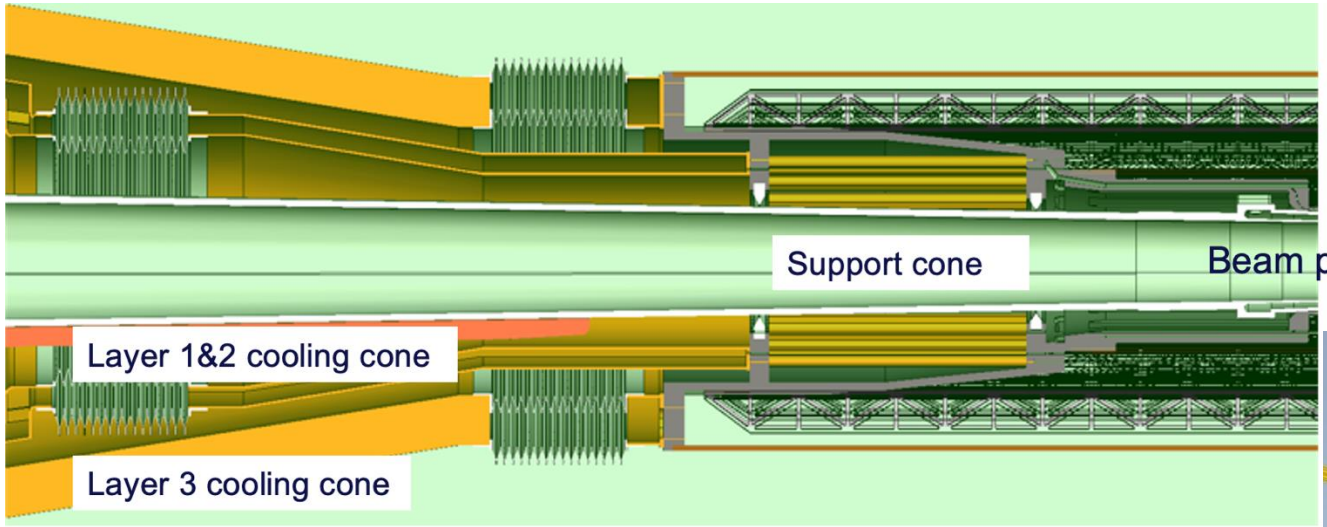

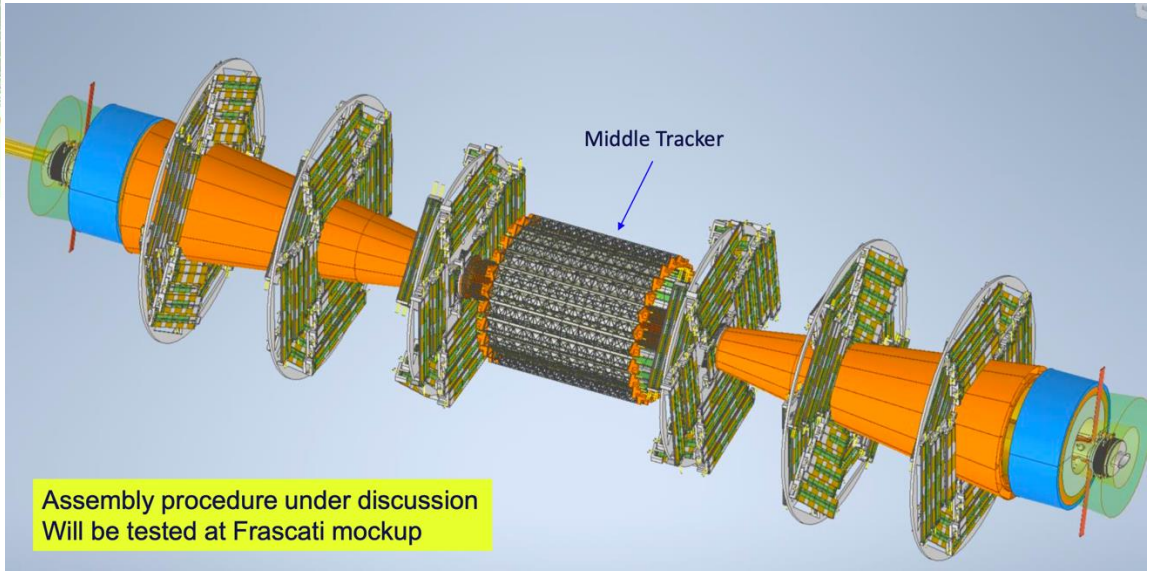

Spatial constraints

To achieve the required performance, it is necessary to have **low material budget** within the LumiCal acceptance (between **50 mrad** and **105 mrad** centered on the outgoing beam pipe).

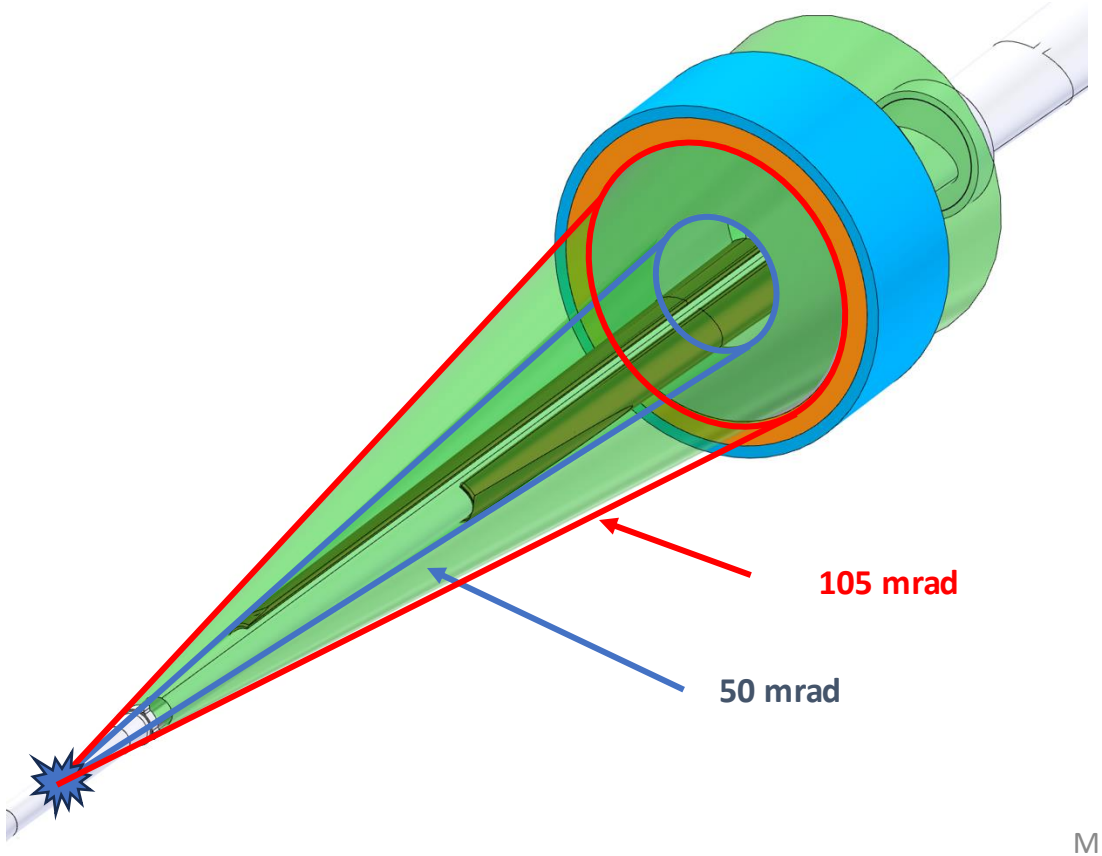

Every component of the MDI must stay inside the **100 mrad detector acceptance** cone.

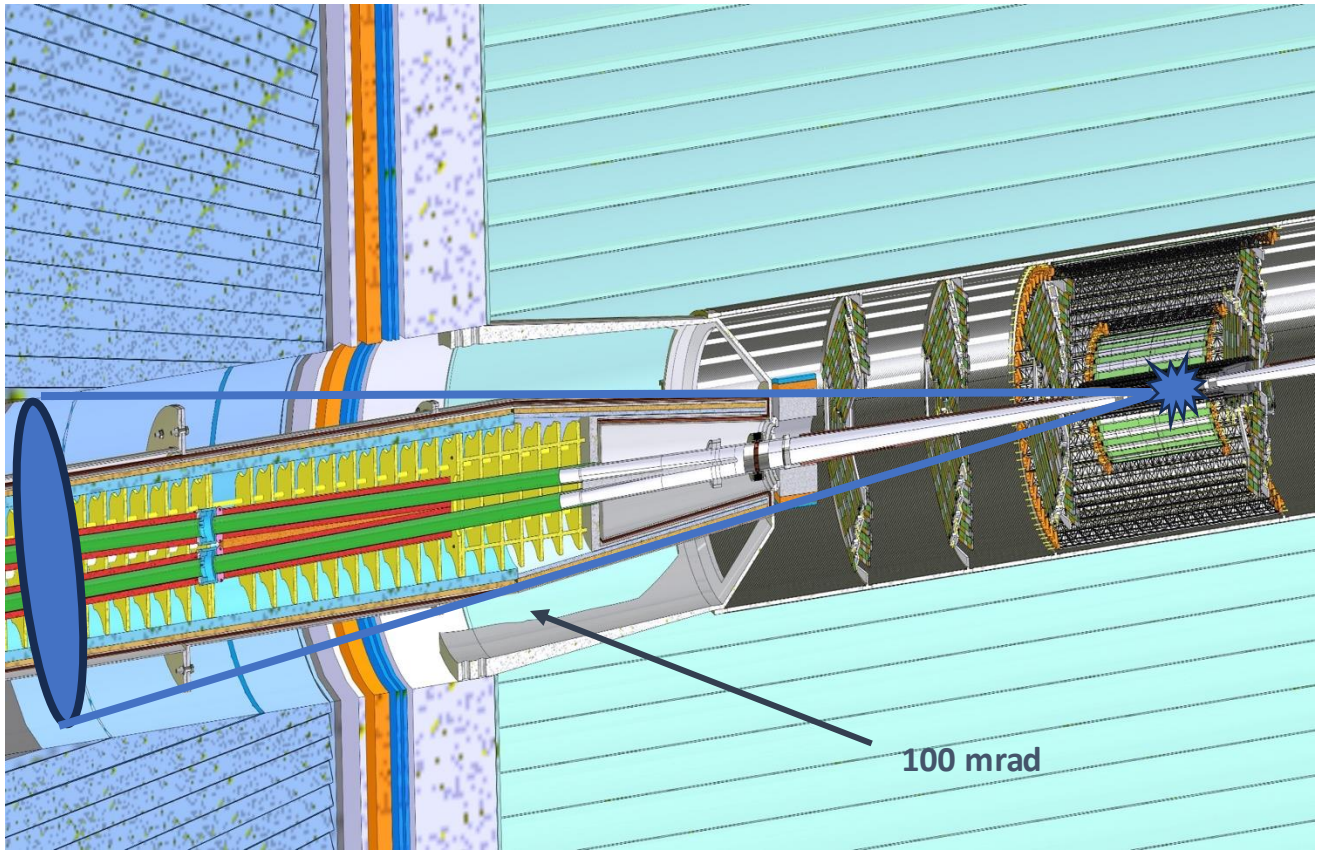

FCC-ee engineered Interaction Region

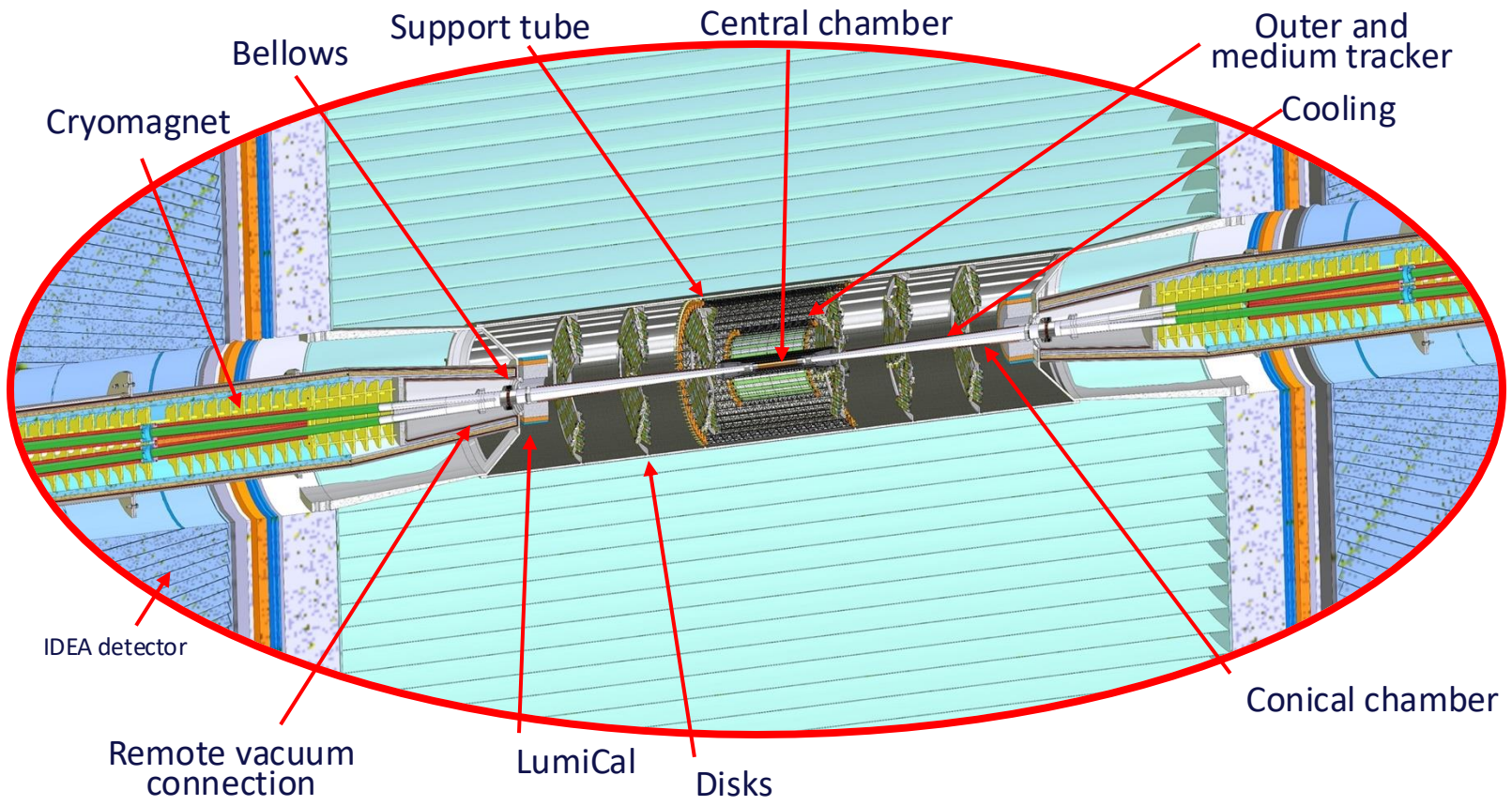

Ref: M B , F. Palla, et al., *Mechanical model for the FCC-ee MDI,* EPJ+ Techn. and Instr., https://doi.org/10.1140/epjti/s40485-023-00103-7

M. B. et al., Progress in the design of the future circular collider FCC-ee interaction region, IPAC24, 18-25 May 2024, Nashville, USA, DOI: 10.18429/JACoW-IPAC2024-TUPC67

LumiCal constraints & requirements

- **Goal: absolute luminosity measurement 10^{-4} at the Z**

- **Standard process Bhabha scattering**
  - Bhabha cross section 12 nb at Z-pole with acceptance **62-88 mrad** wrt the outgoing pipe
  - Requires **50-120 mrad clearance to avoid spoiling the measurement**
  - The LumiCals are centered on the outgoing beamlines with their faces perpendicular to the beamlines
  - Requirements for alignment
    - few hundred μm in radial direction
    - few mm in longitudinal direction

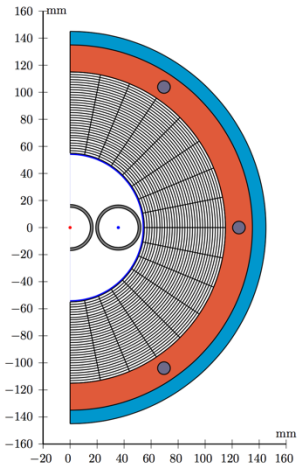

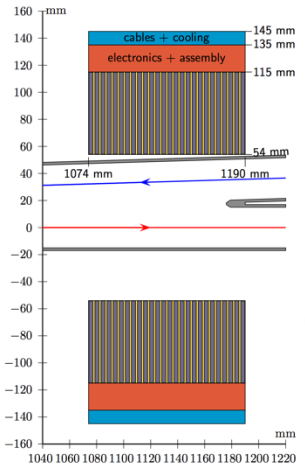

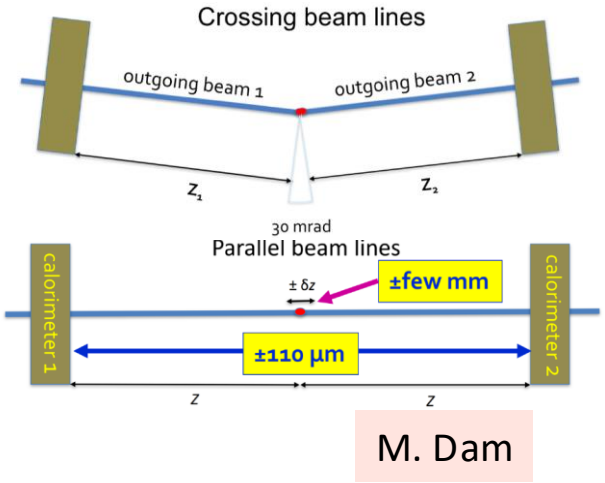

M. Dam

Lumical integration:

- **Asymmetrical cooling system** in conical pipe to provide angular acceptance to lumical

- **LumiCal held by a mechanical support structure**

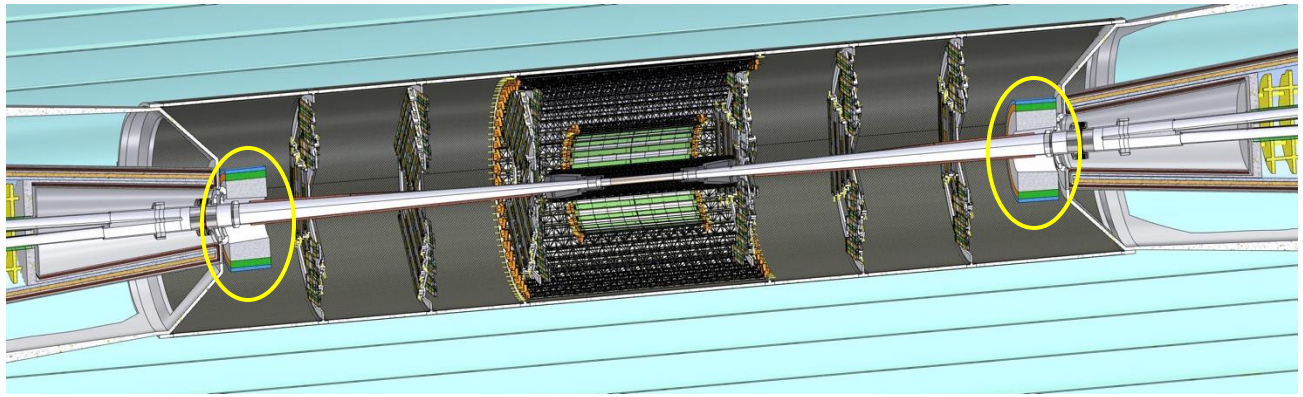

FCC-ee Beamstrahlung Radiation

Radiation from the colliding beams is very intense O(400 kW) at Z

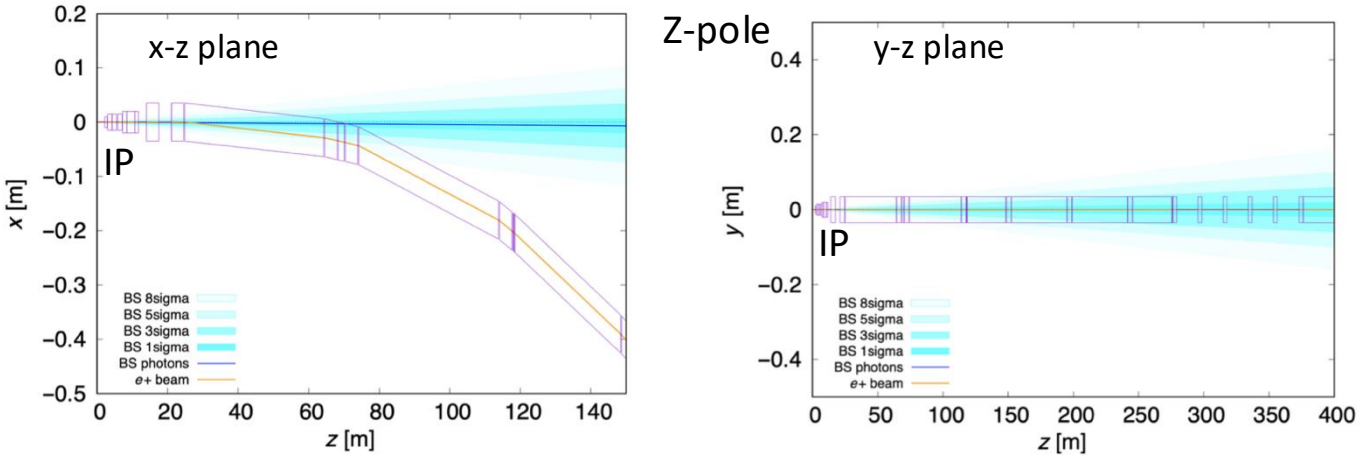

PRAB 26, 111002 (2023), link

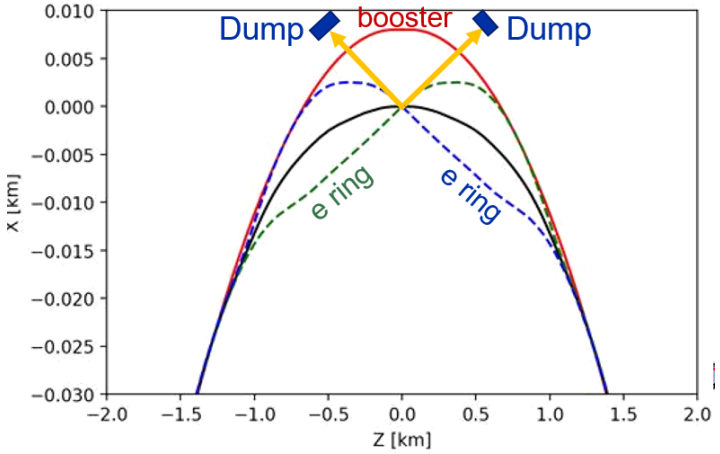

Dump placed 500 m from IP in order to have enough separation from booster / collider
(space for shielding)

High-power beam dump needed to dispose of these BS photons **+ all the radiation from IR**: FLUKA simulation ongoing

- Different targets as dump absorber material are under investigation
- Shielding needed for equipment and personnel protection for radiation environment

Radiation dose from Fluka simulation in the FCC-ee MDI area

Beamstrahlung dump

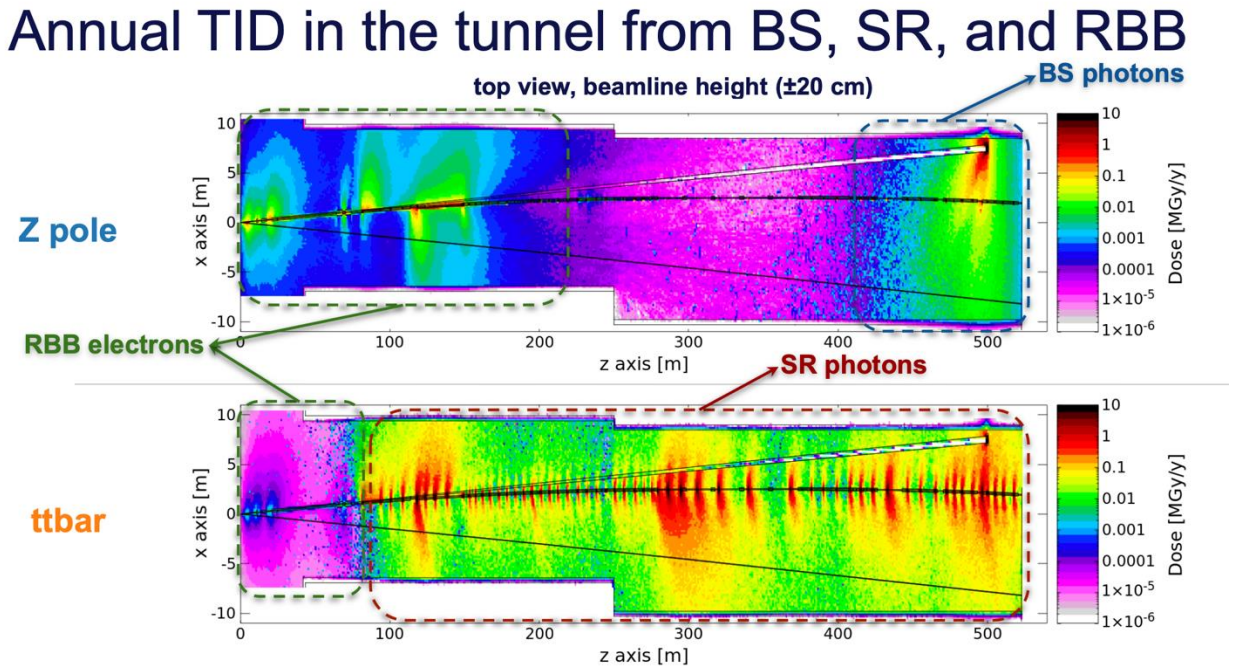

Power deposition in FFQs SC coils from radiative Bhabhas

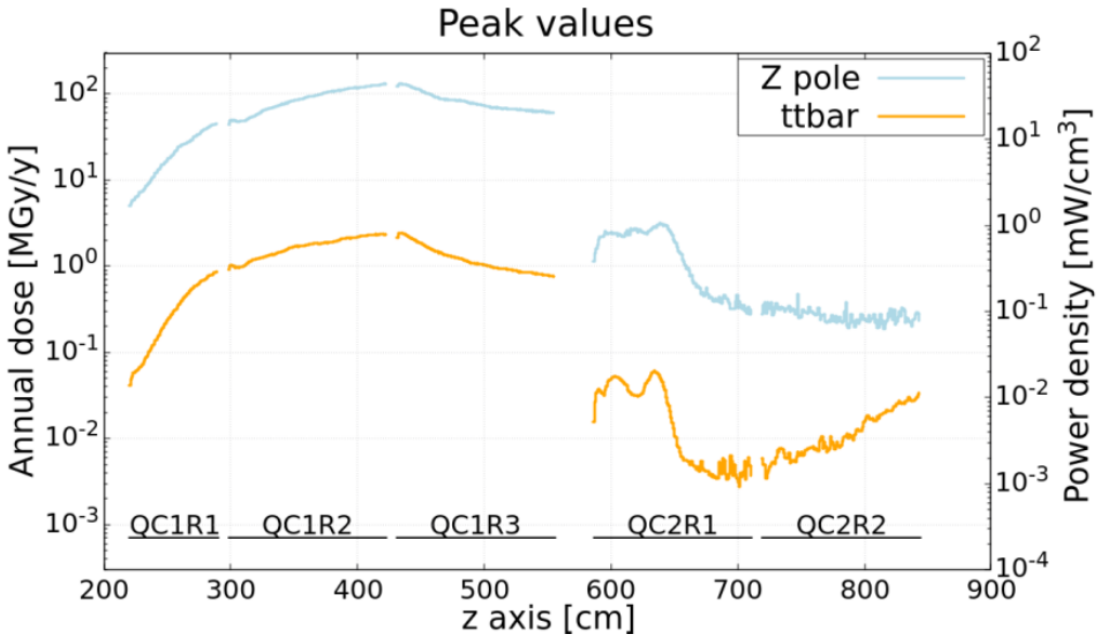

TOTAL POWER DEPOSITED

	Z pole	ttbar
QC1R1	0.30 W	3.4 mW
QC1R2	1.54 W	20.4 mW
QC1R3	2.00 W	29.7 mW
QC2R1	0.20 W	1.9 mW
QC2R2	0.04 W	1.8 mW

5 mm of tungsten ensures

- peak dose: 3 MGy/y
- peak power density deposition: 1 mW/cm^3

Courtesy Alessandro Frasca

Challenge of the FCC-ee IR magnet system

Preferred option for the IR cryostat

IR QC1 and QC2 in different cryostats but one integrated raft (not to scale)

Need to make space for cryogens, leads, and cantilever supports.

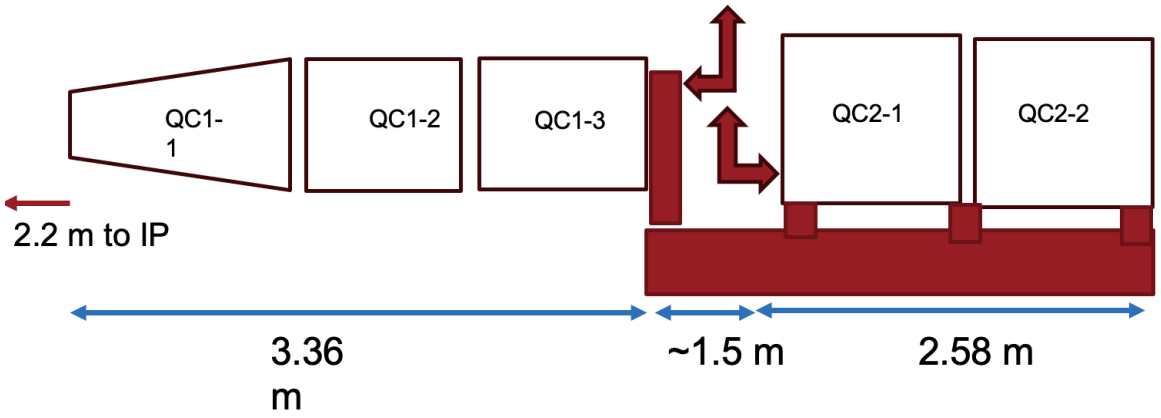

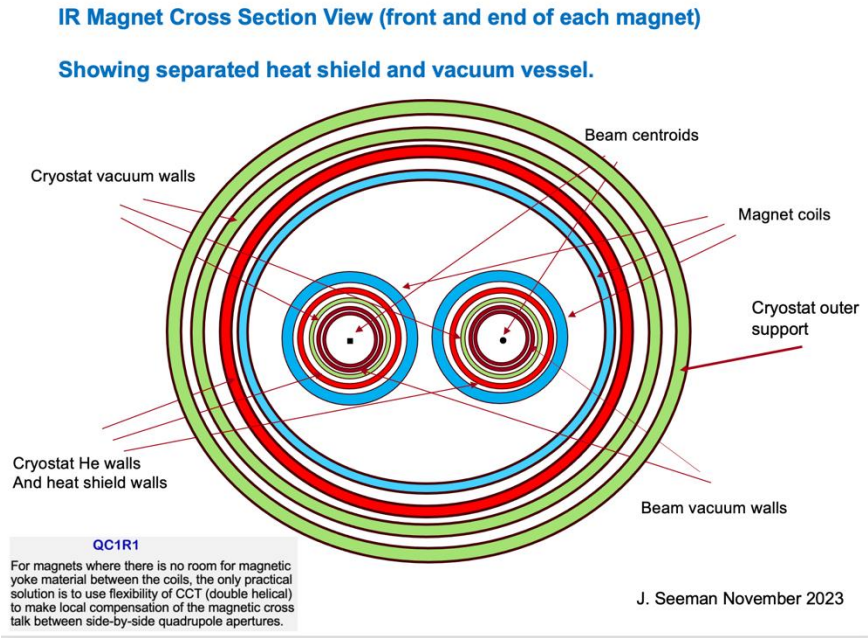

- Radial distance from detector solenoid axis to beam axis:
- conservative/less conservative approach

Courtesy J. Seeman

Solenoid compensation scheme

- Baseline: local compensation (CDR)
- Alternative: non-local compensation https://doi.org/10.18429/JACoW-IPAC2024-TUPC68

Cryogenic approaches for superconducting magnets in the FCC-ee IR

- A preliminary assessment of **local heat extraction** options for the IR magnet QC1 has been carried out, for present **level of heat load O(100 W)** there are **no showstoppers at either 1.9 K, 4.5-5 K or 10-20 K**
- **Aside from local heat extraction, the choice of operating temperature will have a profound impact on the overall MDI/IR zone** → if unavoidable, operation at **1.9 K needs to be justified**
  - **1.9 K** operation is **4x more power consuming than at 4.5 K**, 20x more than at 10-20 K
  - **Cryo distribution line in the tunnel is larger for 1.9 K** operation due to pumping line
  - **Underground cavern space** for cold compressors is a necessity for **1.9 K**
- Integration in the MDI/IR is challenging, would be facilitated by having common temperature levels between different magnets and using cold BPMs
- **Static heat loads** can add up to a significant percentage of the radiation-induced load, once design has matured an estimation should be planned
- **The choice will be driven by its impact on costing, availability, integration constraints**

P. Tavares Borges de Sousa (CERN) link,
MDI Workshop, Frascati 16-17 Nov. '23 https://agenda.infn.it/event/37720/

FCC-ee IP backgrounds

Radiative Bhabha

BBBrem/GuineaPig & SAD/MADX

- characterization of photons
- beam losses from spent beam

Mostly unavoidable and proportional to the luminosity, only the multiturn losses can be mitigated with collimators.

Synchronous with the interaction

Beamstrahlung

GuineaPig /BBWS & SAD/MADX

- multiturn tracking of spent beam – beam losses
- characterization of photons
  - intense radiation collinear with the core of the beam→ BS photon dump
  - **e^+e^- pairs** *GuineaPig, G4 into detector*

    Incoherent Pairs Creation**: Dominant** (real or virtual photon scattering)

    Coherent Pairs Creation: **Negligible (**Photon interaction with the collective field of the opposite bunch, strongly focused on the forward direction)
  - $\gamma\gamma$ **to hadrons** combination of *GuineaPig and Phythia, G4*

    Small effect (Direct production of hadrons, or indirect, where one or both photons interact hadronically)

FCC-ee Single Beam effects

- Synchrotron Radiation
  - main driver of the IR design, studied with various tools (e.g. BDSIM)
  - SR collimators and masks implemented, effect of non-Gaussian tails on the mask tip & effect during top-up injection studied
- Inelastic/ Elastic beam-gas scattering
  - First studies done for the CDR
  - First multiturn tracking and loss maps with X-suite with realistic pressure maps.
- Thermal photons
  - Only first studies done for the CDR
  - Implementation in X-suite planned.
- Touschek
  - Expected not to be relevant due to high beam energy, but to be studied, especially at the Z-pole, due to the dense beam (high bunch current and low emittance)

CEPC MDI

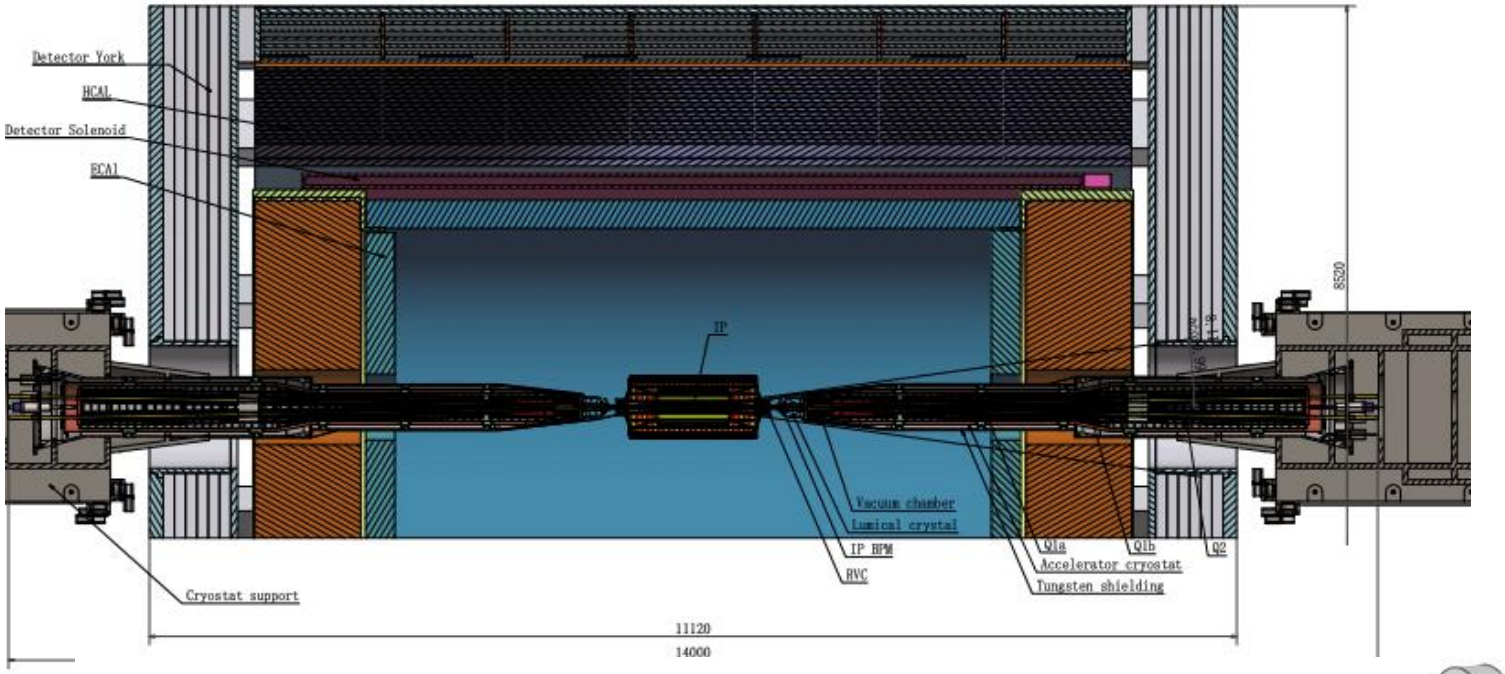

B(detector)=3 T (2T for Z-pole)
L*=1.9 m
crossing angle = 33 mrad

Central Be beam pipe radius = 20 mm
with double layer for liquid cooling

SR masks and gold coating

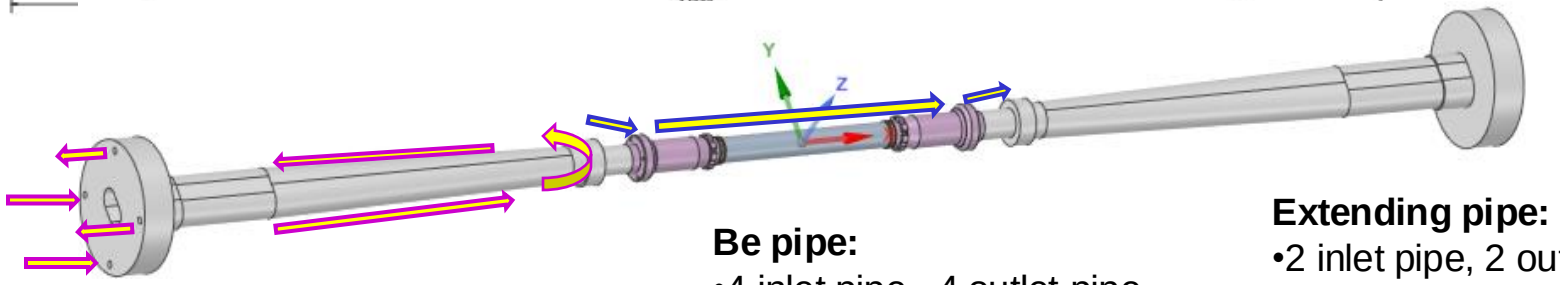

Extending pipe:
- 2 inlet pipe, 2 outlet pipe
- Coolant: water
- Inlet temperature: 20℃
- Inlet velocity: 0.5m/s（1.7L/min）

Be pipe:
- 4 inlet pipe, 4 outlet pipe
- Coolant: water
- Inlet temperature: 20℃
- Inlet velocity: 0.5m/s（0.8L/min）

Extending pipe:
- 2 inlet pipe, 2 outlet pipe
- Coolant: water
- Inlet temperature: 20℃
- Inlet velocity: 0.5m/s（1.7L/min）

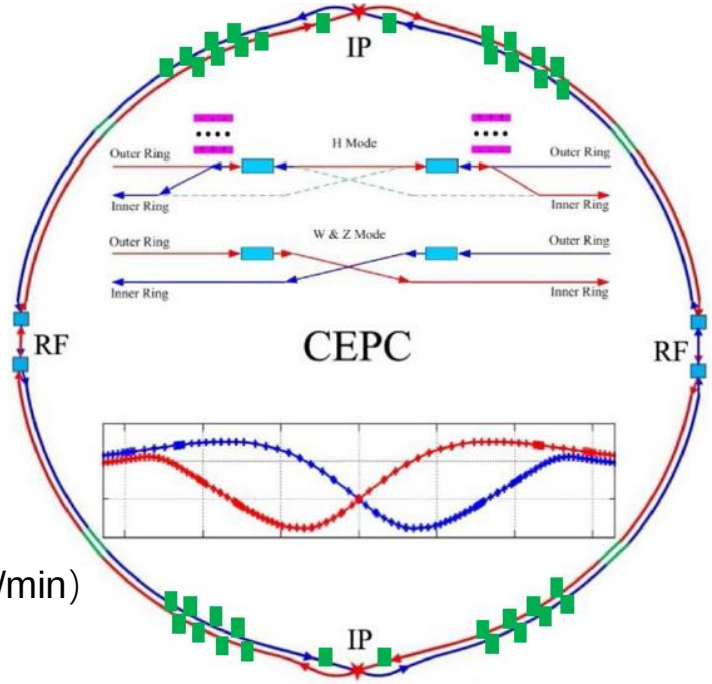

CEPC SC magnet support system

- After the optimization of the supports in the cryostat, the total weight of the cryostat and the devices inside is 2790 Kg.

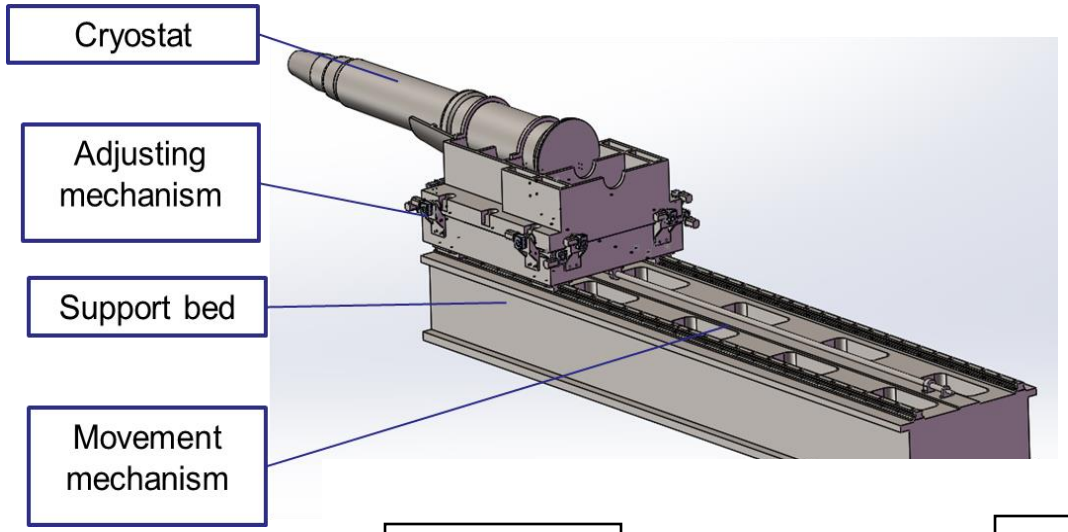

- The cryostat is about 5.6m long. The cantilever length is 5283mm.
- The resolution requirement of the adjusting mechanism < 5 μm.

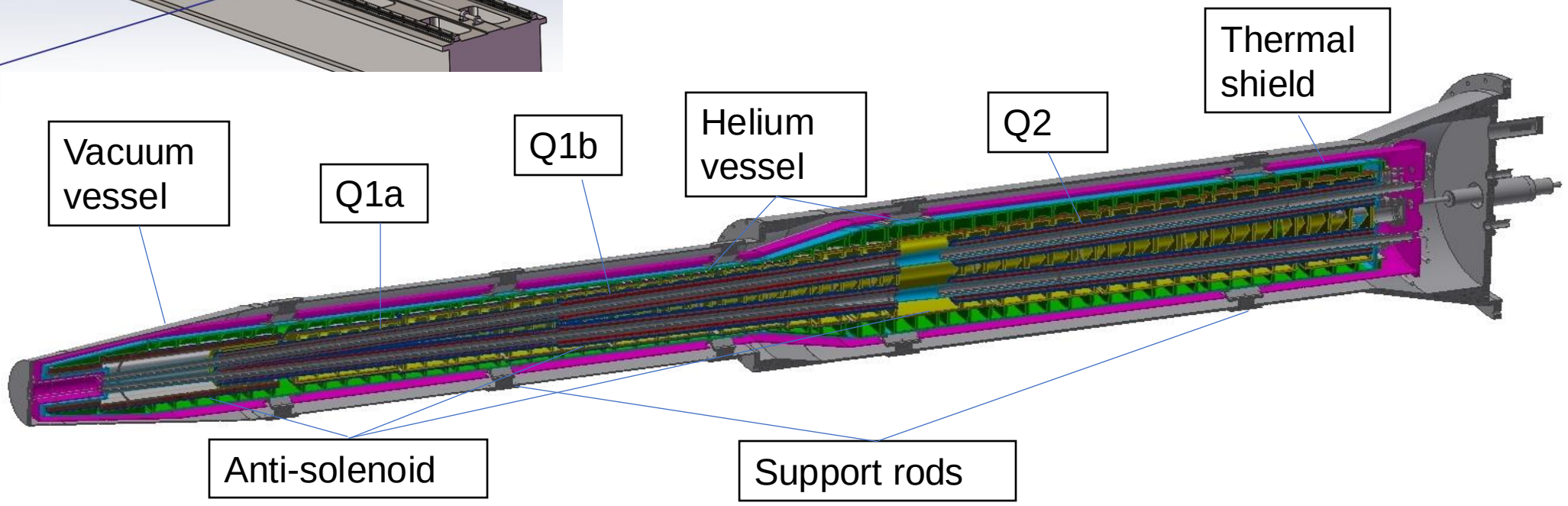

FCC-hh

	HL-LHC	FCC-hh
Cms energy [TeV]	14	100
Int. L., 2 det. [ab^{-1}]	6	30
Operation [years]	12	25
L [10^{34}cm^{-2}s^{-1}]	5	20-30
Circumference	26.7	97.75
Arc dipole field [T]	8	16
Bunch dist. [ns]	25	25
Backgr. events/bx	135	<1020
Bunch length [cm]	7.5	8
L* [m]	23	40

[CDR]

31 GHz of pp collisions

Pile-up 1000

4 THz of tracks

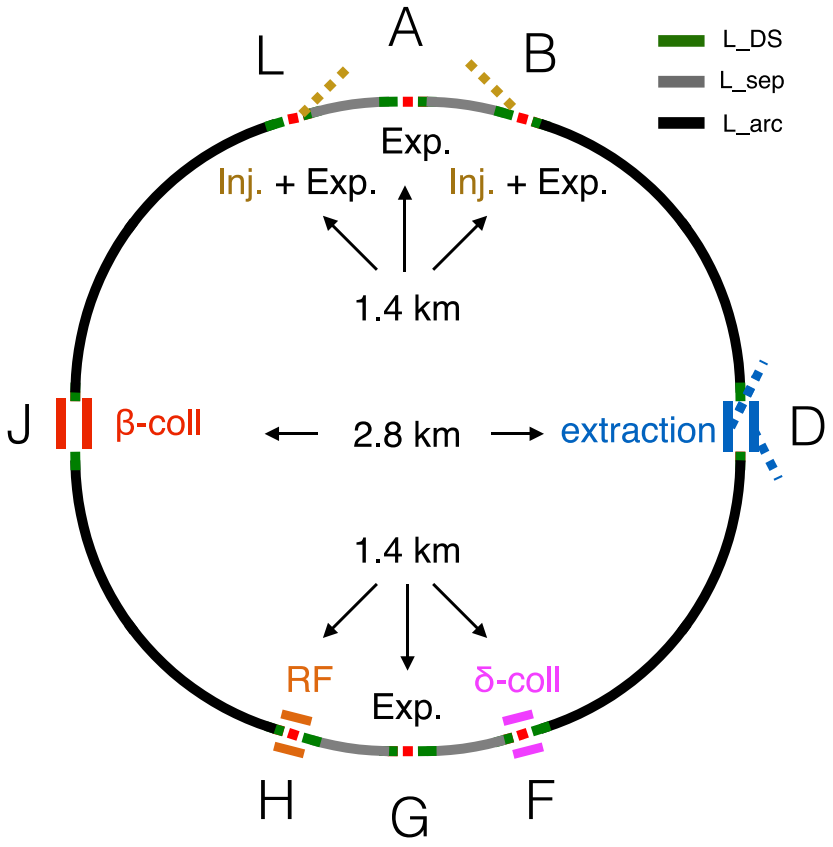

Two main IP's in A, G for both machines

Two High Luminosity IPs A/G

Two Lower Luminosity IPs L/B

Similar to layout at LHC

Unprecedented particle flux and radiation levels

10 GHz/cm2 charged particles

≈ 10^{18} cm^{-2} 1 MeV-n.eq. fluence for 30ab^{-1} (first tracker layer, fwd calo)

signal events from "Light" SM particles produced with increased forward boost

–> spreads out particles by 1-1.5 units of rapidity

FCC-hh MDI

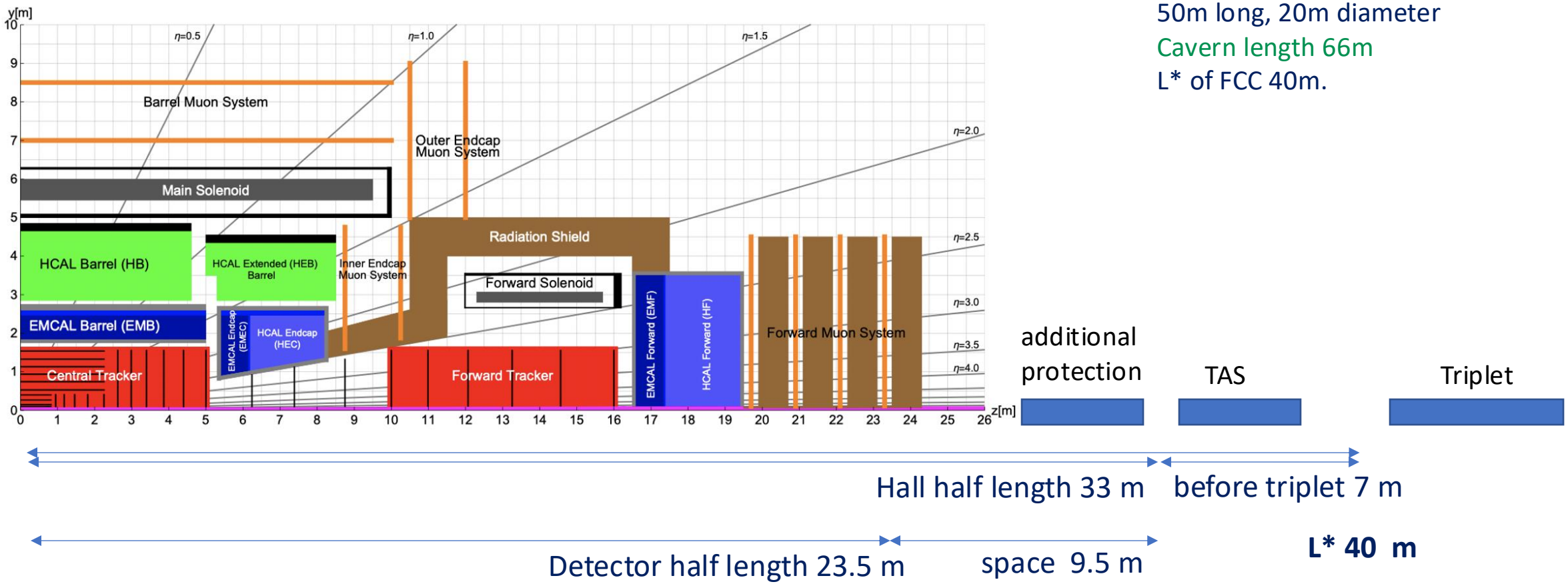

50m long, 20m diameter
Cavern length 66m
L* of FCC 40m.

500 kW power into detector and accelerator (CNGS target!)
radiation in magnets requires some improvements of radiation hardness, considered feasible

FCC-hh IR optics

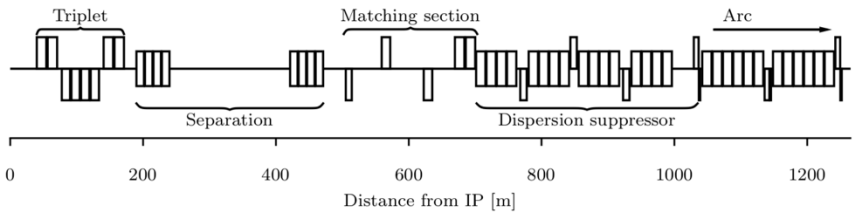

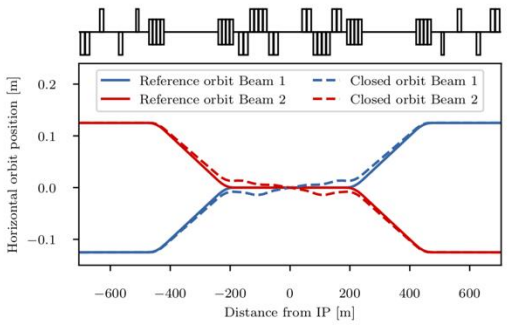

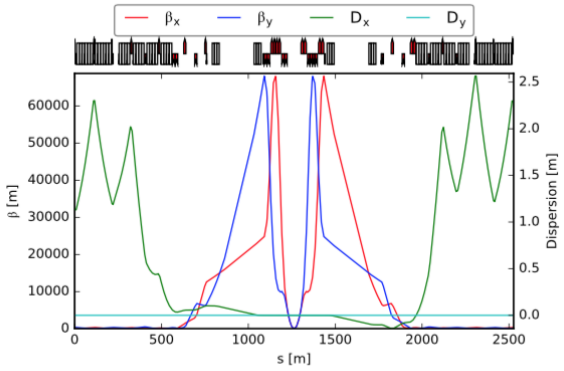

(a) Interaction region: LSS-PA-EXP & LSS-PG-EXP

- Design follows the structure of the LHC IR
- small β* at IP (∝1/√E): demanding IR optics design & large aperture in final focus triplet
- Challenge for magnet, protection design and collimation system (to intercept tail particles that could hit the triplet)
- 1.4 km required
- Final focus is a triplet (superconducting magnets) with a single aperture followed by normal conducting dipoles that separate the beams in individual aperture
- **Design of the final focus system is driven by energy deposition from collision debris from the IP**: short drift between IP and quad and large aperture in FF quads
- 20 m reserved for crab cavities

FCC-hh Reference Detector

- 4T, 10m solenoid, unshielded
- Forward solenoids, unshielded
- Silicon tracker
- Barrel ECAL LAr
- Barrel HCAL Fe/Sci
- Endcap HCAL/ECAL LAr
- Forward HCAL/ECAL LAr

50m length, 20m diameter
similar to size of ATLAS

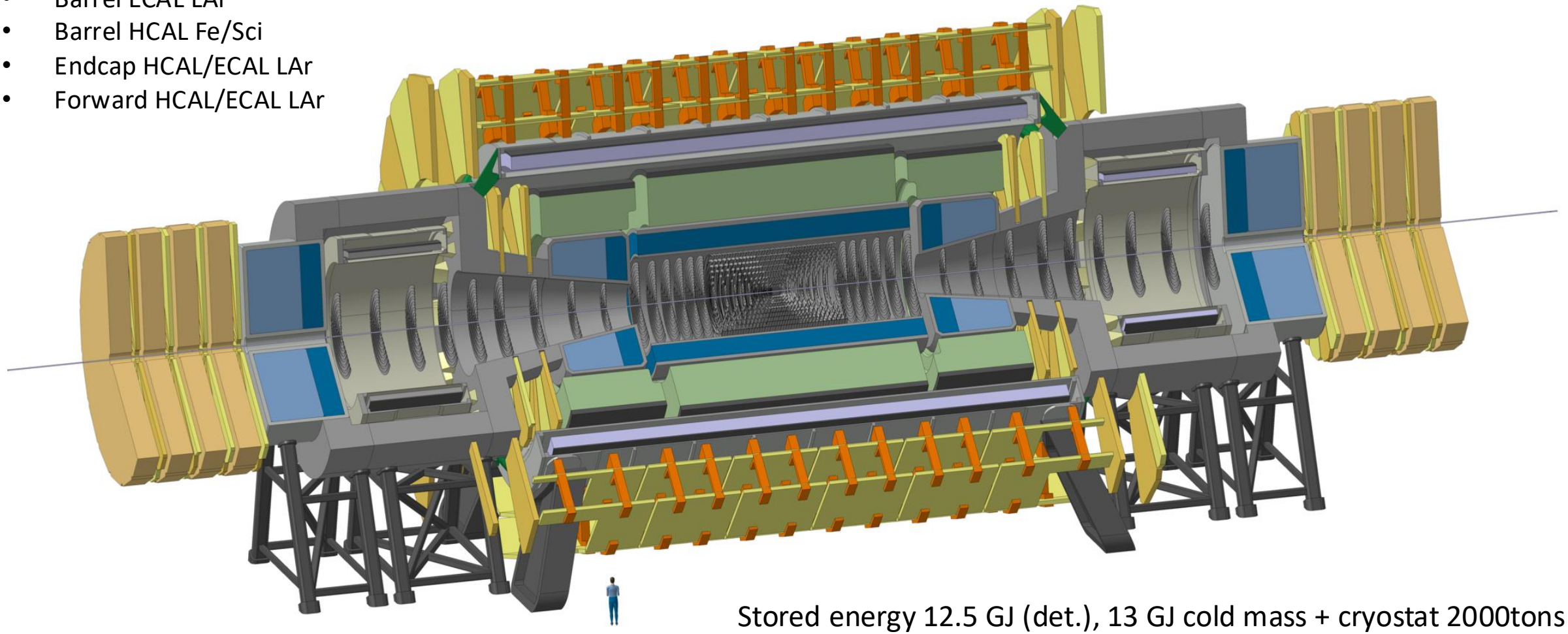

Stored energy 12.5 GJ (det.), 13 GJ cold mass + cryostat 2000tons

Comparison to ATLAS & CMS

ATLAS

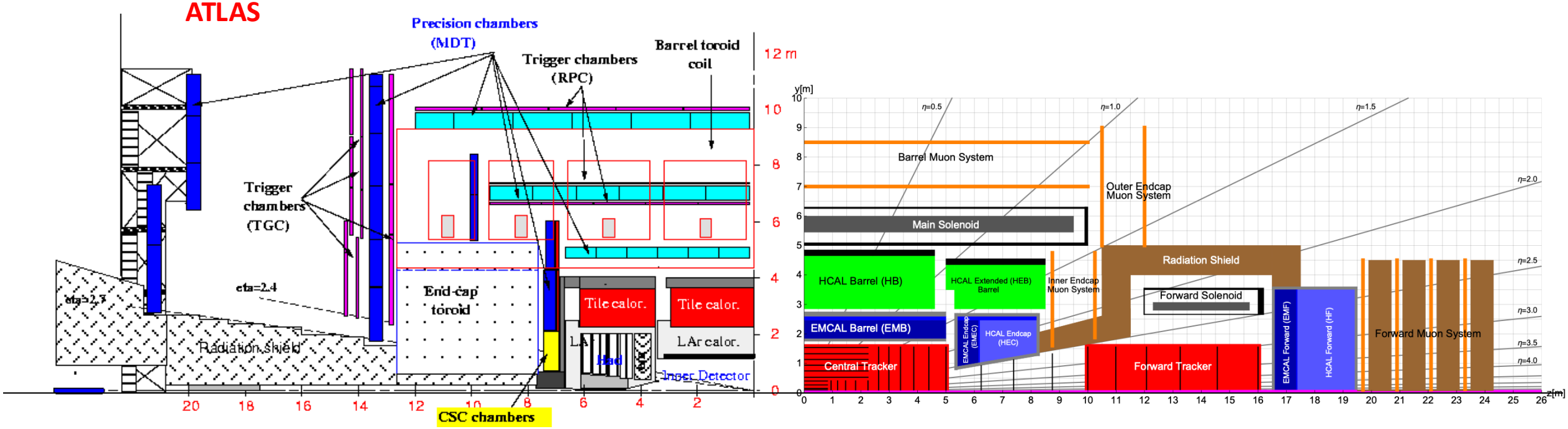

CMS

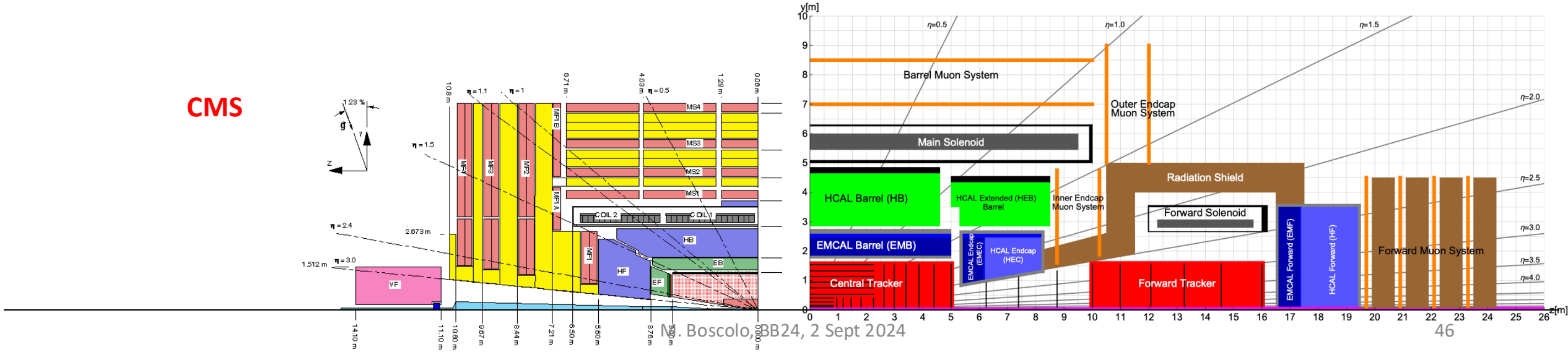

FCC-hh Radiation Studies for L=3x10^{35} cm^{-2}s^{-1} and 30 ab^{-1}

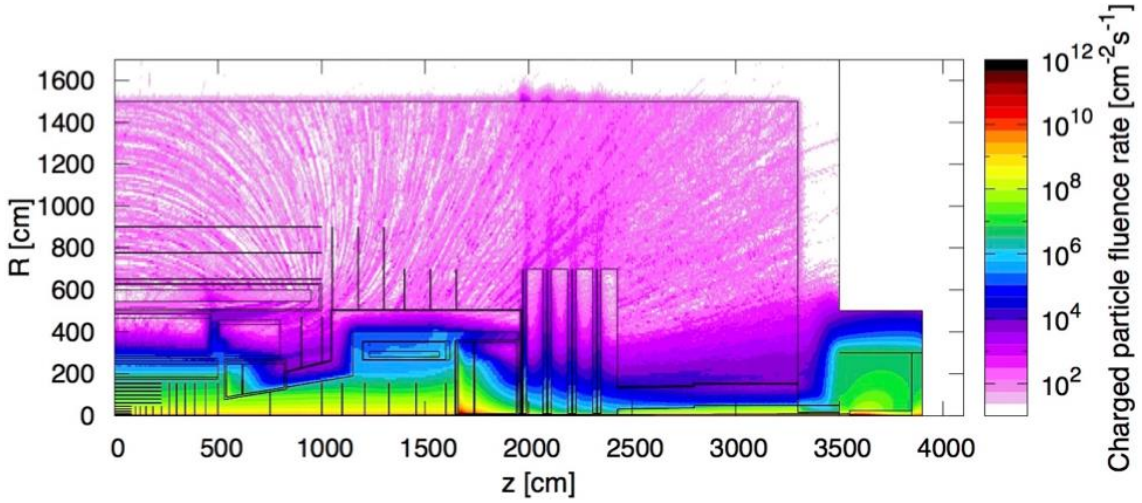

Maximum of 10kHz/cm^2 of charged particle rate in the Barrel and Forward Muon System, similar to HL-LHC Muon Systems.

In the tracker volume the charged particle rate is just a function of distance from the beampipe with rather small dependence on z.

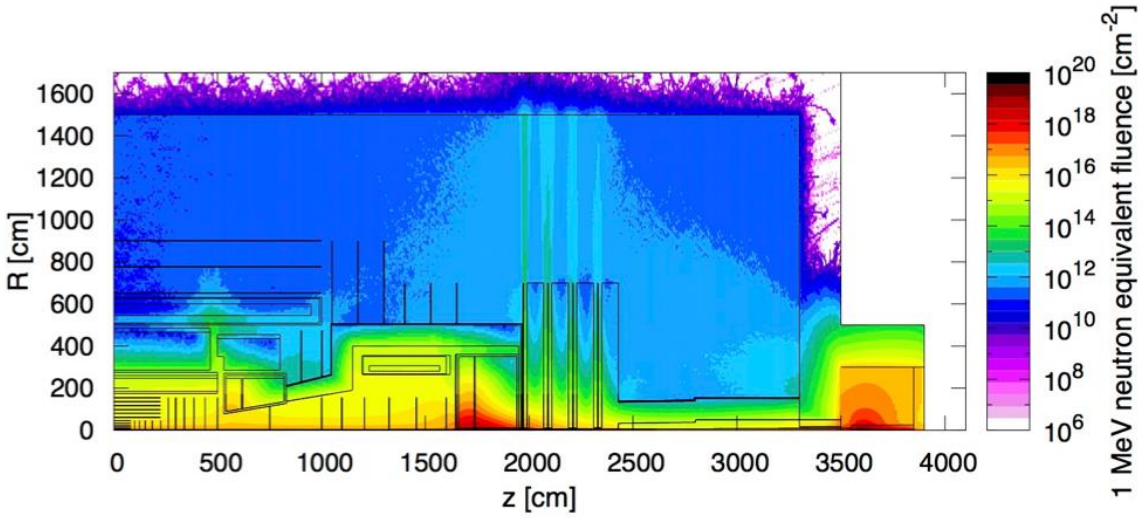

Hadron fluence in the order of 10^{18} /cm^2 close to the beampipe and 10^{15} -10^{16} /cm^2 (HL-LHC levels) for r>40cm.

Extreme fluences in the forward calorimeter …

Triplet (z=40m), Triplet shielding TAS (z=35m) and related radiation are nicely 'buried' inside the tunnel.

EIC IR & MDI

E_{cm}=104.9 GeV (h275/e-10)
$\mathcal{L}$ =10^{34} $cm^{-2}s^{-1}$
N [10^{10}]= 6.9 h/ 17.2 e-
L*= 4.5 m

Rear Direction

Forward Direction

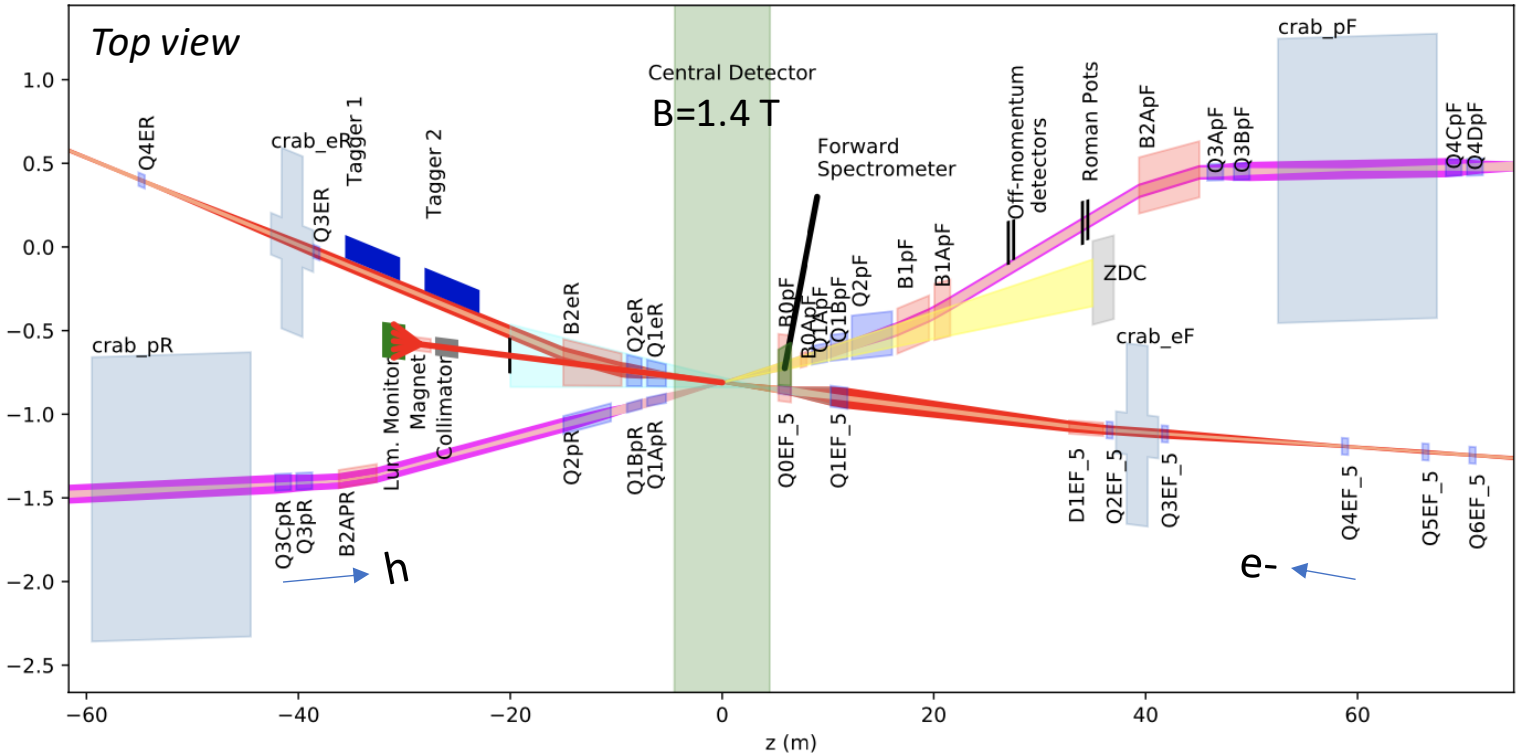

IR Design integrates

- FF magnets
- luminosity and neutron detectors
- e- taggers
- spectrometer
- near-beam detectors (Roman pots for h)
- crab cavities
- spin rotators both beams

- **Squeezed beams**, esp. vertically, small βy* : small L* & strong FF quads (esp. hadron beam)
  Chromaticity needs to be compensated by nonlinear sextupoles which in turn reduce dynamic aperture
- **Large acceptance of protons scattered off the IP** required**: very large apertures** also for FF quads, scattered protons and neutrons are detected far downstream the IP
- **Near-beam-detectors,** placed **along the forward hadron beam pipe**
- **Crossing angle** (25 mrad): trade-off between the space for **neutron detector at zero degree (**forward direction) and **luminosity monitor** (e- exit) and **crab cavities (small voltage for beam dynamics issues)**

EIC IR & MDI

Rear Direction

Forward Direction

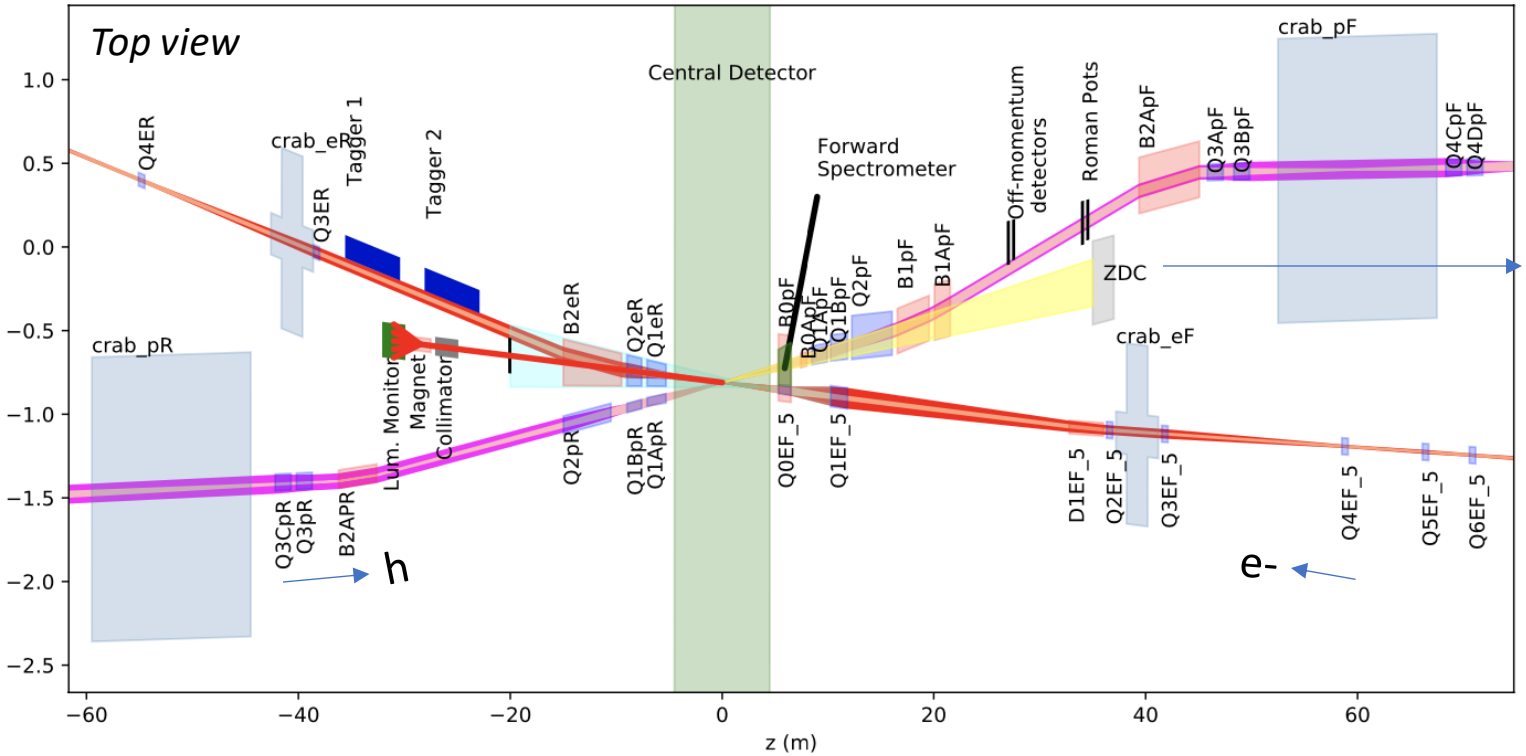

ZDC 60cm x 60cm x 2m @~30 m

Synchrotron radiation background *(HERA experience)*

- No bending upstream for leptons (up to ~35m from IP)
- Rear lepton magnets: aperture dominated by sync fan

Lepton magnet aperture 15 σ beam size aperture (determined by the Syn. Rad cone)

Hadron magnets: 10σ beam size aperture

Requirements for hadron beam direction

- B0pF: Forward Spectrometer (6 - 20 mrad)
- Neutron Detector (+/-4 mrad)
- Roman pots (sensitive 1 to 5 mrad)

Mostly interleaved magnets

- Exception: B0 and Q1BpF/Q1eF

Large apertures of proton forward magnets

EIC

EIC CDR (2021)

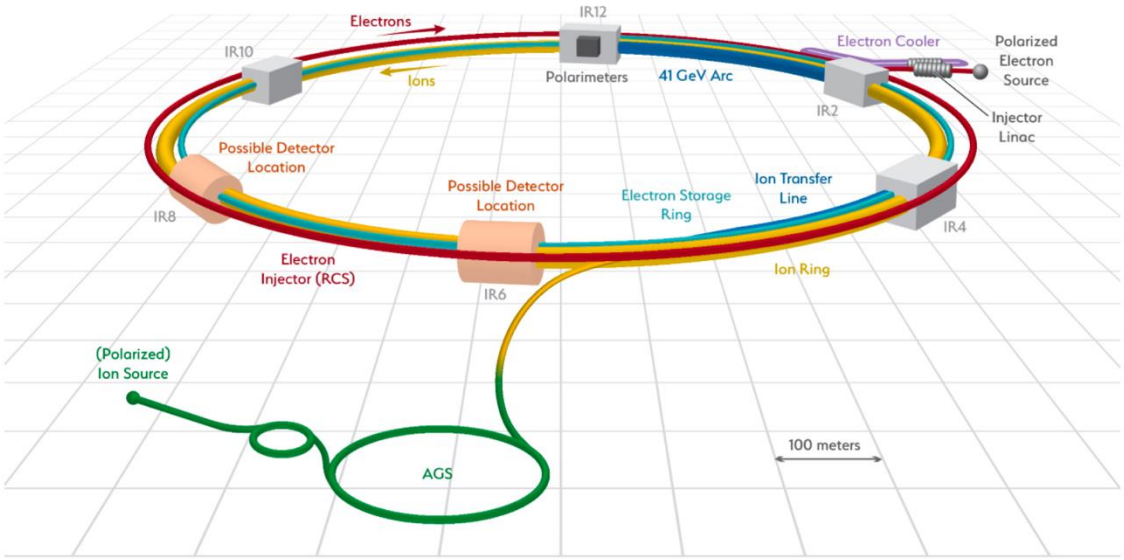

Table 1.1: Maximum luminosity parameters.

Parameter	hadron	electron
Center-of-mass energy [GeV]	104.9	
Energy [GeV]	275	10
Number of bunches	1160	
Particles per bunch [10^{10}]	6.9	17.2
Beam current [A]	1.0	2.5
Horizontal emittance [nm]	11.3	20.0
Vertical emittance [nm]	1.0	1.3
Horizontal β-function at IP β_x^* [cm]	80	45
Vertical β-function at IP β_y^* [cm]	7.2	5.6
Horizontal/Vertical fractional betatron tunes	0.228/0.210	0.08/0.06
Horizontal divergence at IP $\sigma_{x'}^*$ [mrad]	0.119	0.211
Vertical divergence at IP $\sigma_{y'}^*$ [mrad]	0.119	0.152
Horizontal beam-beam parameter ξ_x	0.012	0.072
Vertical beam-beam parameter ξ_y	0.012	0.1
IBS growth time longitudinal/horizontal [hr]	2.9/2.0	-
Synchrotron radiation power [MW]	-	9.0
Bunch length [cm]	6	0.7
Hourglass and crab reduction factor [17]	0.94	
Luminosity [$10^{34}\,\mathrm{cm}^{-2}\,\mathrm{s}^{-1}$]	1.0	

Central vacuum chamber

High electron beam current **2.5 A** -> (related issues: vacuum, photodesorption, heat load)

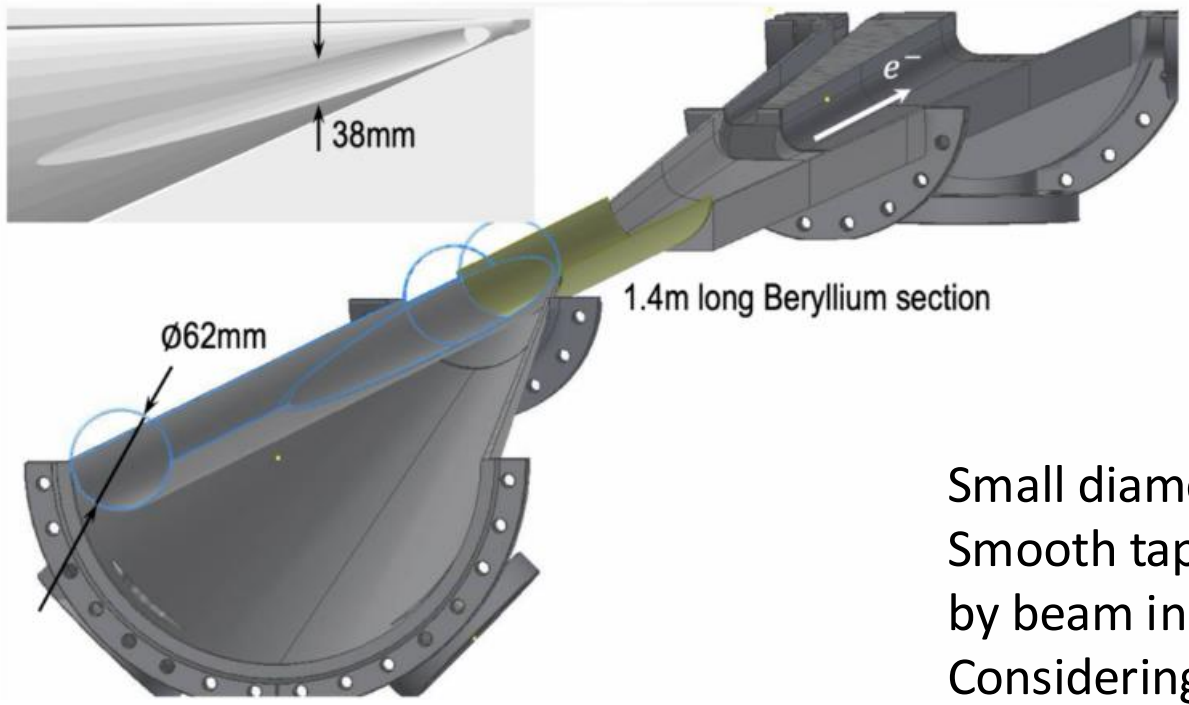

Small diameter, thin **walled Be in center region.**
Smooth tapers and transitions to limit energy deposited by beam in trapped modes (wakes).
Considering **HOM absorbers**

LHeC IR

ArXiv:2007.14491 (2020)

Head-on electron-proton collisions with dipoles in IR

On one side the beams should be fast separated, but this enhances the SR in the detector region, as a trade-off L* is increased and compromise for the β* values found (same achromatic telescopic squeezing implemented for HL)

Parameter	Unit	LHeC				FCC-eh	
		CDR	Run 5	Run 6	Dedicated	E_p=20 TeV	E_p=50 TeV
E_e	GeV	60	30	50	50	60	60
N_p	10^{11}	1.7	2.2	2.2	2.2	1	1
ϵ_p	μm	3.7	2.5	2.5	2.5	2.2	2.2
I_e	mA	6.4	15	20	50	20	20
N_e	10^9	1	2.3	3.1	7.8	3.1	3.1
β^*	cm	10	10	7	7	12	15
Luminosity	$10^{33}\,\mathrm{cm}^{-2}\mathrm{s}^{-1}$	1	5	9	23	8	15

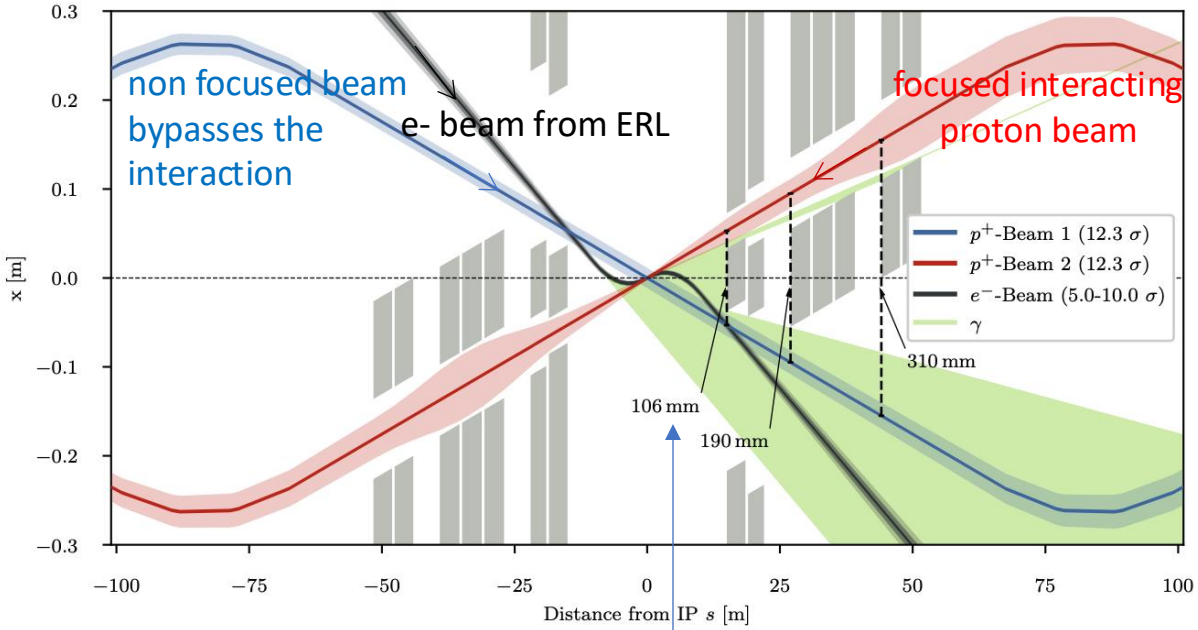

- A dipole (B0) of 0.21 T separates e-/p at the entrance of the first quad
- Nb_3Sn CS for the proton triplet quads

To be incorporated in the HL-LHC lattice -> some constraints

L*(proton) = 15 m (was 10 m in CDR)

E(e-) = 49.19 GeV, I=20mA
P_{SR} = 38 kW
$E_{critical}$ =283 keV

- Challenge from the SR in the IR is a bit relaxed with longer L*
- Challenge on beam current > 20 mA
- sub-μm level stability at IP required
- The beam pipe radius is an experimental challenge coping with strong SR and the forward tagging acceptance (similar to LHC challenges but there there is no pile-up in ep)

Intense e+ source would be needed for LHeC, R&D on e+ sources as joined effort for LC and LEMMA would be of interest

LHeC

ArXiv:2007.14491 (2020)

Detector concept

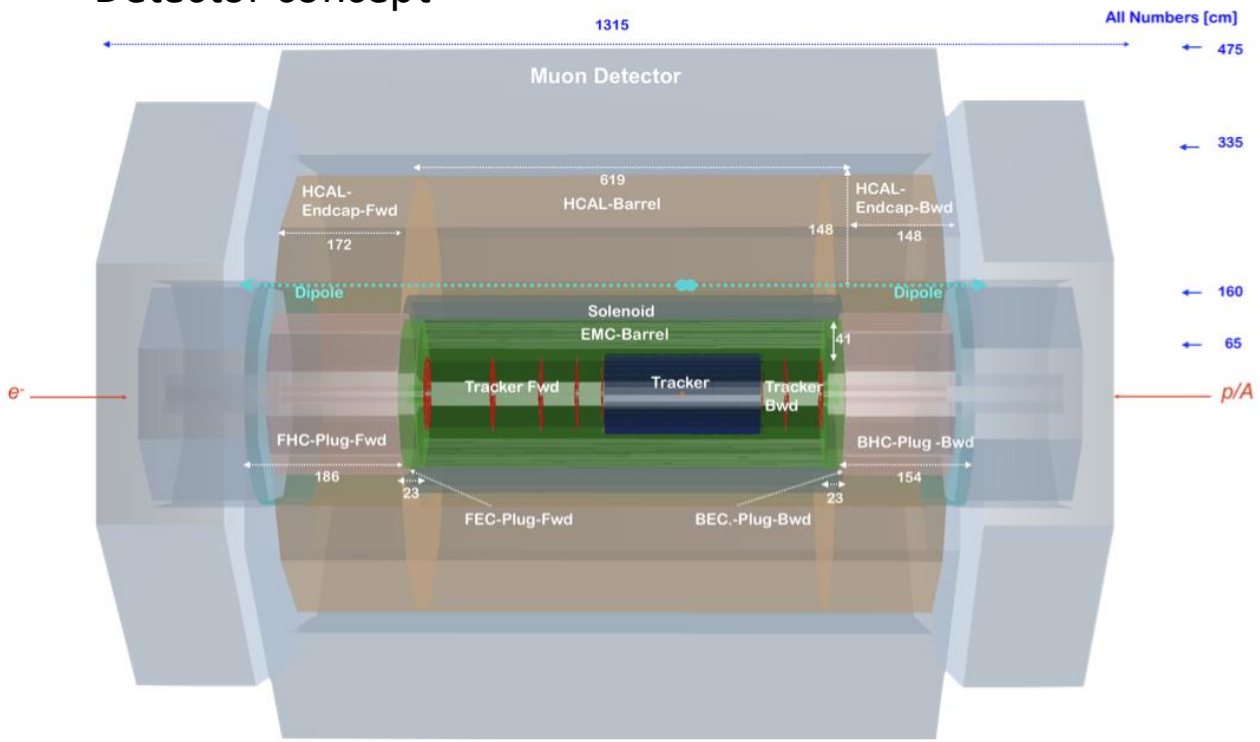

Complex magnet configuration

- Solenoid Detector Magnet (**3.5T**)
- Dual dipole magnets (**0.15 – 0.3 T**) throughout detector region (**|z| < 14m**)
  - to guide e-beam in and out
  - bend e-beam into head-on collision with p-beam
  - Safely extract the distorted e-beam
- 3.5T superconducting NbTi/Cu solenoid in 4.6K liquid helium cryostat

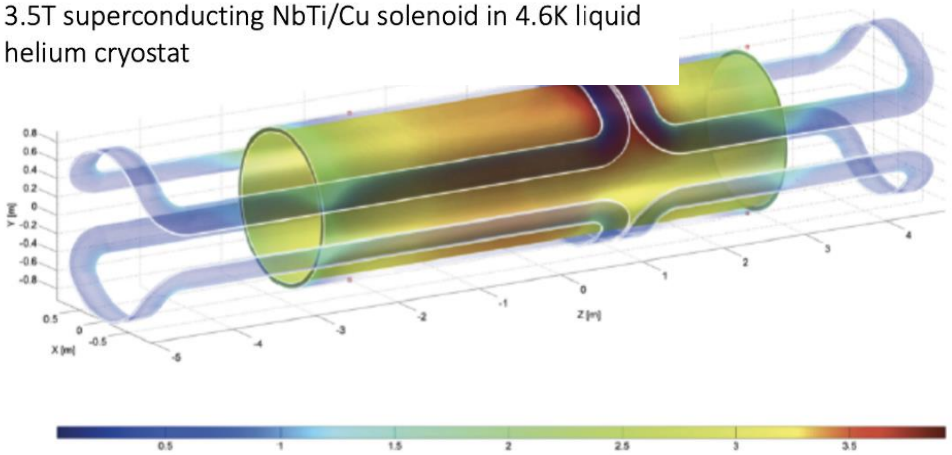

Solenoid and dipoles system housing in a common cryostat free bore 1.8 m extending along the detector for 10 m

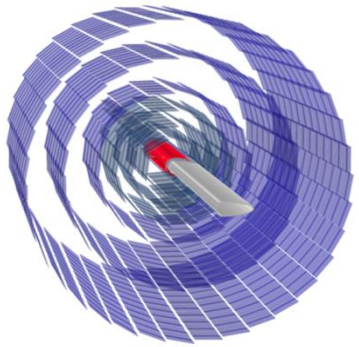

inner barrel tracker layers around the beam pipe

elliptical shape chosen for the beam pipe to allocate the three beams envelopes (15σ for p beam, 20σ for e- beam)

MDI challenge at Muon Colliders

- **Next-to-next** collider. R&D proof-of-principles stage.
- MAP project: a design study was done, with experiment on cooling (MICE), proton target (MERIT). Project stopped after Snowmass 2013.
- $\mathcal{L} \sim 10^{35}\text{cm}^{-2}\text{s}^{-1}$ obtained with O($10^{12}\mu$/bunch) inducing **radiation hazard due to the neutrino production**, **fast muon decay**. The MDI design is challenging.
- Dedicated backgrounds simulation were performed +/-200 m from the IP. Fcm@1.5 TeV muon decay induced backgrounds

To protect SC magnets and detector, 10 and 20 cm W masks with $5\sigma_{x,y}$ elliptic openings are placed in the IR magnet interconnection regions and a sophisticated W cone inside the detector. (**nozzles** – crucial role)

[N. Mokhov]

see dedicated talk by D. Calzolari

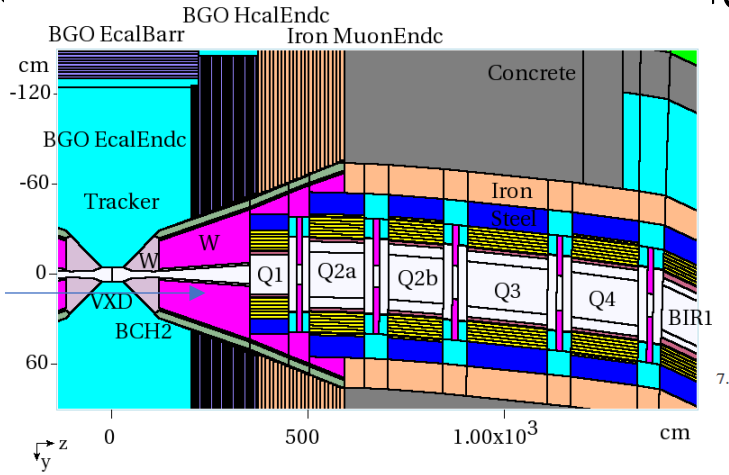

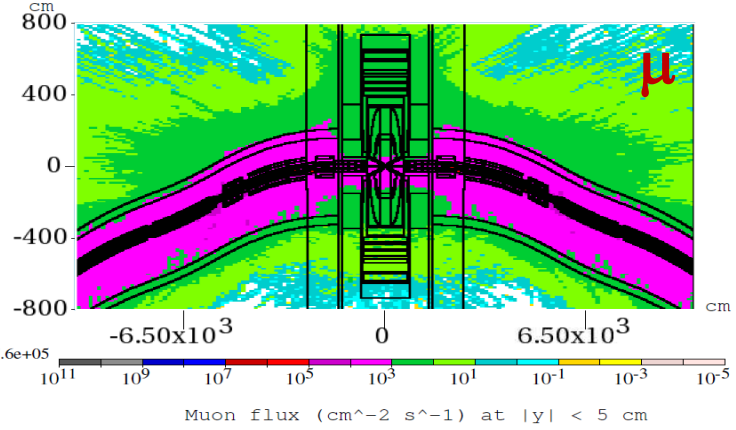

Positron-driven source MC (**LEMMA**) would have the great advantage of aiming at high luminosity with low-emittance muon beams, allowing to reduce the muons/bunch, reducing the backgrounds, relaxing the challenge on the MDI (the main challenge for high luminosity is on the high e+ production rate)

Summary

- **MDI can be the key for success/unsuccess for any collider → it is really mandatory to dedicate the proper R&D and effort in the optimization of its design.**

- Some of the main challenges and R&D discussed for different projects:
  - strong SC magnets, compact and high field magnets design, magnets integration with detector
  - experience in synchrotron radiation mitigation, including vacuum chambers technology
  - low impedance vacuum chamber, material and thickness optimization, radius (great impact on vertex detector!)
  - vacuum chamber cooling due to heat load
  - alignment systems inside the detector
  - BEAM INDUCED BACKGROUNDS & SYNCHROTRON RADIATION BKG: correct and reliable modeling essential for a successful MDI design, R&D not easy, experience on present (and past) colliders really important.

Some References

- *FCC-ee: The Lepton Collider*, **Eur. Phys. J. Spec. Top. 228**, 261–623 (2019)
- *FCC-hh: The Hadron Collider*, **Eur. Phys. J. Spec. Top. 228**, 755-1107 (2019)
- K. Oide et al., **Phys. Rev. Accel. Beams 19**, 111005 (2016)
- Crab-waist collision scheme: ArXiv.070233

- The Compact Linear e+e- Collider (CLIC): Project Implementation Plan (2018), ArXiv:1903.08655
- The Compact Linear e+e- Collider (CLIC): Accelerator and detector, A. Robson (2018)
- CLIC MDI arXiv:1202.6511.pdf (2011)
- The International Linear Collider A global Project, ArXiv:1903.01629v3 (2019)
- ILC TDR

- EIC CDR, doi:10.2172/1765663 (2021)

- The LHeC at the HL-LHC, LHeC and FCC-eh study group, CERN-ACC-Note-2020-0002, ArXiv: 2007.14491 (2020)
- LHeC CDR, J. Phys. G: Nucl. Part. Phys. **39** 075001, arXiv:1206.2913 (2012)

- Muon collider design meetings: https://indico.cern.ch/category/12762/
- The future prospects of muon colliders and neutrino factories, RAST 10, 189 (2019), ArXiv:1808.01858 and Refs. therein

Spare slides

From LCs to FCCee

From CLICdet to CLD

MAX-PLANCK-INSTITUT FÜR PHYSIK

- A LC-inspired FCCee detector concept - retaining key performance parameters
  Evolving from CLIC to CLD

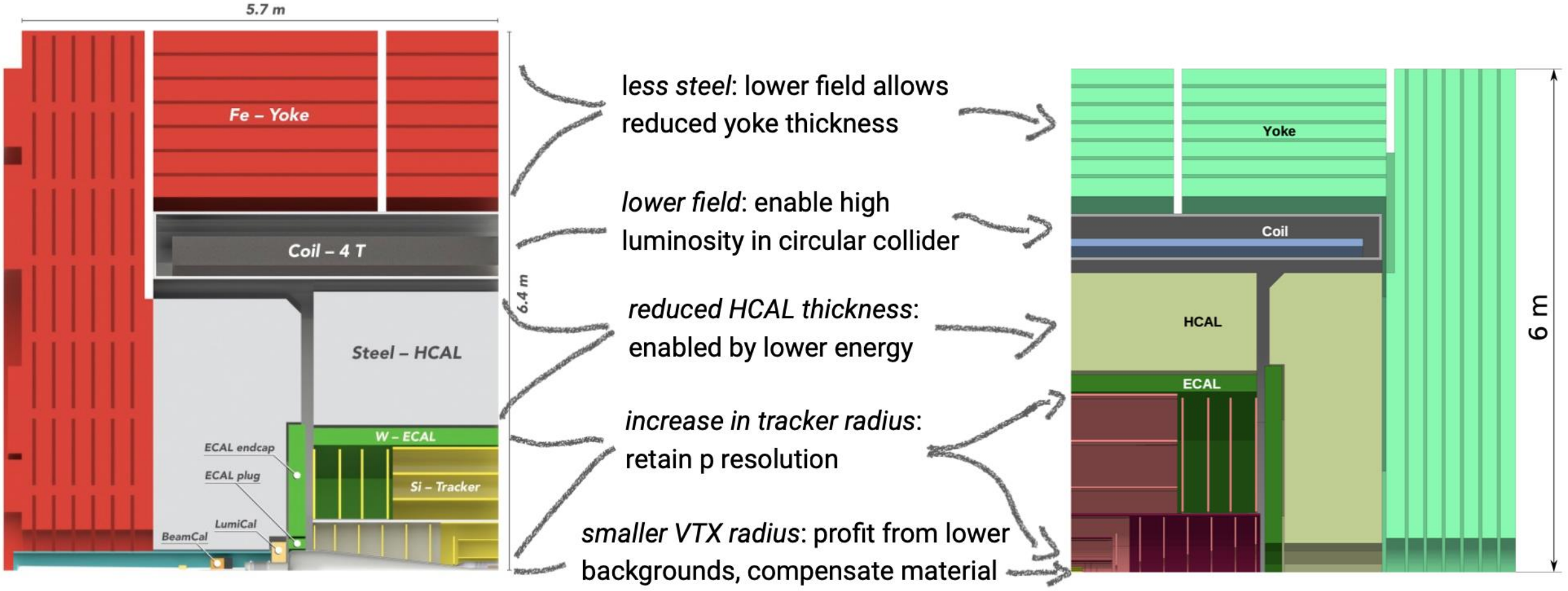

ILC collimators

- The collimation apertures required are approximately ∼6–9σx in the x plane and ∼40–60σy in the y plane. These correspond to typical half-gaps of the betatron spoiler of ∼1 mm in the x plane and ∼0.5 mm in the y plane.
- The spoilers are 0.5–1 X_0 (radiation length) thick, the absorbers are 30 X_0, and the protection collimators are 45 X_0.
- Electromagnetic showers created by primary beam particles in the collimators produce penetrating muons that can easily reach the collider hall. The muon flux through the detector is reduced by a 5 m-long magnetised iron shield 330 m upstream of the collision point that fills the cross-sectional area of the tunnel and extends 0.6 m beyond the ID of the tunnel ((with B= 1.5 T), also as radiation protection.

Belle II Detector

K_L and muon detector:
Resistive Plate Counter (barrel outer layers)
Scintillator + WLSF + MPPC (end-caps, inner 2 barrel layers)

EM Calorimeter:
CsI(Tl), waveform sampling

Particle Identification
Time-of-Propagation counter (barrel)
Prox. focusing Aerogel RICH (fwd)

electron (7GeV)

Beryllium beam pipe
2cm diameter

Vertex Detector
2 layers DEPFET + 4 layers DSSD

positron (4GeV)

Central Drift Chamber
He(50%):C_2H_6(50%), Small cells, long lever arm, fast electronics

COMPUTING

0110001

Lots of Data

Superkekb FF quads

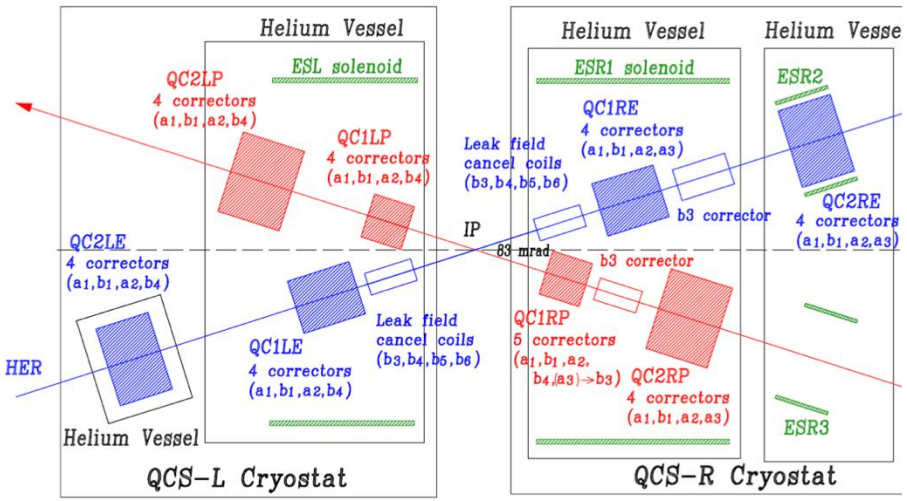

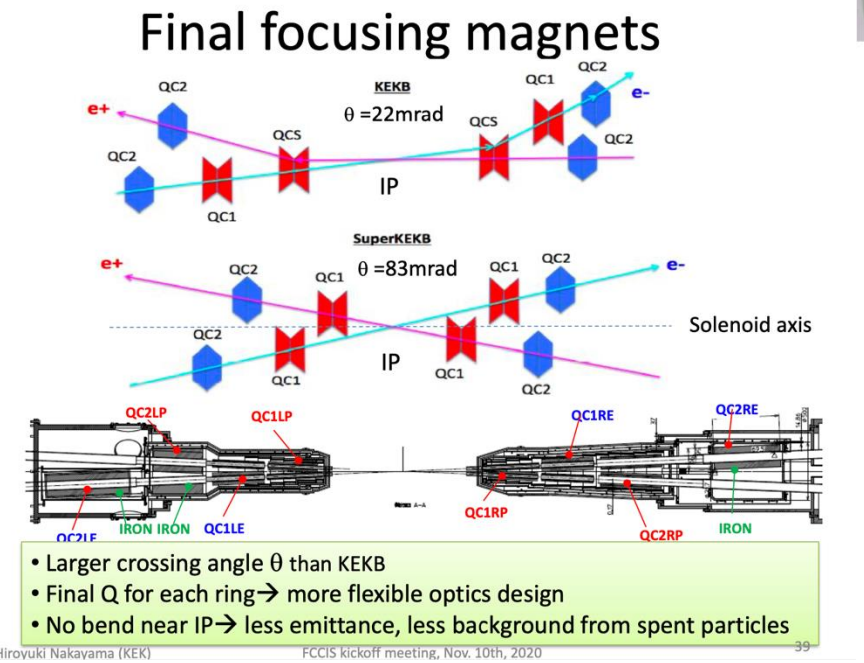

Figure 6: Four SC coils for QC1LP.

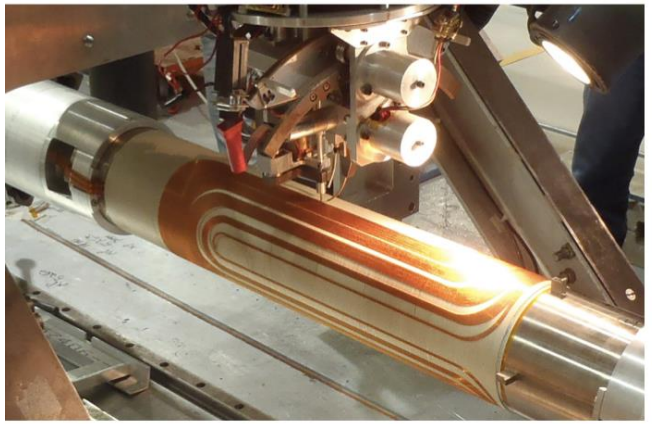

Figure 8: Winding process of corrector magnets in BNL.

Parameter	QC1P	QC1E	QC2P	QC2E
G_D, T/m	76.37	91.57	31.97	36.39
I_D, A	1,800	2,000	1,000	1,250
B_P, T	4.56	3.5	2.43	2.63
LR, %	72.3	73.4	44	39
R_C, mm	25.0	33.0	53.8	59.3
R_{Yo}, mm	NA	70.0	93.0	115.0
L_{PM}, mm	409.3	455.4	495.5	618.9
L_{EM}, mm	333.6	373.1	409.9	537.0
Cable	NbTi	NbTi	NbTi	NbTi
θ_K, deg.	2.1	1.6	1.0	0.94

G_D: design field gradient at the magnet center, I_D: magnet design current, B_P: maximum field in the coil at I_D, LR: load line ratio to the critical point, R_C: SC coil inner radius, R_{Yo}: yoke outer radius, L_{PM}: magnet physical length, L_{EM}: effective magnetic length, θ_K: key stone angle of the SC cable

The SC quadrupole magnet consists of the two layer SC coils (double-pancake structure). For the coils, the Rutherford type NbTi cables were used. The cable consists of 10 strand wires of ϕ0.5 mm. SC corrector magnets had been developed from 2011 in BNL, and 43 corrector magnets were completed in February 2015. The winding of the SC coil was performed by the computer controlled winding robot, and the SC wire of ϕ0.35 mm was directly stuck on the outer surface of the sup- port bobbin as the helium inner vessel.

SR spectra and outgassing loads

- Z-Pole: very high photon flux (→ large outgassing load);
- Z-pole: compliance with scheduled operation (integrated luminosity first 2 years), requires quick commissioning to I_{NOM}=1.390 A;
- t-pole (182.5): extremely large and penetrating radiation, critical energy 1.25 MeV;
- t-pole (and also W and H): needs design which minimizes activation of tunnel and machine components;
- W, H-pole: intermediate between Z and T; still E_{crit} > Compton edge (~100 keV)

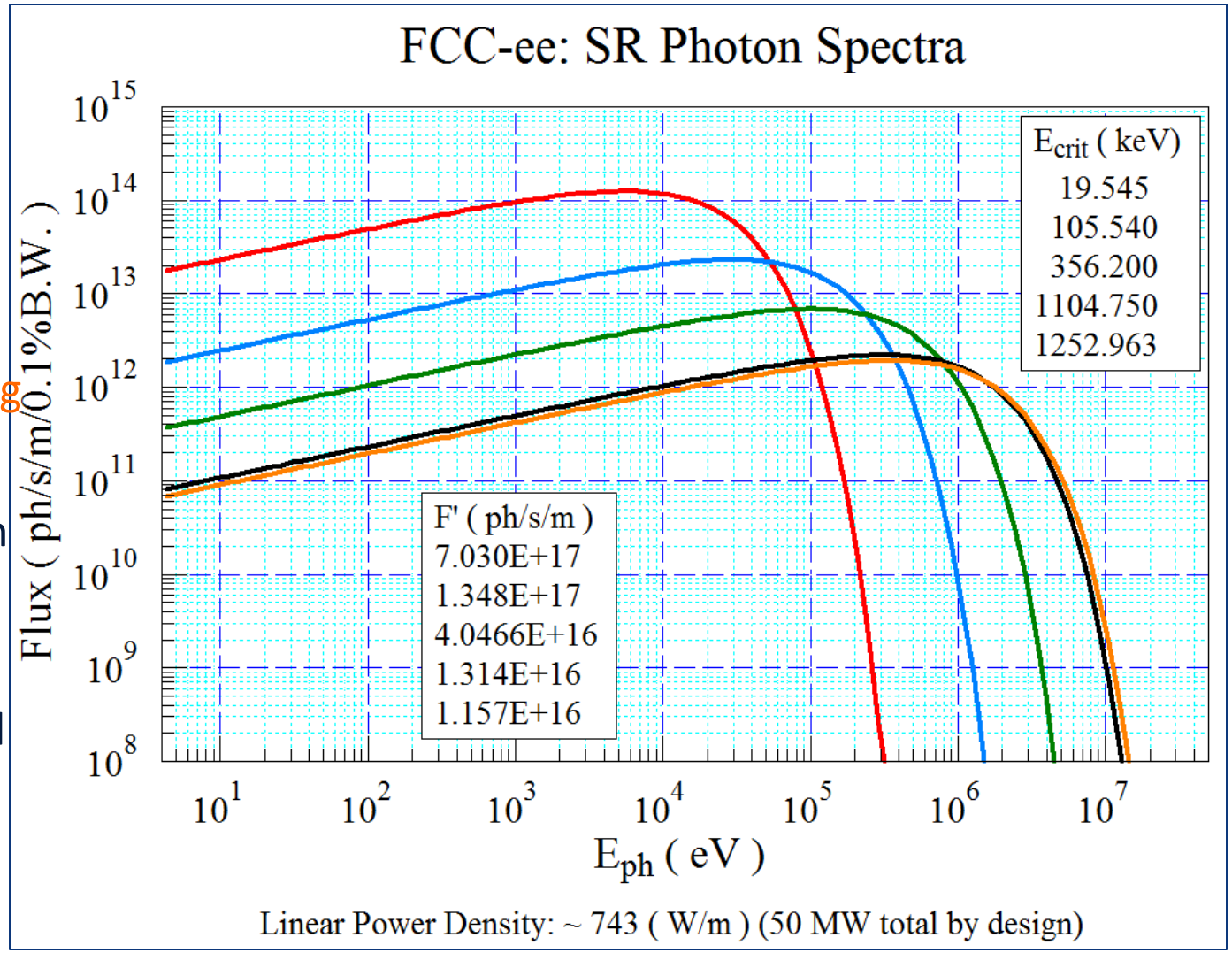

ALICE 3 – MDI R&D and Challenges

- Fast and ultra-thin detector with precise tracking and timing
- Fast -> for higher luminosity
- R&D on vertex layers
- Inner tracker
  - (futuristic) retractable detector for minimal distance from IP
  - ultra-thin layout MAPS sensors
  - small pixel pitch fro position resolution O(1 μm)
- Outer tracker
  - low material budget, lightweight mechanics, cooling and services
  - cost-effective sensors & modules
- Dedicated forward detector for soft photon, low p_T

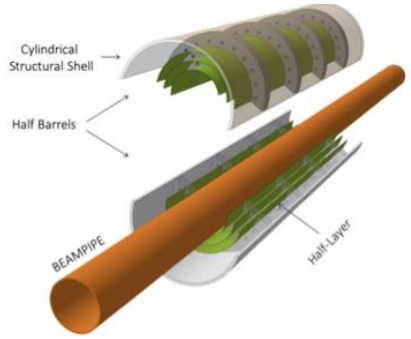

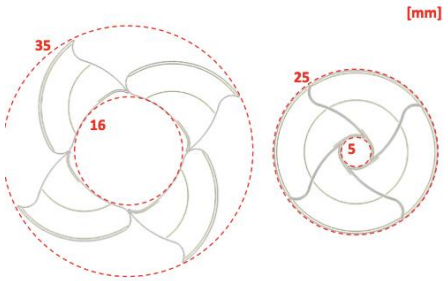

Radiation Studies for L=3x10^{35} cm^{-2}s^{-1} and 30ab^{-1}

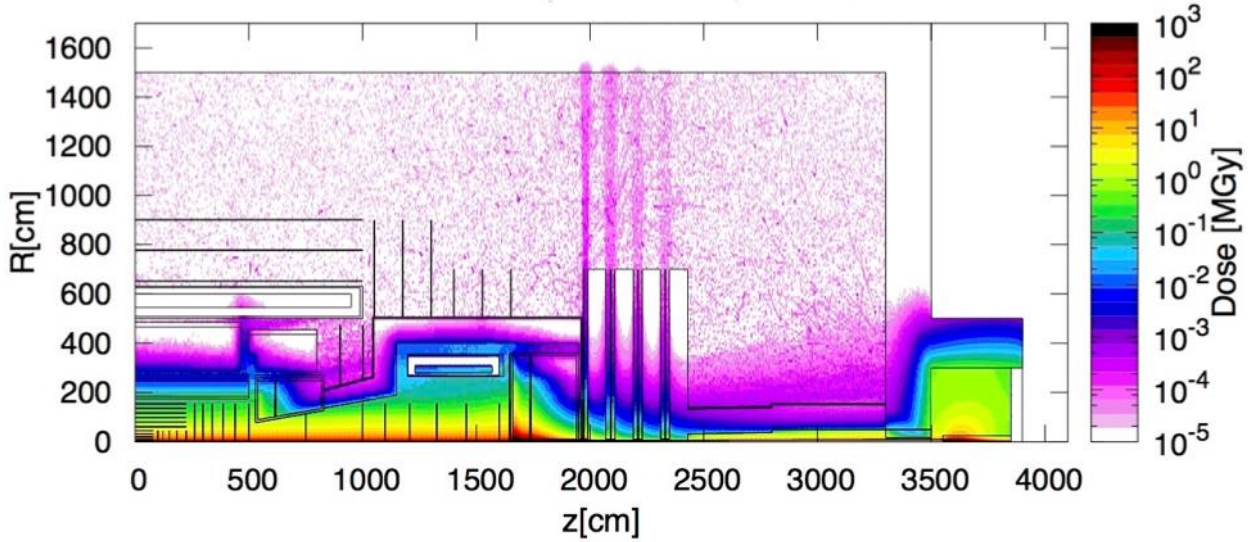

Dose of 300MGy in the first tracker layers.
<10kGy in HCAL barrel and extended barrel.

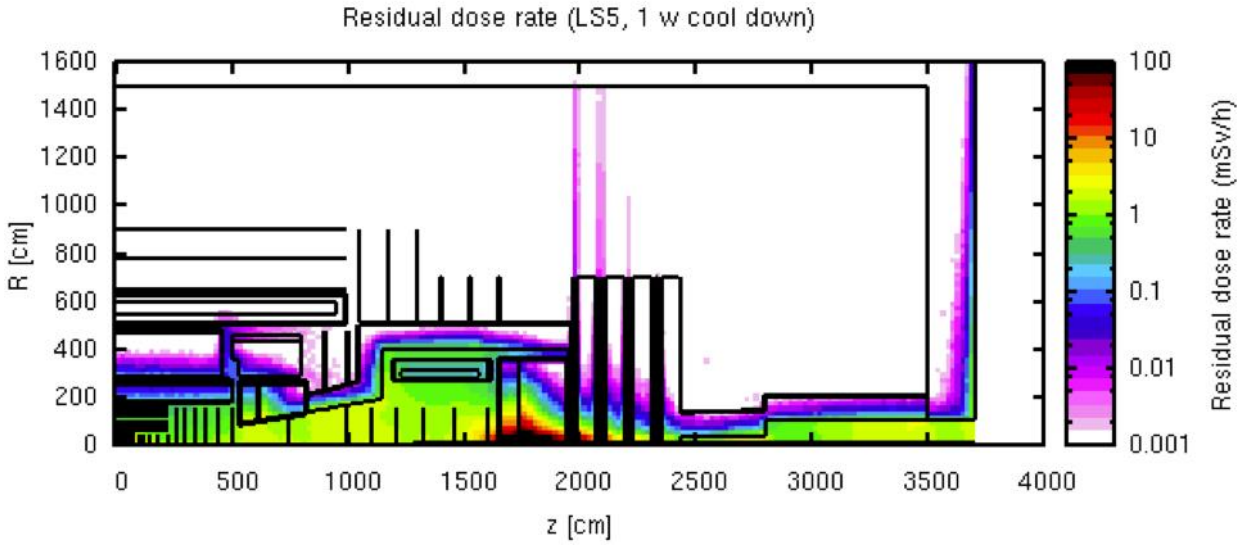

Dose from activation towards the end of FCC operation, 1 week of cooldown, so significant decrease for 1month, 1 year.

EIC MDI – IR Challenging Integration

- Requirements:
  - **Large rapidity** coverage, -4 < eta < 4 and behond especially in far-forward detectors
  - **small micro-vertex and large radius tracking**
  - Detector hermeticity

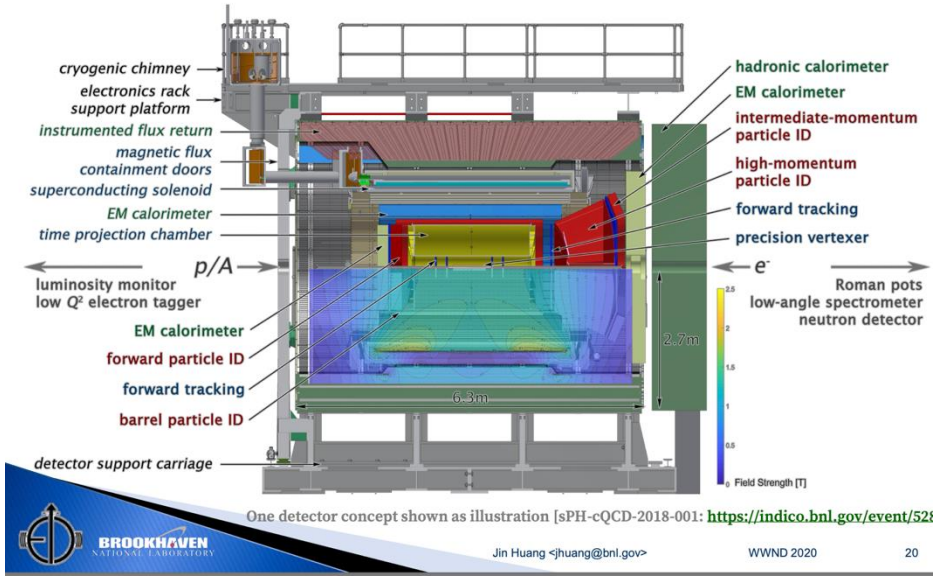

- **Challenge:** large acceptance for diffraction, tagging, neutrons from nuclear breakup ->
- **Integration challenge:** many ancillary detectors integrated in the beamline: low-Q2 tagger, Roman Pots, Zero-Degree Cal.,
- **Luminosity meas**.: hadron control of systematics, also for e- and hadron polarimetry

Vertex: small micro-vertex: MAPS, options: 6-layer barrel, 5+5 disks Si, option GEM for the most external. Hybrid option: SiV+TPC (barrel), 7 Si disks, opt1 TPC+ext.l.MPGD; opt2 coaxial layers of microRW. 20 mu m pitch (10 mu m considered)

LHeC

[ArXiv:2007.14491 (2020)]

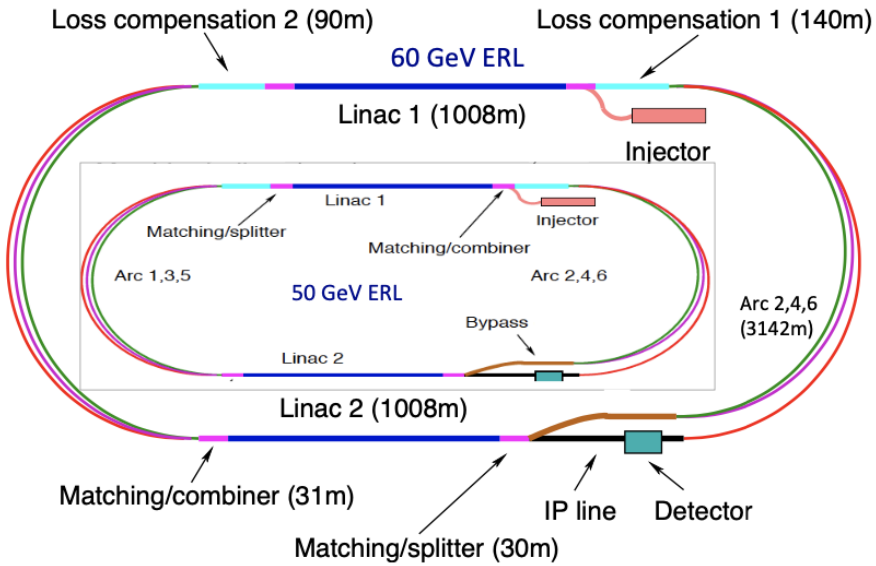

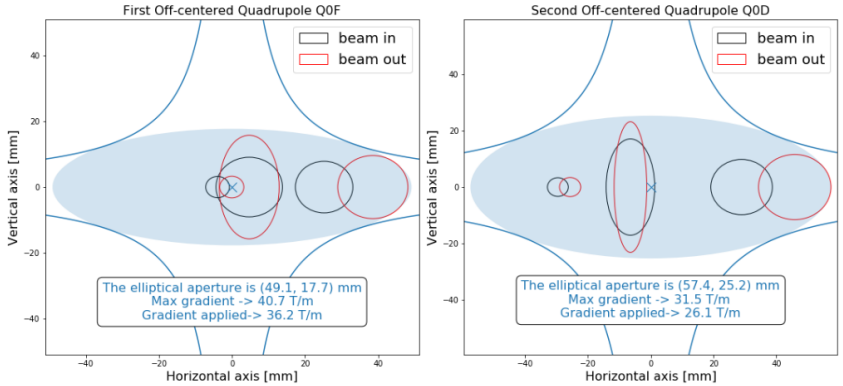

Figure 10.42: The position of the three beams at the entrance (black) and exit (red) of the electron doublet magnets. Following the internal convention, $15\,\sigma$ plus 20 % beta beating plus 2 mm orbit tolerances beam envelopes are chosen for the proton beams. The beam size of the electrons refer to $20\,\sigma$. From left to right the three beams are respectively the non colliding proton beam (tiny circles), electron beam (squeezed ellipses) and the colliding proton beam.

IR

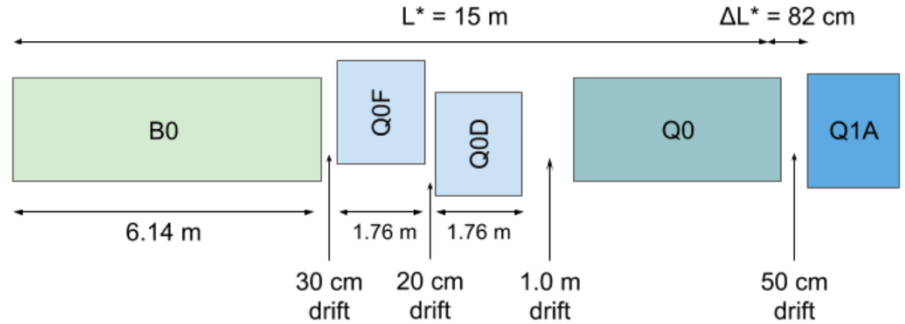

e-: doublet that optimises SR

Parameter	Unit	Q0F	Q0D
$\gamma\varepsilon_e$	mm·mrad	50	50
$\gamma\varepsilon_p$	mm·mrad	2.50	2.50
Gradient	T/m	36.2	26.1
Min. pole-tip radius	mm	28.9	38.1
Length	m	1.86	1.86

Magnet	Gradient [T/m]	Length [m]	Free aperture radius [mm]
Q1A	252	3.5	20
Q1B	164	3.0	32
Q2 type	186	3.7	40
Q3 type	175	3.5	45

Table 10.21: Parameters of the final focus quadrupole septa. The parameters of Q1A/B and Q2 are compatible with the Nb_3Sn based designs from [845] assuming the inner protective layer of Q2 can be reduced to 5 mm thickness.

LHeC – The Large Hadron-Electron Collider at the HL-LHC

Calorimeters

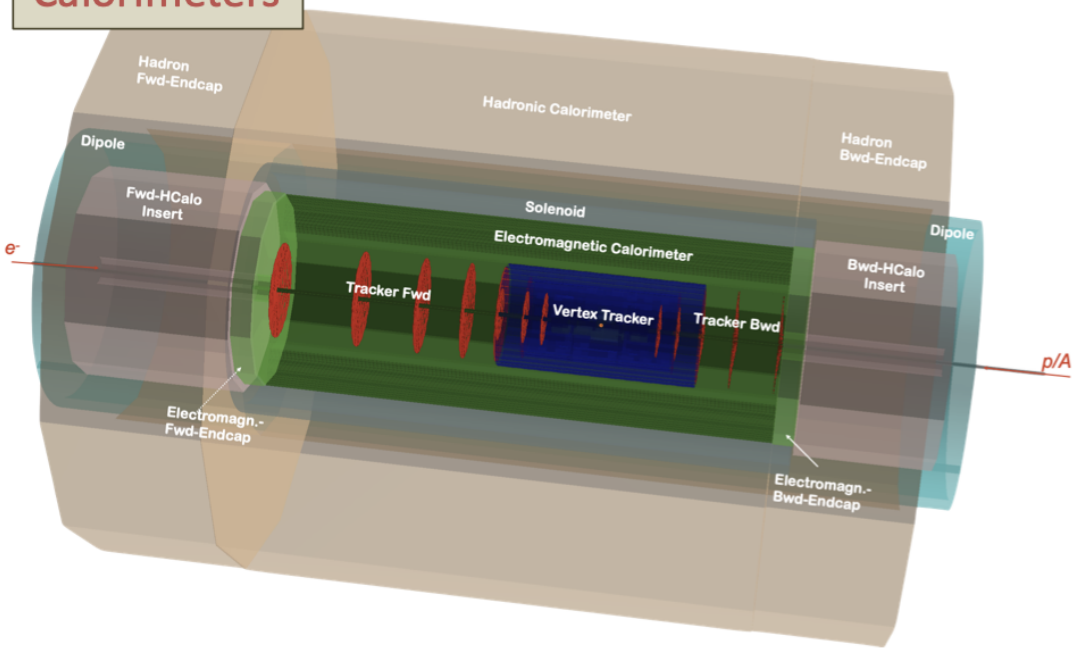

- Complete coverage: $-5 < \eta < +5.5$
- Forward Region: dense, high density jets of few TeV
- Backward Region: in DIS only deposit of $E < E_e$
- Calorimeter depth
  - ECAL: 30 X_0 barrel & backward, ~ 50X_0 forward
  - HCAL: 7.1-9.3 Λ_I barrel & backward; 9.2-9.6 Λ_I forward
- Detector technologies (ala ATLAS):
  - ECal: Pb/LAr with accordeon geometry
  - HCAL: Pb/Scintillating tiles
  - Alternative: ECAL: Pb/Scintillator ⇨ eliminate cryogenics

Barrel Calorimeters

Calo (LHeC)		EMC	HCAL		
		Barrel	Ecap Fwd	Barrel	Ecap Bwd
Readout, Absorber		Sci,Pb	Sci,Fe	Sci,Fe	Sci,Fe
Layers		38	58	45	50
Integral Absorber Thickness	[cm]	16.7	134.0	119.0	115.5
η_{max}, η_{min}		2.4, −1.9	1.9, 1.0	1.6, −1.1	−1.5, −0.6
$\sigma_E/E = a/\sqrt{E} \oplus b$	[%]	12.4/1.9	46.5/3.8	48.23/5.6	51.7/4.3
Λ_I / X_0		$X_0 = 30.2$	$\Lambda_I = 8.2$	$\Lambda_I = 8.3$	$\Lambda_I = 7.1$
Total area Sci	[m^2]	1174	1403	3853	1209

Forward/Backward Calorimeters

Calo (LHeC)		FHC Plug Fwd	FEC Plug Fwd	BEC Plug Bwd	BHC Plug Bwd
Readout, Absorber		Si,W	Si,W	Si,Pb	Si,Cu
Layers		300	49	49	165
Integral Absorber Thickness	[cm]	156.0	17.0	17.1	137.5
η_{max}, η_{min}		5.5, 1.9	5.1, 2.0	−1.4, −4.5	−1.4, −5.0
$\sigma_E/E = a/\sqrt{E} \oplus b$	[%]	51.8/5.4	17.8/1.4	14.4/2.8	49.5/7.9
Λ_I / X_0		$\Lambda_I = 9.6$	$X_0 = 48.8$	$X_0 = 30.9$	$\Lambda_I = 9.2$
Total area Si	[m^2]	1354	187	187	745

CDR-2020 (arXiv:2007:14491), tables 12.3 and 12.4

ILC BDS

Ref. TDR

The main subsystems of the BDS are (beam direction):

• a section containing emittance measurement and matching (correction) sections, trajectory feedback, polarimetry and energy diagnostics;

• a **collimation section** which removes beam-halo particles that would otherwise generate unacceptable background in the detector, and also contains magnetised iron shielding to deflect and/or absorb muons generated in the collimation process;

• the **final focus** (FF), which uses **strong compact superconducting quadrupoles** to focus the beam at the IP, with sextupoles providing local chromaticity correction;

• the interaction region, containing the experimental detectors. The final-focus quadrupoles closest to the IP are **integrated into the detector** to facilitate detector "push-pull";

• the extraction line, which has a large enough bandwidth to transport the heavily disrupted beam cleanly to a high-powered water-cooled dump. The extraction line also contains important polarisation and energy diagnostics.

The beam-delivery optics provides demagnification factors of typically several hundreds in the beam size, resulting in very large beta functions (several thousand kilometres) at critical locations, leading to the tightest alignment tolerances in the entire machine. In addition, careful correction of the strong chromaticity and geometric aberrations requires a delicate balance of higher-order optical terms. The tight tolerances on magnet motion (down to tens of nanometres), makes continuous trajectory correction and the use of fast beam-based feedback systems mandatory. Furthermore, several critical components (e.g. the final focusing doublet) may well require mechanical stabilisation.

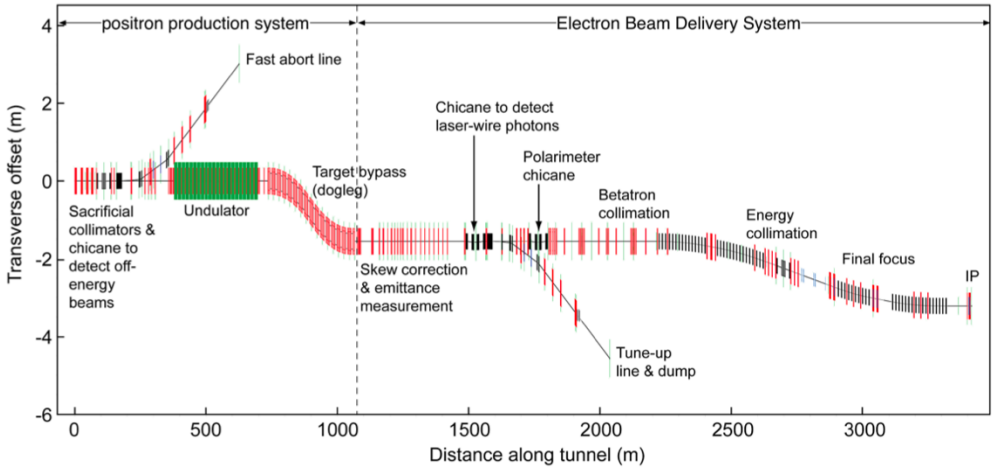

Parameter Tables

FCC-ee collider parameters (stage 1)

parameter	Z	WW	H (ZH)	ttbar
beam energy [GeV]	45	80	120	182.5
beam current [mA]	1390	147	29	5.4
no. bunches/beam	16640	2000	393	48
bunch intensity [10^{11}]	1.7	1.5	1.5	2.3
SR energy loss / turn [GeV]	0.036	0.34	1.72	9.21
total RF voltage [GV]	0.1	0.44	2.0	10.9
long. damping time [turns]	1281	235	70	20
horizontal beta* **[m]**	0.15	0.2	0.3	1
vertical beta* [mm]	0.8	1	1	1.6
horiz. geometric emittance [nm]	0.27	0.28	0.63	1.46
vert. geom. emittance [pm]	1.0	1.7	1.3	2.9
bunch length with SR / BS [mm]	3.5 / 12.1	3.0 / 6.0	3.3 / 5.3	2.0 / 2.5
luminosity per IP [10^{34} $cm^{-2}s^{-1}$]	230	28	8.5	1.55
beam lifetime rad Bhabha / BS [min]	68 / >200	49 / >1000	38 / 18	40 / 18

PDG 2020

Table 31.1: Tentative parameters of selected future e^+e^- high-energy colliders. Parameters associated with different beam energy scenarios are comma-separated.

	FCC-ee	CEPC	ILC	CLIC
Species	e^+e^-	e^+e^-	e^+e^-	e^+e^-
Beam energy (GeV)	46, 120, 183	46, 120	125, 250	190, 1500
Circumference / Length (km)	97.75	100	20.5, 31	11, 50
Interaction regions	2	2	1	1
Est. integrated luminosity per experiment (ab^{-1}/year)	26, 0.9, 0.17	4, 0.4	0.2, 0.2	0.2, 0.6
Peak luminosity ($10^{34}/cm^2/s$)	230, 8.5, 1.6	32, 3	1.4, 1.8	1.5, 6
Time between collisions (μs)	0.015, 0.75, 8.5	0.025, 0.68	0.55	0.0005
Energy spread (rms, 10^{-3})	1.3, 1.65, 2.0	0.4, 1.0	e^-: 1.9, 1.2 e^+: 1.5, 0.7	3.5
Bunch length (rms, mm)	12.1, 5.3, 3.8	8.5, 3.3	0.3	0.09, 0.044
IP beam size (μm)	H: 6.3, 14, 38 V: 0.03, 0.04, 0.07	H: 5.9, 21 V: 0.04, 0.07	H: 0.52, 0.47 V: 0.008, 0.006	H: 0.15, 0.04 V: 0.003, 0.001
Injection energy (GeV)	on energy (topping off)	on energy (topping off)	5.0 (linac)	9.0 (linac)
Transv. rms emittance (pm)	H: 270, 630, 1340 V: 1, 1, 3	H: 170, 1210 V: 2, 3	H: 20, 10 V: 0.14, 0.07	H: 2.4, 0.22 V: 0.8, 0.01
β^* at interaction point (cm)	H: 15, 30, 100 V: 0.08, 0.1, 0.16	H: 20, 36 V: 0.1, 0.15	H: 1.3, 2.2 V: 0.041, 0.048	H: 0.8, 0.69 V: 0.01, 0.0068
Full crossing angle (mrad)	30	33	14	20
Crossing scheme	crab waist	crab waist	crab crossing	crab crossing
Piwinski angle $\phi = \sigma_z\theta_c/(2\sigma_x^*)$	28.5, 5.8, 1.5	23.8, 2.6	0	0
Beam-beam param. ξ_y (10^{-3})	133, 118, 144	72, 109	n/a	n/a
Disruption parameter D_y	0.9, 1.1, 1.9	0.3, 1.0	34, 25	8, 12
Average Upsilon Υ	0.0002,0.0004,0.0006	0.0001,0.0005	0.03, 0.06	0.26, 3.4
RF frequency (MHz)	400, 400, 800	650	1300	11994
Particles per bunch (10^{10})	17, 15, 27	8, 15	2	0.52, 0.37
Bunches per beam	16640, 328, 33	12000, 242	1312 (pulse)	352, 312 (trains at 50 Hz)
Average beam current (mA)	1390, 29, 5.4	19.2	6 (in train)	1660, 1200 (in train)
RF gradient (MV/m)	1.3, 9.8, 19.8	3.6, 19.7	31.5	72, 100
Polarization (%)	≥10, 0, 0	5–10, 0	e^-: 80% e^+: 30%	e^-: 70% at IP
SR power loss (MW)	100	64	n/a	n/a
Beam power/beam (MW)	n/a	n/a	5.3, 10.5	3, 14
Novel technology	—	—	high grad. SC RF	two-beam accel.

	LHeC	HE-LHC	FFC-hh	SPPC	μ collider
Species	ep	pp	pp	pp	$\mu^+\mu^-$
Beam Energy (TeV)	0.06(e), 7 (p)	13.5	50	37.5	0.063, 3
Circumference (km)	9(e), 26.7 (p)	26.7	97.75	100	0.3, 6
Interaction regions	1	2 (4)	4	2	1, 2
Estimated integrated luminosity per experiment (ab^{-1}/year)	0.1	0.5	0.2–1.0	0.4	0.001, 1.0
Peak luminosity ($10^{34}/cm^2/s$)	0.8	16	5–30	10	2.2, 71
Time between collisions (μs)	0.025	0.025	0.025	0.025	1, 20
Energy spread (rms, 10^{-3})	0.03 (e), 0.1(p)	0.1	0.1	0.2	0.04, 1
Bunch length (rms, mm)	0.06 (e), 75.5(p)	80	80	75.5	63, 2
IP beam size (μm)	4.3 (round)	8.8	6.7-3.5 (init.)	6.8 (init.)	75, 1.5
Injection energy (GeV)	1(e), 450(p)	1300	3300	2100	on energy
Transverse emittance (rms, nm)	0.45(e), 0.27(p)	0.17	0.04 (init.)	0.06 (init.)	335, 0.9
β^*, amplitude fcn. at IP (cm)	5.0(e), 7.0(p)	45	110–30	75	1.7, 0.25
Beam-beam parameter/IP (10^{-3})	−(e), 0.4(p)	12	5–15	7.5	20, 90
RF frequency (MHz)	800(e), 400(p)	400	400	400/200	805
Particles per bunch (10^{10})	0.23(e), 22(p)	22	10	15	400, 200
Bunches per beam	−(e), 2808(p)	2808	10600	10080	1
Average beam current (mA)	15(e), 883(p)	1120	500	730	640, 16 (peak)
Length of standard cell (m)	52.4(e arc), 107(p)	137	213	148	N/A
Phase advance per cell (deg)	310/90(eH/V) 90(p)	90	90	90	N/A
Peak magnetic field (T)	0.264(e), 8.33(p)	16	16	12	10
Polarization (%)	90(e), 0(p)	0	0	0	0
SR power loss/beam (MW)	30(e), 0.01(p)	0.1	2.4	1.1	3×10^{-5}, 0.068
Novel technology	high-energy ERL	16T Nb_3Sn magnets	16T Nb_3Sn magnets	HTS magnets	muon prod.

https://pdg.lbl.gov/2020/reviews/rpp2020-rev-accel-phys-colliders.pdf

KEKB and SuperKEKB

Table 1: Machine Parameters of KEKB and SuperKEKB. Values in parentheses for SuperKEKB denote parameters without intrabeam scattering. Note that horizontal emittance increases by 30% owing to intrabeam scattering in the LER. The KEKB parameters are those achieved at the crab crossing [2], where the effective crossing angle was 0. (*)Before the crab crossing, the luminosity of $1.76 \times 10^{34}\mathrm{cm}^{-2}\mathrm{s}^{-1}$ was achieved at the half crossing angle of 11 mrad, where $\phi_{\mathrm{Piw}} \sim 1$ [6].

		KEKB		SuperKEKB		
		LER (e+)	HER (e-)	LER (e+)	HER (e-)	Units
Beam energy	E	3.5	8.0	4.0	7.007	GeV
Circumference	C	3016.262		3016.315		m
Half crossing angle	θ_x	0 ($11^{(*)}$)		41.5		mrad
Piwinski angle	ϕ_{Piw}	0	0	24.6	19.3	rad
Horizontal emittance	ε_x	18	24	3.2 (1.9)	4.6 (4.4)	nm
Vertical emittance	ε_y	150	150	8.64	12.9	pm
Coupling		0.83	0.62	0.27	0.28	%
Beta function at IP	β_x^*/β_y^*	1200/5.9	1200/5.9	32/0.27	25/0.30	mm
Horizontal beam size	σ_x^*	147	170	10.1	10.7	μm
Vertical beam size	σ_y^*	940	940	48	62	nm
Horizontal betatron tune	ν_x	45.506	44.511	44.530	45.530	
Vertical betatron tune	ν_y	43.561	41.585	46.570	43.570	
Momentum compaction	α_p	3.3	3.4	3.20	4.55	10^{-4}
Energy spread	σ_ε	7.3	6.7	7.92(7.53)	6.37(6.30)	10^{-4}
Beam current	I	1.64	1.19	3.60	2.60	A
Number of bunches	n_b	1584		2500		
Particles/bunch	N	6.47	4.72	9.04	6.53	10^{10}
Energy loss/turn	U_0	1.64	3.48	1.76	2.43	MeV
Long. damping time	τ_z	21.5	23.2	22.8	29.0	msec
RF frequency	f_{RF}	508.9		508.9		MHz
Total cavity voltage	V_c	8.0	13.0	9.4	15.0	MV
Total beam power	P_b	~3	~4	8.3	7.5	MW
Synchrotron tune	ν_s	-0.0246	-0.0209	-0.0245	-0.0280	
Bunch length	σ_z	~7	~7	6.0 (4.7)	5.0 (4.9)	mm
Beam–beam parameter	ξ_x/ξ_y	0.127/0.129	0.102/0.090	0.0028/0.088	0.0012/0.081	
Luminosity	L	2.108×10^{34}		8×10^{35}		$\mathrm{cm}^{-2}\mathrm{s}^{-1}$
Integrated luminosity	$\int L$	1.041		50		ab^{-1}

ILC TDR

Table 2.1. Summary table of the 200–500 GeV baseline parameters for the ILC. The reported luminosity numbers are results of simulation [12]

Centre-of-mass energy	E_{CM}	GeV	200	230	250	350	500
Luminosity pulse repetition rate		Hz	5	5	5	5	5
Positron production mode			10 Hz	10 Hz	10 Hz	nom.	nom.
Estimated AC power	P_{AC}	MW	114	119	122	121	163
Bunch population	N	$\times 10^{10}$	2	2	2	2	2
Number of bunches	n_b		1312	1312	1312	1312	1312
Linac bunch interval	Δt_b	ns	554	554	554	554	554
RMS bunch length	σ_z	μm	300	300	300	300	300
Normalized horizontal emittance at IP	$\gamma\epsilon_x$	μm	10	10	10	10	10
Normalized vertical emittance at IP	$\gamma\epsilon_y$	nm	35	35	35	35	35
Horizontal beta function at IP	β_x^*	mm	16	14	13	16	11
Vertical beta function at IP	β_y^*	mm	0.34	0.38	0.41	0.34	0.48
RMS horizontal beam size at IP	σ_x^*	nm	904	789	729	684	474
RMS vertical beam size at IP	σ_y^*	nm	7.8	7.7	7.7	5.9	5.9
Vertical disruption parameter	D_y		24.3	24.5	24.5	24.3	24.6
Fractional RMS energy loss to beamstrahlung	δ_{BS}	%	0.65	0.83	0.97	1.9	4.5
Luminosity	L	$\times 10^{34}$ cm^{-2} s^{-1}	0.56	0.67	0.75	1.0	1.8
Fraction of L in top 1% E_{CM}	$L_{0.01}$	%	91	89	87	77	58
Electron polarisation	P_-	%	80	80	80	80	80
Positron polarisation	P_+	%	30	30	30	30	30
Electron relative energy spread at IP	$\Delta p/p$	%	0.20	0.19	0.19	0.16	0.13
Positron relative energy spread at IP	$\Delta p/p$	%	0.19	0.17	0.15	0.10	0.07

Table 8.2. Energy-dependent parameters of the Beam Delivery System [84].

		Center-of-mass energy, $E_{\rm cm}$ (GeV)							
		Baseline				Upgrades			
Parameter		200	250	350	500	500	1000 (A1)	1000 (B1b)	Unit
Nominal bunch population	N	2.0	2.0	2.0	2.0	2.0	1.74	1.74	$\times 10^{10}$
Pulse frequency	$f_{\rm rep}$	5	5	5	5	5	4	4	Hz
Bunches per pulse	$N_{\rm bunch}$	1312	1312	1312	1312	2625	2450	2450	
Nominal horizontal beam size at IP	$\sigma_{\rm x}^*$	904	729	684	474	474	481	335	nm
Nominal vertical beam size at IP	$\sigma_{\rm y}^*$	7.8	7.7	5.9	5.9	5.9	2.8	2.7	nm
Nominal bunch length at IP	$\sigma_{\rm z}^*$	0.3	0.3	0.3	0.3	0.3	0.250	0.225	mm
Energy spread at IP, e^-	$\delta E/E$	0.206	0.190	0.158	0.124	0.124	0.083	0.085	%
Energy spread at IP, e^+	$\delta E/E$	0.190	0.152	0.100	0.070	0.070	0.043	0.047	%
Horizontal beam divergence at IP	$\theta_{\rm x}^*$	57	56	43	43	43	21	30	μrad
Vertical beam divergence at IP	$\theta_{\rm y}^*$	23	19	17	12	12	11	12	μrad
Horizontal beta-function at IP	$\beta_{\rm x}^*$	16	13	16	11	11	22.6	11	mm
Vertical beta-function at IP	$\beta_{\rm y}^*$	0.34	0.41	0.34	0.48	0.48	0.25	0.23	mm
Horizontal disruption parameter	$D_{\rm x}$	0.2	0.3	0.2	0.3	0.3	0.1	0.2	
Vertical disruption parameter	$D_{\rm y}$	24.3	24.5	24.3	24.6	24.6	18.7	25.1	
Energy of single pulse	$E_{\rm pulse}$	420	526	736	1051	2103	3409	3409	kJ
Average beam power per beam	$P_{\rm ave}$	2.1	2.6	3.7	5.3	10.5	13.6	13.6	MW
Geometric luminosity	$L_{\rm geom}$	0.30	0.37	0.52	0.75	1.50	1.77	2.64	$\times 10^{34}$ cm^{-2} s^{-1}
– with enhancement factor		0.50	0.68	0.88	1.47	2.94	2.71	4.32	$\times 10^{34}$ cm^{-2} s^{-1}
Beamstrahlung parameter (av.)	$\Upsilon_{\rm ave}$	0.013	0.020	0.030	0.062	0.062	0.127	0.203	
Beamstrahlung parameter (max.)	$\Upsilon_{\rm max}$	0.031	0.048	0.072	0.146	0.146	0.305	0.483	
Simulated luminosity (incl. waist shift)	L	0.56	0.75	1.0	1.8	3.6	3.6	4.9	$\times 10^{34}$ cm^{-2} s^{-1}
Luminosity fraction within 1 %	$L_{1\%}/L$	91	87	77	58	58	59	45	%
Energy loss from BS	$\delta E_{\rm BS}$	0.65	0.97	1.9	4.5	4.5	5.6	10.5	%
e^+e^- pairs per bunch crossing	$n_{\rm pairs}$	45	62	94	139	139	201	383	$\times 10^3$
Pair energy per B.C.	$E_{\rm pairs}$	25	47	115	344	344	1338	3441	TeV

Figure 8.3
BDS optics, subsystems and vacuum chamber aperture; S is the distance measured from the entrance.

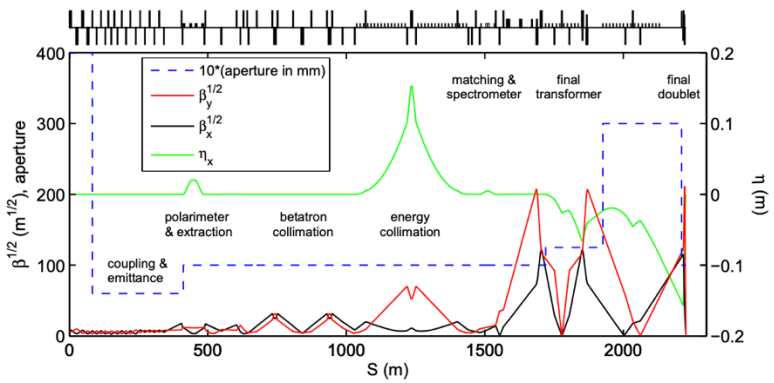

Table 8.1
Key parameters of the BDS [12]. The range of L^*, the distance from the final quadrupole to the IP, corresponds to values considered for the existing SiD and ILD detector concepts.

Parameter	Value	Unit
Length (start to IP distance) per side	2254	m
Length of main (tune-up) extraction line	300 (467)	m
Max. Energy/beam (with more magnets)	250 (500)	GeV
Distance from IP to first quad, L^*, for SiD / ILD	3.51 / 4.5	m
Crossing angle at the IP	14	mrad
Normalized emittance $\gamma\epsilon_{\rm x}$ / $\gamma\epsilon_{\rm y}$	10 000 / 35	nm
Nominal bunch length, σ_z	300	μm
Preferred entrance train to train jitter	<0.2–0.5	σ_y
Preferred entrance bunch to bunch jitter	< 0.1	σ_y
Typical nominal collimation aperture, x/y	6-10 / 30-60	beam sigma
Vacuum pressure level, near/far from IP	0.1 / 5	μPa

ILC 2019

Quantity	Symbol	Unit	Initial	$\mathcal{L}$ Upgrade	TDR	Upgrades	
Centre of mass energy	$\sqrt{s}$	GeV	250	250	250	500	1000
Luminosity	$\mathcal{L}$	$10^{34}\mathrm{cm}^{-2}\mathrm{s}^{-1}$	1.35	2.7	0.82	1.8/3.6	4.9
Polarisation for $e^-(e^+)$	$P_-(P_+)$		80 %(30 %)	80 %(30 %)	80 %(30 %)	80 %(30 %)	80 %(20 %)
Repetition frequency	f_{rep}	Hz	5	5	5	5	4
Bunches per pulse	n_{bunch}	1	1312	2625	1312	1312/2625	2450
Bunch population	N_{e}	10^{10}	2	2	2	2	1.74
Linac bunch interval	Δt_{b}	ns	554	366	554	554/366	366
Beam current in pulse	I_{pulse}	mA	5.8	5.8	8.8	5.8	7.6
Beam pulse duration	t_{pulse}	μs	727	961	727	727/961	897
Average beam power	P_{ave}	MW	5.3	10.5	10.5	10.5/21	27.2
Norm. hor. emitt. at IP	$\gamma\epsilon_{\mathrm{x}}$	μm	5	5	10	10	10
Norm. vert. emitt. at IP	$\gamma\epsilon_{\mathrm{y}}$	nm	35	35	35	35	30
RMS hor. beam size at IP	σ^*_{x}	nm	516	516	729	474	335
RMS vert. beam size at IP	σ^*_{y}	nm	7.7	7.7	7.7	5.9	2.7
Luminosity in top 1 %	$\mathcal{L}_{0.01}/\mathcal{L}$		73 %	73 %	87.1 %	58.3 %	44.5 %
Energy loss from beamstrahlung	δ_{BS}		2.6 %	2.6 %	0.97 %	4.5 %	10.5 %
Site AC power	P_{site}	MW	129		122	163	300
Site length	L_{site}	km	20.5	20.5	31	31	40

TABLE I: Summary table of the ILC accelerator parameters in the initial 250 GeV staged configuration (with TDR parameters at 250 GeV given for comparison) and possible upgrades. A 500 GeV machine could also be operated at 250 GeV with 10 Hz repetition rate, bringing the maximum luminosity to $5.4 \cdot 10^{34}\,\mathrm{cm}^{-2}\mathrm{s}^{-1}$ [10].

FCC-hh

Table 2.11. Baseline parameters and estimated peak luminosities of future electron–proton collider configurations for the electron ERL when used in concurrent ep and pp operating mode.

Parameter (unit)	LHeC CDR	ep at HL-LHC	ep at HE-LHC	FCC-eh
E_p (TeV)	7	7	12.5	50
E_e (GeV)	60	60	60	60
$\sqrt{s}$ (TeV)	1.3	1.3	1.7	3.5
Bunch spacing (ns)	25	25	25	25
Protons per bunch (10^{11})	1.7	2.2	2.5	1
$\gamma\epsilon_p$ (μm)	3.7	2	2.5	2.2
Electrons per bunch (10^9)	1	2.3	3.0	3.0
Electron current (mA)	6.4	15	20	20
IP beta function β_p^* (cm)	10	7	10	15
Hourglass factor H_{geom}	0.9	0.9	0.9	0.9
Pinch factor H_{b-b}	1.3	1.3	1.3	1.3
Proton filling H_{coll}	0.8	0.8	0.8	0.8
Luminosity ($10^{33}\,\mathrm{cm}^{-2}\,\mathrm{s}^{-1}$)	1	8	12	15

Parameter Table

Table 7.1: Key numbers relating the detector challenges at the different accelerators.

Parameter	Unit	LHC	HL-LHC	HE-LHC	FCC-hh
Total number of pp collisions	10^{16}	2.6	26	91	324
Charged part. flux at 2.5 cm, est.(FLUKA)	GHz cm^{-2}	0.1	0.7	2.7	8.4 (10)
1 MeV-neq fluence at 2.5 cm, est.(FLUKA)	10^{16} cm^{-2}	0.4	3.9	16.8	84.3 (60)
Total ionising dose at 2.5 cm, est.(FLUKA)	MGy	1.3	13	54	270 (300)
$dE/d\eta\|_{\eta=5}$ [331]	GeV	316	316	427	765
$dP/d\eta\|_{\eta=5}$	kW	0.04	0.2	1.0	4.0
90% $b\bar{b}$ $p_T^b > 30$ GeV/c [332]	$\|\eta\|<$	3	3	3.3	4.5
VBF jet peak [332]	$\|\eta\|$	3.4	3.4	3.7	4.4
90% VBF jets [332]	$\|\eta\|<$	4.5	4.5	5.0	6.0
90% H $\rightarrow 4l$ [332]	$\|\eta\|<$	3.8	3.8	4.1	4.8

First tracking layer:

10GHz/cm^2 charged particles

10^{18} hadrons/cm^2 for 30ab^{-1}

Increased Boost at 100TeV 'spreads out' light SM physics by 1-1.5 units of rapidity.

Heavy Ions

Table 7.4: Key parameters defining the detector requirements for PbPb collisions.

Parameter	unit	LHC	HL-LHC	HE-LHC	FCC-hh
E_{cm} per nucleon	TeV	5.5	5.5	10.6	39.4
Circumference	km	26.7	26.7	26.7	97.8
Peak $\mathcal{L}$	10^{27} cm^{-2}s^{-1}	1	6.5	15-50	320
Bunch spacing	ns	100	50	50	50
Number of bunches		1232	1232	1232	5400
Goal $\int \mathcal{L}$	nb^{-1}	1	10	10/month	110/month
σ_{inel}	b	7.8	7.8	8	9
σ_{tot}	b	515	515	530	597
BC rate	MHz	13.8	13.8	13.8	16.6
Peak PbPb collision rate	kHz	7.8	50.7	400	2880
RMS luminous region σ_z	mm	50-70	50-70	35-70	30-60
$dN_{ch}/d\eta\|_{\eta=0}$		500	500	610	900
Charged tracks per collision N_{ch}		5800	5800	7500	12500
Rate of charged tracks	GHz	0.05	0.3	3	36
$< p_T >$	GeV/c	0.47	0.47	0.49	0.55
Bending radius for $< p_T >$ at B=4T	cm	39	39	41	46

The general purpose detector will also be able to perform well for PbPb collisions at the predicted Luminosities.

Continuous readout, PID from TOF with the timing detectors are good features for Heavy Ion Physics.

Operating at a lower field than 4T would of course be desirable (calibration questions to be worked out …)

The significantly lower radiation requirement allows of course optimized detector solutions that can outperform a general purpose detector.

We definitely have to keep the door open for a dedicated HI experiment setup.